Finite-State Machine Abstractions of Continuous Systems

by

Stéphane Blouin

A thesis submitted to the Department of
Chemical Engineering in conformity with the requirements for
the degree of Doctor of Philosophy

Queen's University
Kingston, Ontario, Canada
October, 2003

to Marie-Claude

Abstract

Many manufacturing processes involve an interplay of logical and continuous control objectives. Here, emphasis is put on the class of continuous plants controlled by a discrete-event supervisor. For the supervisor synthesis, we favor an approach by abstraction. This amounts to extracting a finite-state machine realization that is dynamically equivalent to the continuous dynamics. In particular, we aim for abstractions that are independent of specifications. Moreover, we seek a computational method capable of generating such an abstraction in finite time.

In our procedure, a partition of a state-space region of the continuous plant yields the state structure of the abstraction. The transition structure of the abstraction is then obtained by analyzing the continuous trajectories with respect to the partition. The proposed partitioning technique is model-based since the state-space decomposition uses dynamical invariants of the continuous dynamics. The present method applies to a class of continuous systems satisfying an integrability property. Moreover a dynamical equivalence between the original and the abstract systems is based on a correspondence between continuous trajectories and sequences of discrete transitions.

First we show how to use dynamical invariants for constructing partitions. Then we identify a transversality property of continuous trajectories with respect to partition boundaries. We also characterize this property for two classes of systems before providing sufficient conditions. This leads to a technique for evaluating the transition structure with a reduced number of points. We can fully exploit this feature if the partition satisfies a certain boundedness property, for which we supply sufficient conditions. For two-dimensional systems we present sufficient conditions ensuring the finiteness of computation of the abstraction. Simulation results demonstrate that one usually obtains an abstraction with nondeterministic transitions. Moreover, the dynamical equivalence between the abstract and the original system is, in general,

violated. To circumvent those difficulties we recommend the use of an extended abstraction transition mapping that could take into account the timing information as well as the hyperplanes through which continuous trajectories transit. Finally we extend the above method to a class of systems for which a Lyapunov function can be determined.

Acknowledgments

for their extraordinary support during the last weeks of my Ph.D.

Many thanks to my parents, brother and sisters for their love and support during all these years.

Spécialement, je tiens à remercier Marie-Claude pour sa charmante compagnie, sa jovialité, son indéfectible patience, et sa complicité tout au long de ma thèse.

Statement of Originality

In this thesis, a theory is developed for generating finite-state machine abstractions for a class of continuous systems with nonlinear dynamics. More specifically, the claims of originality are as follows:

- a class of nonlinear systems satisfying an integrability property is identified;

- for those systems, a technique for generating abstractions based on invariants and independent of specifications is proposed;

- sufficient conditions are provided for obtaining abstractions with transversality characteristics;

- two abstraction boundedness properties are defined and sufficient conditions are given;

- for two-dimensional systems, a set of sufficient conditions and an algorithm ensure the computation of abstractions in finite time; a method for verifying a notion of dynamical equivalence between the original and the abstract system is also suggested;

- an extension of the theory and the algorithm is performed for a class of systems for which Lyapunov functions can be determined.

Contents

List of Tables

List of Figures

List of Symbols

Roman Letters

$\mathcal{A}$ Finite-state machine abstraction

$\mathcal{C}, \mathcal{C}'$ Set of critical points of ψ, approximate set of critical points of ψ

$\mathcal{E}, \mathcal{E}'$ Subset of critical points, approximate subset of critical points

$\mathcal{F}$ Zero-level set of $\widetilde{\psi}$

$\mathcal{G}$ Set of non-transversal points that are linearly dependent with respect to a leaf

$\mathcal{I}_\Sigma$ Index set of Σ

$\mathcal{I}_S$ Index set of slices

$\mathcal{R}, \widetilde{\mathcal{R}}, \hat{\mathcal{R}}$ Sets of regular values of first integrals

$\mathcal{S}_\sigma$ Set of equilibrium points induced by the input value σ, $\mathcal{S}_\sigma \subset D$

$\mathcal{U}$ Class of admissible controls

$\mathcal{U}_d$ Class of piecewise-constant admissible controls, $\mathcal{U}_d \subset \mathcal{U}$

B_p^δ Ball centered at p and of radius $\delta > 0$

c Real constant or concentration

C_k^r Set of first integral constants associated to γ_j^k

D Subset of $\mathbb{R}^n$ where the ODE is defined

D', D'' State-space regions where first integrals are defined, $D', D'' \subset D$

E State-space region where a partition is performed, $E \subset D$

h Height of liquid

$H_{\Omega(\hat{\Gamma})}(p)$ Set of vectors tangent to $\Omega(\hat{\Gamma})$ at point p

$L_{j,k}^c$ Leaf induced by the first integral $\gamma_j^k \in \Gamma$ and the real constant c

m Dimension of the input space

n Dimension of the continuous system

$N(\partial, p)$ Normal to a boundary ∂ at a point p

N_i Index set of partition cells neighbor to cell q_i, $N_i \subset Q$

p Arbitrary point in D

Q Index set for the subsets of a partition π

q Partition subset, $q \subset E$

s Sequence of input values, $s \in \Sigma^+$

$S_{j,k}$ Set of slices associated to γ_j^k

T Temperature

t Time variable, time period

$T_p M$ Tangent space of a manifold M at a point p

U Set of input values

V Lyapunov function

v Vector

Greek Letters

δ Finite-state machine transition map

ϵ Small positive real number

Γ Set of all first integrals induced by Σ

Γ^k Set of all first integrals induced by input value $\sigma_k \in \Sigma$

γ_j^k jth first integral induced by input value $\sigma_k \in \Sigma$

$\hat{\Gamma}$ Subset of Γ

ω One-form or a covector

$\Omega(\hat{\Gamma})$ Locations where $\hat{\Gamma}$ has less than n independent first integrals

∂ Set of boundary points

Φ Composition of flows induced by s and τ

Φ^* Trajectory induced by s and τ

ϕ_k Flow induced by the input value $\sigma_k \in \Sigma$

ϕ_k^* Trajectory under input value $\sigma_k \in \Sigma$

Π Collection of partitions

π Partition over a region E

$\psi, \widetilde{\psi}$ Non-transversality function, approximate non-transversality function

Σ, Σ' Set of input values, approximate set of input values

Σ^+ Set of input sequences

σ_k Input value, an element of Σ with $k \in \mathcal{I}_\Sigma$

τ Sequence of switching times

Vectors and Matrices

f Vector field

u Vector of input values of dimension m

x State variable in a n-dimensional space

y Vector of output variables

Operators and Symbols

$=, \neq$ Equal to, not equal to

$\#$ Cardinality

$\cap, \cup$ Intersection, union

$\cdot$ Inner product

$\Delta^\perp$ Codistribution

$\dot{z}$ Time derivative of variable $z(t)$, i.e., dz/dt

$\exists$ There exists

$\forall$ For all

$\frac{\partial}{\partial t}$ Partial derivative with respect to time

$\in, \notin$ Element of, not an element of

$\circ$ Composition of mappings

$\overline{A}$ Closure of set A

$\setminus$ Set difference

$\star$ Refinement of partitions

$\subset$, $\subseteq$ Strict subset of, a subset of

$\sum$ Summation sign

$\times$ Cartesian product

$|\cdot|$ Absolute value of enclosed expression

$\wedge$ Wedge product

$A(x)|_{x=p}$ Evaluation of $A(x)$ at $x = p$

A^c Complement of set A in the containing set

d Differential with respect to x

$dim(B)$ Dimension of subspace B

g^{-1} Preimage of mapping g

$int(A)$ Interior of set A

lim Limit

$rank(g)$ Rank of mapping g

sup Supremum (least upper bound)

v^T Transpose of vector v

$\mathbb{N}$, $\mathbb{N}^+$ Natural numbers $\{0, 1, 2, \dots\}$, positive natural numbers $\{1, 2, \dots\}$

$\mathbb{R}^n$ Euclidean space of dimension n

$\mathbb{R}$, $\mathbb{R}_{\geq 0}$ Real numbers, non-negative real numbers

Abbreviations

CSS Controlled switched system

FIC First integral constant

FSM Finite-state machine

HCS Hybrid control system

HIBC Hybrid in-block controllability

ICSS Integrable controlled switched system

NTSM Non-transversality submanifold

Chapter 1

Introduction

The theory of Hybrid Systems consists of a formalism enabling the modelling and analysis of systems that involve both continuous and discrete behaviour. In the last decade, Hybrid Systems have proven their relevance in various fields such as the automotive industry, air traffic control, and robotics. In the chemical industry, this framework is particularly well-suited to capture some physical phenomena such as liquid-gas phase transitions and changes in reaction pathways.

Of particular interest, one finds the class of systems that exhibit switchings among various continuous dynamics. Either a switching arises when certain physical constraints are attained (as for a bouncing ball when hitting the ground) or it is induced by some qualitative or logical rules. A situation where logical rules are present consists of the safety procedures for manufacturing processes such as shut-down or actuator saturation.

A large portion of the literature on Hybrid Systems is devoted to the task of *verification*, i.e., ensuring that a set of logical rules can be enforced. Verification often reduces to checking that the plant states reach, or avoid, a certain region when initialized in a given departure set. In the theory of continuous control systems, the notion of stabilization (respectively, set-stabilization), i.e., stabilizing a system to a

point (resp., set of points), is also of crucial importance.

There exists no unique formalism for modelling general Hybrid Systems. However, the model presented in (Branicky *et al.*, 1998) subsumes a large family of cases. In the last few years some important classes of Hybrid Systems have emerged such as Switched Systems (Liberzon and Morse, 1999), Hybrid Output Feedback Systems (Artstein, 1996), and Quantized Systems (Lunze, 1994; Liberzon, 2002). This thesis focuses on a family of Hybrid Systems that is introduced next.

1.1   A Class of Hybrid Systems

In manufacturing processes, many situations involve an interplay of logical rules with continuous control objectives. One such situation considers the use of logic controllers for continuous processes (such as programmable logic controllers), which represent a significant industrial application of continuous dynamics altered by logical rules.

The special class of *Hybrid Control Systems* is particularly adapted for studying the control of a continuous plant subject to continuous and logical control goals. This class of Hybrid Systems was first introduced in (Stiver and Antsaklis, 1993) and further developed in (Stiver *et al.*, 1995*a*; Yang *et al.*, 1995; Caines and Wei, 1998; Stiver *et al.*, 2001). A Hybrid Control System consists of three components: a discrete-event controller, a continuous plant, and an interface — as illustrated in Figure 1.1. That is, the continuous plant (possibly equipped with a continuous controller) is controlled by the discrete-event controller via the interface. The input and output signals of the plant are real-valued whereas those of the controller are of a symbolic nature. In the sequel the adjective "symbolic" refers to a qualitative statement such as "on", "off", "too high", etc. The sets of controller input and output symbols are assumed to be finite. Therefore, the interface converts the continuous plant output y into a controller symbolic input s_i and the controller symbolic output

s_o into the plant input u. The discrete-event controller updates its output symbol s_o only when a change in s_i, the qualitative plant measurement, occurs. In the literature some authors refer to the above setup as *symbolic control* or *supervisory control* of continuous systems (Raisch, 1995; Raisch and O'Young, 1998; Lunze, 1998).
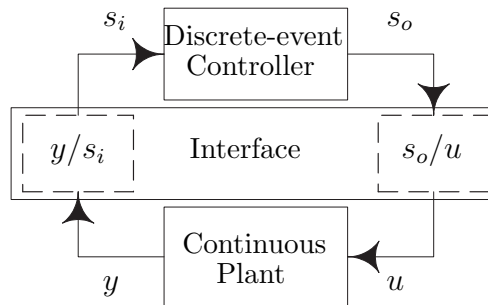
Figure 1.1: A Hybrid Control System

Hybrid Control Systems are especially relevant when a continuous plant is subject to coarse or high-level control tasks. The simplest example of a Hybrid Control System equipped with a coarse control objective is the temperature controller of a room. Indeed, the thermostat reads the room temperature as either "too low" or "too high" and reacts accordingly by turning "on" or "off" the heating or cooling system, which then alters the room temperature. As for the interface, the "on" and "off" symbols are converted into a piecewise-constant signal of the current sent to the heating system (resp., of the heat supplied to the room) if the actuator dynamics are (resp., are not) incorporated into the room energy-balance model. Also, the "too low" and "too high" qualifiers can simply be assigned by the test $T < T_s$ and $T \geq T_s$, respectively, where T_s is the set temperature and T the room temperature.

Many industrial processes possess a hierarchical structure, into which the control objectives are aggregated in "low-level" and "high-level" categories. Usually the low-level control objectives (such as set-point tracking) are continuous in nature whereas high-level objectives (such as set-point change) are better described by a sequence of

events than by a continuous flow of information. In this context a Hybrid Control System can be used to enforce high-level control objectives over the continuous plant.

Two distinct problems can be identified with the class of Hybrid Control Systems. In both cases, the plant continuous dynamics, the set of manipulated variables and the output function are known *a priori*. The first problem assumes that the interface is given and therefore it focuses on control issues, such as stabilization or controllability (Stiver and Antsaklis, 1993; Yang *et al.*, 1995; Caines and Lemch, 1998). This area of research includes the class of Quantized Systems (both in measurements and inputs) consisting of Hybrid Control Systems equipped with quantizers in place of the interface (Lunze, 1994; Liberzon, 2002).

The second problem concentrates on developing the interface. In particular the second problem arises when a qualitative representation of the continuous dynamics is beneficial for the task at hand. For instance, a qualitative model may be required in the presence of the following situations:

(COND. 1) processes with an actuation taking finite values ("on", "half-open", etc.),

(COND. 2) systems with qualitative control requirements such as specifications.

Other situations where a qualitative model is needed can be found in (Lunze, 1998; Stursberg *et al.*, 2000; Stiver *et al.*, 2001; Bernard and Gouzé, 2002).

In the above condition (COND. 2), we understand by "specification" some logic statement of the form *"if event A occurs then perform action B"*. For instance, if a fault is detected, a piece of equipment may have to be shut down rapidly and safely by enforcing some actions while disabling some others. In the presence of many specifications one must check for the occurrence of conflicts, which happen whenever one specification is enforced at the price of violating another one.

In the chemical industry, many actuators (e.g., pumps and valves) operate with a finite number of modes. The room-temperature controller, with its "on" and "off"

modes, falls in this category. Therefore condition (COND. 1) is sometimes inherent to the process. Another instance where condition (COND. 1) appears naturally is in the design of a high-level controller for a plant with complex continuous dynamics. Indeed, in the presence of condition (COND. 2) a continuous plant behaviour may be reduced to its key triggering events, thus leading to (COND. 1). The oilsand extraction process discussed in (Blouin *et al.*, 2001) is an example where this strategy is used. As one notices, conditions (COND. 1) and (COND. 2) do not exclude continuous control objectives.

In the remaining chapters emphasis is put on those systems for which both (COND. 1) and (COND. 2) apply.

1.1.1 An Illustrative Example

In order to illustrate some of the concepts, a physical system where both (COND. 1) and (COND. 2) hold is introduced. The system is composed of two tanks connected via a pipe as shown in Figure 1.2. The variables of the system are the levels of liquid in Tank 1 and Tank 2 measured from a reference level, h_1 and h_2, respectively. Tank 1 has an inlet flow and an outlet flow whose rates are recorded in F. The tanks interact via a pipe with a flowrate controlled by a valve, whose opening value is denoted by β. The cross-section areas of Tank 1 and Tank 2 are A_1 and A_2, respectively.
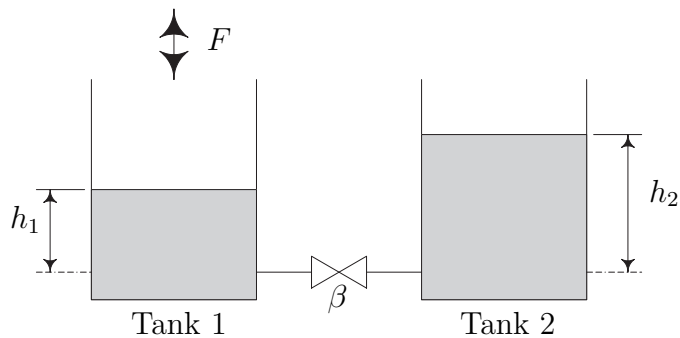
Figure 1.2: A two-tank system

The control variables are the flowrate F and the valve opening β. The flowrate F results from a pump (or a group of pumps) that has finite modes ("pumping from", "off", and "pumping towards") while the pipe's valve has "open" and "close" modes. In the actual approach, it is assumed that each controller output symbol corresponds, in a one-to-one manner, to a plant input value. This assumption holds for a large number of computer-controlled systems since it is usually required for the digital-to-analog conversion of the control signal originating from the computer and directed to the actuators. Therefore one can assume that the control variables in the above example take real values, say $\beta \in \{0, 0.9\}$ and $F \in \{-10.5, 0, 10.5\}$, thus satisfying condition (COND. 1). The converted symbolic output value then becomes a piecewise-constant signal due to the presence of a zero-hold device (Stiver and Antsaklis, 1993).

A mass balance performed on the system provides the set of differential equations

$$
\begin{aligned}
\dot{h}_1(t) &= \frac{F}{A_1} - \frac{\beta\alpha}{A_1}\sqrt{h_1(t) - h_2(t)} \\
\dot{h}_2(t) &= \frac{\beta\alpha}{A_2}\sqrt{h_1(t) - h_2(t)}
\end{aligned}
\quad , \text{ for } h_1(t) \geq h_2(t) \tag{1.1}
$$

$$
\begin{aligned}
\dot{h}_1(t) &= \frac{F}{A_1} + \frac{\beta\alpha}{A_1}\sqrt{h_2(t) - h_1(t)} \\
\dot{h}_2(t) &= -\frac{\beta\alpha}{A_2}\sqrt{h_2(t) - h_1(t)}
\end{aligned}
\quad , \text{ for } h_1(t) \leq h_2(t), \tag{1.2}
$$

where $\dot{h}_i$ denotes the time derivative of h_i, $i \in \{1, 2\}$, and α is some real constant. The above system dynamics are nonlinear and are characterized by the differential equations (1.1) and (1.2), each of which holds on a different side of the hypersurface satisfying $h_1 = h_2$. This model differs from the two-tank model

$$
\begin{aligned}
\dot{h}_1(t) &= \frac{F}{A_1} + \frac{\beta\alpha}{A_1}(h_2(t) - h_1(t)) \\
\dot{h}_2(t) &= -\frac{\beta\alpha}{A_2}(h_2(t) - h_1(t))
\end{aligned}
\quad , \tag{1.3}
$$

6

found in (Raisch and O'Young, 1998) and where the nonlinearity (the square root) has been omitted. We refer to (1.1) and (1.2) as the *nonlinear model* and to (1.3) as the *linear model* of the two-tank system. Unlike the linear model, the nonlinear model one is hybrid as the system's dynamics experience a change whenever $h_1 = h_2$.

A qualitative requirement for the two-tank system is the specification "do not overflow". Such a task does not require the full knowledge of the underlying continuous dynamics. For instance, it can be verified by using the level qualifiers "low", "medium" and "high". Another example of a qualitative statement is "if Tank 2 reaches the high level, then bring both tanks to low and then stop the process".

1.2   Research Objectives and Motivations

As defined in the previous section, the second problem of Hybrid Control Systems influences the first one. Moreover, a thorough understanding of the interface design is believed to provide insights on the control capabilities of Hybrid Control Systems. Indeed some authors integrate the interface design within the controller synthesis (Artstein, 1996; Raisch, 2000; Stiver *et al.*, 2001). Therefore, the second problem is investigated first with the assumption that one is given the finite set of output symbols of the controller (s_o in Figure 1.1).

If one lumps together the interface and the continuous dynamics of Figure 1.1 then the second problem is to determine a discrete model which approximates or mimics the continuous dynamics paired with the interface. In the sequel we refer to the plant discrete model as an "abstraction" and we adopt the finite-state machine formalism as a representation. A more precise definition of an abstraction is given in subsequent chapters. Usually, abstractions are used for two purposes: (i) to "throw away" information (thus making the abstract system simpler to analyze), and (ii) to "preserve a property of interest" (Kokar, 1995). A common technique to initiate

an abstraction is to decompose, or *partition*, a plant signal space (state space, input space, output space, or a combination of those) into sets of points and identify each of these sets with a single qualitative symbol, thus throwing away some information (point (i) above). Then the abstraction transition structure is deduced from analysis of the continuous dynamics with respect to the partition. Once an abstraction is obtained then a controller can be synthesized by using the finite-state machine theory only. This represents the main benefit of the approach by abstractions since controller synthesis in a continuous framework is usually more difficult to achieve, especially in the presence of condition (COND. 1).

Figure 1.3 represents a Hybrid Control System setup with an abstraction as part of the interface. With this configuration the plant symbolic output s_i is induced by the abstraction. Also the plant input signal u is generated from the set of controller output symbols s_o and an interface similar to that of the two-tank example. As mentioned before it is assumed that s_o takes values in a finite set. Therefore the abstraction dynamics are completely governed by the occurrence of discrete events only. The presence of y as an input signal to the abstraction in Figure 1.3 is there to emphasize the fact that plant events s_i also depend on continuous output data.
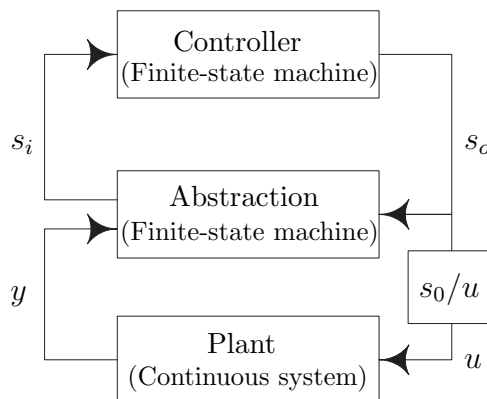
Figure 1.3: A Hybrid Control System with an abstraction

Rather than proceeding by abstractions, an alternative is to consider a continu-

ous equivalent of the hybrid control problem, a procedure referred to as "continuation" in (Branicky, 1995). A consequence of this approach is that formal methods (Cuadrado, 1994) for checking conflicts among specifications cannot be used. Moreover, there are situations where continuation is intentionally avoided. This is the case for complex continuous systems where continuation is dropped to simplify the exceedingly complex models that may result. A closely related field is that of generating continuous abstractions of continuous systems. Indeed, in (Pappas and Simic, 2002) the authors use a smooth surjective mapping to abstract affine control systems while preserving the reachability properties of the original system.

Among the various abstraction techniques, one can choose to make the abstraction tailored to a particular specification (or a set of them). For instance, an abstraction may be used for a verification purpose so that its transition and state structures capture the reachability of a target set from a given source set. We denote by *s-abstractions* such specification-oriented abstractions. From a practical point of view, s-abstractions are suitable for finite sequences of actions (such as start-up and shut-down). The alternative is to consider abstractions that are independent of specifications. We simply refer to those as *abstractions*. The s-abstractions usually require less analysis and computation than abstractions since the information that does not relate to the specification can be dropped. Stabilization through abstractions can be investigated as shown in (Hsu, 1987; Lunze, 1995), whereas converting a stabilization task into a finite set of s-abstractions may not be trivial. Indeed, the construction of abstractions can be seen as the first stage of a control synthesis technique. This approach is potentially relevant for systems with nonlinear dynamics and bounded inputs for which no general strategy for synthesizing a controller exists. Unlike s-abstractions, abstractions are also amenable to hierarchical control (Caines and Wei, 1998), logical control of continuous process (Stursberg *et al.*, 2000), model validation (Bernard and Gouzé, 2002), and integrated process design (fifth conference

paper on page 162). Therefore we favor abstractions because (i) continuous control tasks can be achieved, (ii) verification can always be performed, and (iii) they can lead to hierarchical control or integrated design solutions, which are applications of interest in chemical engineering.

In summary, the interface of Hybrid Control Systems is part of the design procedure being undertaken. Also the approach by abstractions is preferred due to the nature of the envisioned control tasks. Therefore given a continuous plant, the problem of interest is to develop a technique to generate a finite-state machine abstraction so that each plant trajectory corresponds to a sequence of discrete transitions in the abstraction, and vice versa. This notion of relationship between trajectories and discrete transitions will be made clearer in further chapters.

1.3   Overview of the Thesis

In Chapter 2, a literature review of various abstraction techniques is performed. Chapter 3 contains the theoretical background for the subsequent chapters. Therein the notions of transversality, finiteness, consistency, and deterministic behaviour are introduced, prior to formulating a precise problem statement. Also a class of nonlinear systems is defined and some preliminary results are provided. Then in Chapter 4 we state a transversality requirement and establish its relation to the deterministic behaviour of the abstraction's transition structure. Chapter 5 presents the notion of L-boundedness, its relevance for a family of abstractions, and a set of sufficient conditions. In Chapter 6 the finiteness of computation is resolved for two-dimensional systems and case studies are presented. Chapter 7 introduces an extension of the theory to systems for which a Lyapunov function can be determined. Finally Chapter 8 contains the conclusions.

Chapter 2

Literature Review

Prior to abstracting the continuous dynamics of a Hybrid Control System we begin by reviewing and comparing the various contributions related to the general area of abstractions. For this purpose we present in Section 2.1 a brief description of abstraction techniques found in the literature. Then in Section 2.2 a qualitative comparison of the existing approaches is performed. A discussion of the comparative analysis follows in Section 2.3.

2.1   Review of Approaches

The interest for abstracting continuous dynamics by discrete realizations originated a decade ago. At the same time Hybrid Systems experienced an increase in popularity in various fields of science. As of today, research efforts on discrete abstractions of continuous systems take place in broad areas of engineering such as chemical engineering, electrical engineering, and biological engineering. This is one of the reasons why the references are presented by research group in the chronological order of their first known contribution. Also, due to similarities with the abstraction task some achievements in the field of verification (reachability analysis or s-abstractions) and qualitative modelling are cited. As a guideline, almost all techniques presented here

follow a generic procedure, first a partition of some space is performed, followed by the construction of a transition structure based on the partition.

Throughout their work, Lunze and coworkers (Lunze, 1992; Lunze, 1994; Lunze, 1998; Lunze *et al.*, 1999) show an interest in eliminating spurious solutions by targeting abstractions with deterministic behaviour. *Spurious solutions* are those solutions (i.e., sequences of transitions) generated by an abstraction for which there exists no corresponding continuous trajectory. In other words, the presence of spurious solutions implies that an abstraction over-approximates the underlying continuous dynamics. A transition structure of an abstraction is *deterministic* if from any partition subregion a given input value leads to a unique partition subregion. The early work of Lunze (Lunze, 1992; Lunze, 1994; Lunze, 1998) covers the qualitative modelling of continuous dynamics whose input and state signals are quantized. It was shown that a quantization of state variables induces a partition over the state space of the system. Among the various modelling approaches presented in (Lunze, 1998), the representation by discrete-event systems is favored. For the class of unforced sampled-data systems, necessary and sufficient conditions for obtaining a deterministic automaton are provided (Lunze, 1994). As those conditions are rather restrictive the automaton is, in general, nondeterministic, thus leading to the use of stochastic automata. The author illustrates the approach by applying it to the practical stability of an inverted pendulum in (Lunze, 1992). Recently Lunze and coworkers (Lunze *et al.*, 1999) have taken a slightly different approach. Instead of considering a predetermined quantization, the authors investigate conditions under which a partitioning of the state space leads to deterministic automata. Sufficient conditions are provided for the class of continuous linear systems with fixed input values.

In (Stiver and Antsaklis, 1993), Stiver and Antsaklis extend the notions of controllability and of supremal controllable language presented in (Ramadge and Wonham, 1982) to analyze abstractions of the continuous part of Hybrid Control Systems.

In this setup, the interfaces are given and abstractions are assumed to be nondeterministic. Stiver and coworkers (Stiver *et al.*, 1995*a*; Stiver *et al.*, 1995*b*) then consider the case where the interface must be designed in order to build s-abstractions. Therein the design of a controller and the interface is performed together based on natural invariants of the continuous dynamics. A control goal, such as the reachability of a target set from a departing set, and control input values are utilized for the interface design. Recently Stiver et al. (Stiver *et al.*, 2001) extended some of the previous results to linear hybrid systems. In this recent article the controller design approach is explained extensively.

In (Zhao, 1994), Zhao proposes a computational method for analyzing the qualitative behaviour of a class of nonlinear systems with known input values. The qualitative representation is based on a state-space analysis in terms of equilibrium points, limit cycles, stability regions, and an equivalence class of trajectories. Those entities serve to partition a region of interest of the state space into qualitatively distinct regions. The method applies to systems satisfying a hyperbolicity condition, a transversality condition, and a certain condition on the trajectories bounding stability regions. The class of structurally stable systems naturally fulfill the first two conditions.

Unlike other researchers, Yang *et al.* assume that a nondeterministic abstraction of the continuous plant is given (Yang *et al.*, 1995). This work is worth mentioning because new definitions of nondeterministic behaviour and controllability are provided. Moreover the authors develop a procedure for generating the supremal live sublanguage of a specification language.

In (Kokar, 1995), the author investigates how to partition some signal space of a continuous system so that one can analyze continuous dynamics from the abstraction only. This leads to a notion of *consistency*, which precludes the existence of spurious solutions. The approach uses hypersurfaces to partition various signal spaces (output space, state space, and input-state-time space). In this context hypersurfaces define

an abstraction mapping. The partitioning technique applies to single-output systems possessing a closed-form solution. Therein a consistency postulate is defined on the basis of the exact knowledge of time and initial conditions.

In (Raisch, 1995), the author studies linear switched systems (where switching among various (A, B) pairs occurs) subject to output quantization. In this context the quantization results in a rectangular partition of the output space. For the sub-class of systems with constant drift vector, the author derives necessary and sufficient conditions for the global reachability and controllability in the presence of piecewise-constant input signals. Raisch and O'Young then focus on systems modelled by discrete-time dynamics with disturbances (Raisch and O'Young, 1996). By considering past and present data it is shown how state estimates can be constructed. Recently Raisch has formalized the approach in (Raisch, 2000) by using the behavioural paradigm (Willems, 1991). The technique contains two steps, first an ordered set of behaviours is generated, and then for each behaviour a nondeterministic automaton is constructed as the minimal realization. The accuracy of the abstraction can be tuned to the precision required by the specification. In this setup the automaton representation of the behaviour has its state structure determined by a partitioning of the input-output space.

Bernard and Gouzé (Bernard and Gouzé, 1995) study the class of uncertain continuous models with loop structure and monotonous interactions (i.e., the off-diagonal terms of the vector field Jacobian matrix never vanish), which are common in biological, population and evolution systems. For unforced systems, they provide a technique to obtain finite-state machine abstractions based on the extra-diagonal terms of the Jacobian of the system's vector field. An extension to systems with inputs is performed in (Bernard and Gouzé, 1999). In (Bernard and Gouzé, 2002), the authors provide conditions under which the abstractions can be derived when diagonal terms of the Jacobian are considered. The finite-state machine abstractions thus obtained

are mainly used for the experimental validation of the continuous models.

Broucke (Broucke, 1998) also uses dynamical invariants (more precisely, first integrals) for the verification task of a safety problem (that is, ensure that a forbidden set is not reached when departing from a given set). Therein an equivalence relation among the trajectories of a hybrid system acts as a *bisimulation*, i.e., it is not only the case that the abstraction "simulates" the original system but also the original system "simulates" the abstraction. Analytical representations of bisimulations are constructed from foliations, which consist of state-space decompositions by dynamical invariants. Then for each control location (meaning each input value) an over-approximation of the system trajectories is obtained. Note that the construction of the s-abstraction requires a transversality condition.

In (Caines and Lemch, 1998; Lemch and Caines, 1999) Caines and Lemch build on the Hybrid-In-Block-Controllability (HIBC) and the dynamical consistency (DC) properties introduced in (Caines and Wei, 1998). On one hand, the HIBC property requires that each subregion of a partition forms a controllable subsystem (in the continuous sense). On the other hand, two distinct neighboring partition subregions are dynamically consistent (in a given direction) if for any point of a subregion there exists a control action such that the point can be brought to some point of the other subregion. In order to obtain a lattice of HIBC partitions, Caines and Wei invoke the existence of a flow transversal to the partition boundaries. Moreover, the fountain condition and one of the recurrence conditions provided in (Caines and Lemch, 1998) are sufficient to establish the controllability of nonlinear systems in general, and thus the HIBC property of their partitions. These results hold for the class of admissible controls (defined in §A.4.1), which is a generalization of the type of control involved here (ref. the two-tank example of §1.1.1 on page 5). Also, one notices that no technique is provided in order to build finite-state machine abstractions.

The work of (Stursberg *et al.*, 2000) explores two procedures to extract timed dis-

crete abstractions of continuous dynamics. Both methods are based on a rectangular partition of the state space. The first technique uses interval-arithmetical expressions to capture flows between two partition regions, whereas the second technique considers partition boundaries as additional states in order to establish boundary-to-boundary flows by numerical integration. A comparison between the two methods is performed on the basis of completeness, accuracy, consistency and computational burden. Even though the accuracy of the second method is better than that of the first method, it is limited by the fact that an infinite number of initial conditions must be considered. Systems to which the techniques apply are those modelled by nonlinear dynamics with piecewise-constant input signals.

Since a continuous system is a hybrid system with a single discrete location, the work of Alur and coworkers (Alur *et al.*, 2000) is also of interest. The article reviews the class of hybrid systems for which the construction of an equivalent finite discrete abstraction, through language equivalence relations and bisimulations, is possible. Therein emphasis is put on the decidability of the reachibility problem. For this purpose, existing results require that the continuous dynamics be constrained to that of rectangular automata (that is, continuous dynamics with interval-valued vector fields and decoupled states evolving on a rectangular region). A restriction to a subclass of hybrid systems allows an extension of the continuous dynamics to a class of linear systems.

Finally Lefebvre and coworkers (Lefebvre *et al.*, 2002) abstract continuous dynamics modelled by linear switched systems of dimension two. In essence, the authors show that a state-space partition based on dynamical entities (such as equilibrium points and eigenvalues) provides more efficient abstractions than rectangular grids.

This completes the literature review on abstractions of continuous dynamics. In the following sections we proceed with an analysis of the above results before defining a set of objectives.

16

2.2 Qualitative Comparison

In order to shed some light on potential research directions, we undertake a qualitative comparison between the various approaches described in the previous section. The comparison focuses on three distinct aspects: the continuous dynamics, the abstraction type, and the nature of the partition.

The class of continuous systems that are abstracted can be represented by linear (L) or nonlinear (NL) dynamical models. Among the linear dynamics one finds the discrete-time (LD), continuous (LC), and switched (LS) models. The column labelled "Continuous" in Table 2.1 summarizes the class of systems considered by each research group. The presence of "–" in Table 2.1 stands for an absence of information on the topic. In addition to the previous classification of continuous dynamics, the following properties are required: bidimensionality in (Lefebvre *et al.*, 2002), global controllability in (Caines and Lemch, 1998), structural stability in (Zhao, 1994), uncertain models with loop structure in (Bernard and Gouzé, 2002), models with a single output and closed-form solutions in (Kokar, 1995), and an integrability property in (Broucke, 1998; Stiver *et al.*, 2001).

As seen previously one can generate various types of abstractions. In order to characterize them, emphasis is put on the dependence of the abstraction on continuous time, specifications, and input values. Also the deterministic nature of the transition structure of the abstraction is of interest. For instance, the column "Discrete" in Table 2.1 depicts for each approach if the transition structure refers to time (either timed (T) or untimed (U)) and whether its behaviour is deterministic (D) or nondeterministic (ND). Furthermore, only (Kokar, 1995; Caines and Lemch, 1998; Lunze *et al.*, 1999; Stursberg *et al.*, 2000; Bernard and Gouzé, 2002; Lefebvre *et al.*, 2002) generate abstractions that do not depend on specifications. The synthesis of s-abstractions is denoted by SA in Table 2.1 whereas A stands for the synthesis of abstractions. The technique of a few research groups (Broucke, 1998; Lunze *et al.*, 1999; Lefebvre

et al., 2002; Bernard and Gouzé, 2002) is such that an abstraction or s-abstraction must be generated for each input value. In contrast, the work of (Lemch and Caines, 1999; Raisch, 2000; Stiver *et al.*, 2001) uses a single abstraction or s-abstraction to capture all input values.

Authors	Discrete	Continuous	Partition	Technique
Lunze *et al.* (1992-1999)	U, D, A	LD, LC	S, d	Yes
Stiver *et al.* (1993-2001)	U, ND, SA	NL	S, d	Yes
Zhao (1994)	U, –, –	NL	S, d	Yes
Raisch *et al.* (1995-2000)	U, ND, SA	LS,LD	IO, s	Yes
Kokar (1995)	U, –, A	NL	ES, d	Yes
Bernard and Gouzé (1995-2002)	U, ND, A	NL	ES, s	Yes
Broucke (1998)	U,–,SA	NL	S, d	No
Caines *et al.* (1998-1999)	U, ND, A	NL	S,–	No
Stursberg *et al.* (2000)	T, ND, A	NL	S, s	Yes
Alur *et al.* (2000)	–, –, SA	L	–, –	No
Lefebvre *et al.* (2002)	U, –, A	LS, LC	S, d	Yes

Table 2.1: Qualitative comparison of existing approaches (A: abstraction; D: deterministic transition structure; d: dynamic partition; ES: extended-space partition; IO: input-output space partition; L: linear systems; LC: linear and continuous systems; LD: linear and discrete-time systems; LS: linear and switched systems; ND: nondeterministic transition structure; NL: nonlinear systems; s: static partition; S: state-space partition; SA: s-abstraction; T: timed transition structure; U: untimed transition structure)

Abstractions of continuous dynamics are usually obtained by first partitioning a signal space, such as the state space (S), the input-ouput space (IO), or an extended state-space (ES). Moreover, the partitioning technique is classified as dynamic (d) (resp., static (s)) if it is (resp., is not) a model-based approach. For instance, all partitions performed with a rectangular grid (or induced by quantizers) are static whereas all partitions based on some dynamical features of the model are dynamic. The third column of Table 2.1 summarizes the characteristics of the various types of partitions encountered. Finally the last column in Table 2.1 indicates whether there

exists a technique (either an algorithm or a detailed procedure) for obtaining the partition and the abstraction or s-abstraction.

2.3 Discussion

As seen in the last section there are very few connections between all references cited previously and a definite line of thought is far from apparent. This section is meant to propose research guidelines based on existing techniques.

The physical systems mentioned in Chapter 1 (two-tank and oilsand extraction), like many other systems, inherently possess nonlinear dynamics. Therefore, one would benefit from an abstraction technique that is suitable for this class of systems. Moreover, the steering car example in (Nijmeijer and van der Schaft, 1990) shows that linearization can destroy (continuous) controllability. Therefore an abstraction based on a linearized model may show fewer control capabilities than its original nonlinear form. This is an incentive for considering approaches that apply to nonlinear models.

Among the aforementioned approaches those specific to linear models, i.e., (Lunze *et al.*, 1999; Raisch, 2000; Alur *et al.*, 2000; Lefebvre *et al.*, 2002) are difficult to extend to nonlinear dynamics for various reasons. Whereas the work of (Broucke, 1998; Caines and Lemch, 1998) applies to nonlinear dynamics, the authors do not suggest any technique for obtaining an abstraction or s-abstraction. Also the class of systems defined in (Kokar, 1995) is considered to be restrictive because it requires a closed-form solution, the exact knowledge of initial conditions, and a single-output variable. The remaining techniques that are applicable to nonlinear dynamical systems are those proposed in (Zhao, 1994; Stiver *et al.*, 2001; Stursberg *et al.*, 2000; Bernard and Gouzé, 2002) where only the last two generate abstractions. Therefore, there exists very few specification-independent techniques for abstracting systems with nonlinear dynamics, in general.

The process for abstracting continuous systems can take different forms and target distinct objectives. For instance, an abstraction mapping for continuous systems is introduced in (Kokar, 1995) where the author defines the mapping through the partitioning of various signal spaces. An alternative approach to abstraction mappings amounts to defining an equivalence relation based on languages or trajectories (Broucke, 1998; Alur *et al.*, 2000). Recall that an abstraction is also meant to preserve some property. Among the properties of interest that can be preserved through the abstraction of a continuous system one finds consistency (Kokar, 1995; Caines and Wei, 1998; Stursberg *et al.*, 2000), deterministic behaviour (Lunze *et al.*, 1999), HIBC (Caines and Lemch, 1998), and completeness (Stursberg *et al.*, 2000). Even though various definitions of consistency exist, the weakest notion is a property ensuring that a sequence of transitions in the abstraction has at least one corresponding trajectory in the underlying continuous system. Completeness is the converse of consistency, that is, it ensures that each continuous trajectory is represented by a transition in the abstraction. Indeed, a consistent abstraction does not necessarily capture all trajectories of a continuous system, i.e., it may under-approximate the continuous behaviour. Therefore consistency and completeness are important properties because they enable one to reason about the original system from its abstraction only.

A few observations are worth noting about the technicalities of generating abstractions. First notice that in the work of Lunze the removal of a fixed quantization resulted in a relaxation of conditions to obtain a deterministic automaton. Indeed the necessary and sufficient conditions to have a deterministic automaton for discrete-time models equipped with quantizers are very restrictive. In comparison, the sufficient conditions to obtain a deterministic automaton for a linear continuous system without quantizers are more permissive. Moreover, in (Lefebvre *et al.*, 2002) it is shown that a model-based partitioning provides a more accurate abstraction than a static partitioning, such as those induced by quantizers. This is part of the motivation

20

for exploring the partition techniques based on dynamical invariants similar to the verification approach in (Broucke, 1998; Stiver *et al.*, 2001). Also a transversality condition is often cited as a necessary requirement for abstracting nonlinear continuous systems (Zhao, 1994; Caines and Wei, 1998; Broucke, 1998). Moreover, one must pay attention to the finiteness of computation for constructing abstractions. For example, the accuracy of the abstractions obtained in (Stursberg *et al.*, 2000) increases with the number of initial conditions considered.

In summary, an abstraction technique based on nonlinear models is recommended because (i) it is more accurate than one that refers to the linearized version of the models, and (ii) it applies to a larger class of systems. Since previous results indicate the benefits of dynamical partitions, a partitioning technique using dynamical invariants is favored. At the same time the approach must aim at obtaining, in a finite number of steps, abstractions that are consistent and complete in some sense. Moreover, for such abstractions a characterization of transversality should be performed. In the following chapter, we introduce the necessary material to provide a formal problem definition.

Chapter 3

Theoretical Background

Herein we formalize some of the concepts introduced in the previous chapters. Since the main objective of the thesis is to obtain a finite-state machine (FSM) abstraction of a continuous system, the continuous dynamics of an Hybrid Control System (HCS) are defined first in Section 3.1. This leads to a family of systems called Controlled Switched Systems (CSSs). In Section 3.2 we proceed with a formal characterization of FSM abstractions for CSSs, which is then followed by the formulation of the problem statement. In Section 3.3 we introduce a subclass of systems leading naturally to a partitioning technique, which is a necessary step towards FSM abstractions.

3.1 Continuous Plant Dynamics

The continuous system in an HCS is assumed to be modelled by a set of equations

$$
\begin{aligned}
\dot{x}(t) &= f(x(t), u(t)), \ x(t) \in D \subseteq \mathbb{R}^n, \ u(t) \in U \subset \mathbb{R}^m, \ t \in \mathbb{R}, \\
y(t) &= x(t)
\end{aligned}
\tag{3.1}
$$

where $x(t)$, $u(t)$, and $y(t)$ represent a coordinate function, an input map, and an output function, respectively. In the sequel we refer to x as the *state* variable, to u as

the *input* variable, and to y as the *output* variable (the indication of time t is dropped whenever clear from the context). The set D in (3.1) is assumed to be an open subset of $\mathbb{R}^n$, the n-dimensional Euclidean space, whereas the input space U is assumed to be a nonempty subset of $\mathbb{R}^m$.

A function g defined on an open set A is C^k, i.e., k-differentiable, with $k = 1, 2, \ldots, \infty$, if its partial derivatives of order k exist and are continuous. A C^∞ (or smooth) function g is *analytic* if for each point $p \in A$ and some neighborhood $N \subset A$ of p there exists a convergent power series for all $p' \in N$. The $\mathbb{R}^n$-valued function f, with domain $D \times U$, is referred to as a *vector field*. Throughout the thesis the vector field $f(x, u)$ is assumed to be smooth on its domain $D \times U$.

In the HCS context, the set of input values $\Sigma \subset U$ is assumed to be known *a priori* and taking the form of a finite set of real m-tuples

$$\Sigma := \{\sigma_k := (\sigma_k^1, \ldots, \sigma_k^m)\}_{k \in \mathcal{I}_\Sigma}, \tag{3.2}$$

with $\mathcal{I}_\Sigma \subset \mathbb{N}^+$ the index set for Σ and m the size of the vector of input values. We also assume that the map $u : \mathbb{R}_{\geq 0} \rightarrow \Sigma$ generates piecewise-constant input signals (i.e., u is a piecewise-continuous from the right function). By definition, such an input map is closed under concatenation and therefore it belongs to the class of admissible controls $\mathcal{U}$ (ref. §A.4.1 on page 148). For clarity, the use of piecewise-constant input maps taking value in Σ is emphasized by writing $u(\cdot) \in \mathcal{U}_\Sigma$.

Given a fixed input value $u = \sigma \in \Sigma$, the set of singular points for $f(x, \sigma)$ is defined as

$$\mathcal{S}_\sigma := \{p \in D \mid f(x, \sigma)|_{x=p} = 0\}. \tag{3.3}$$

The set $\mathcal{S}_\sigma$ captures the equilibrium points of $f(x, \sigma)$ in D, i.e., if the system is initialized at $p \in \mathcal{S}_\sigma$ and the input value is σ, then (3.1) has the solution $x(t) = p$ for

all $t \in \mathbb{R}$. If $\sigma = \sigma_k \in \Sigma$ then we denote $\mathcal{S}_{\sigma_k}$ by $\mathcal{S}_k$.

The next step amounts to investigating the nature of the solutions of systems as defined in (3.1) with an input map $u(\cdot) \in \mathcal{U}_\Sigma$. We first consider the case of a fixed input value, prior to extending to a piecewise-constant input signal. The *flow* of the vector field $f(x, u)$ is a mapping $\phi : I \times D \times \Sigma \to D$ satisfying $\phi(t = 0, p, \sigma_k) = p$, for any $p \in D$, $\sigma_k \in \Sigma$, and $\partial\phi(t, x, \sigma_k)/\partial t = f(\phi(t, x, \sigma_k), \sigma_k)$, for each $t \in I \subset \mathbb{R}$ where I is a time interval containing the origin. Therefore the flow of a vector field represents the solution of (3.1) on a time interval given an initial condition and a fixed input value. At this point, we impose a further restriction on the class of input signals $\mathcal{U}_\Sigma$ by requiring that the vector field $f(x, u)$ of (3.1) is *complete*, that is, given any initial condition the solutions of (3.1), with $u(\cdot) \in \mathcal{U}_\Sigma$, are defined over the time interval $I = \mathbb{R}$ (this is a generalization of Definition A.10 provided on page 149). Consequently, the existence (and uniqueness) of a solution on any time interval and in the presence of an input map $u(\cdot) \in \mathcal{U}_\Sigma$ is guaranteed. The following example illustrates that even if a vector field is complete for each input value in Σ (as in Definition A.10), it may not be complete in the above general sense in the presence of a piecewise-constant input signal $u(\cdot) \in \mathcal{U}_\Sigma$, i.e., the existence of a solution on any finite interval is compromised.

Example 3.1 ((Nijmeijer and van der Schaft, 1990)) Consider on $\mathbb{R}^2$ the system

$$
\begin{aligned}
\dot{x}_1 &= (1 + x_2^2)u \\
\dot{x}_2 &= (1 + x_1^2)(1 - u)
\end{aligned}
\tag{3.4}
$$

with input set $\Sigma := \{0, 1\}$. Let the initial value be $(x_1(t = 0), x_2(t = 0)) = (0, 0)$. A

piecewise constant control $u(\cdot) \in \mathcal{U}_\Sigma$ is defined over the time interval $[0, T]$ by

$$u(t) = \begin{cases} 0, & a_n \le t < b_n \\ \\ 1, & b_n \le t < a_{n+1} \end{cases}, \tag{3.5}$$

where

$$b_n = a_n + \frac{1}{1+n^2} \qquad a_{n+1} = b_n + \frac{1}{1+(1+n^2)}, \tag{3.6}$$

with $b_{-1} = 0$, $a_0 = 1$ and such that $lim_{n \to \infty} a_n = T < \infty$. The solution of the system exists over the interval $[0, T)$ but the solution at time T does not exist. In fact, in a finite time u switches infinitely between 0 and 1 while states x_1 and x_2 increase, thus leading to a finite-escape time scenario.●

We now look at the characterization of input signals generated by a map $u(\cdot) \in \mathcal{U}_\Sigma$. Let a *switching time* refer to a time $t \in \mathbb{R}_{\ge 0}$ at which a change of input value occurs, i.e., $u(t^-) \ne u(t)$. Thus a piecewise-constant input signal can be described by a sequence of input values $s := \sigma_1 \cdots \sigma_r \in \Sigma^+$, $r \in \mathbb{N}^+$, where Σ^+ represents the set of all possible sequences of elements of Σ (except for the empty sequence), together with a sequence of switching times $\tau := t_1 \cdots t_r$, such that $u(t) = \sigma_i$ for all $t \in [t_{i-1}, t_i)$ with t_0 the initial time. The lower graph in Figure 3.1 shows an input sequence where at switching times the input value undergoes a change.

Let us now consider cases where sequences of input values are implemented. For this purpose, let the flow induced by a fixed input value $\sigma_k \in \Sigma$ on an interval I be denoted as a mapping $\phi_k : I \times D \to D$. Given some input and time sequences s and τ, let $p_i = \phi_i(t_i - t_{i-1}, p_{i-1})$, $i \in \{1, \ldots, r\}$, $r \in \mathbb{N}^+$, represent the locations in D where the vector field experiences a change of input value, and let $\phi_i^*([t_{i-1}, t_i), p_{i-1}) :=$

$\bigcup_{t \in [0, t_i - t_{i-1})} \phi_i(t, p_{i-1})$ be the trajectory connecting p_{i-1} to p_i under input value σ_i. Thus

a trajectory initiated at a point $p = p_0$ and induced by s and τ consists of the set of points $\Phi^*(p_0 = p, t_0, s, \tau) := \bigcup_{i \in \{1, \ldots, r\}} \phi_i^*([t_{i-1}, t_i), p_{i-1})$. Also, the composition of flows $\Phi(p_0 = p, t_0, s, \tau) := \phi_r(t_r - t_{r-1}, \cdot) \circ \cdots \circ \phi_1(t_1 - t_0, p_0)$ yields p_r, the point reached under s and τ when departing from $p_0 = p$ at t_0. Consequently, the solutions are continuous and continuously differentiable everywhere except at switching times. The top diagram of Figure 3.1 shows a sample trajectory initiated at p and induced by the input sequence illustrated in the lower diagram of Figure 3.1.
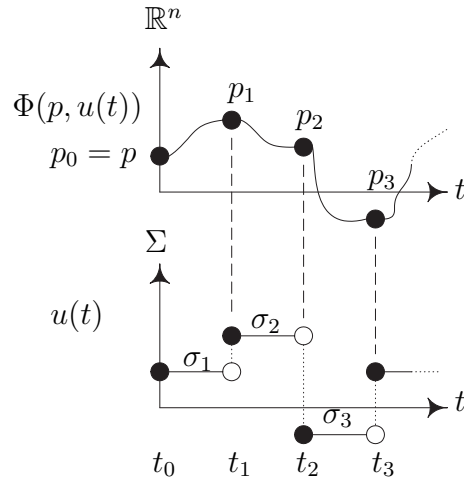
Figure 3.1: A sample input sequence $u(t)$ and its corresponding trajectory

We complete the characterization of the continuous dynamics of an HCS by formalizing the above setup in a definition.

Definition 3.2 (CSS) A system characterized by (3.1) with input map $u(\cdot) \in \mathcal{U}_\Sigma$ and an analytic[1] and complete vector field is said to be a *Controlled Switched System* (or CSS).$\diamond$

In the following section we continue the definition of an HCS by introducing a formal description of a finite-state machine abstraction of a CSS, its state structure and its transition structure.

---

[1] In further results, we identify when the analyticity requirement cannot be dropped.

3.2 Finite-State Machine Abstractions

In the present approach, the state structure of an FSM abstraction is defined through a partitioning of a state-space region of a CSS. The transition structure is then deduced from the partition and the continuous dynamics. For this reason we first present the properties of a partition, followed by a definition of the transition structure of an FSM abstraction. Prior to formulating the problem definition, we investigate some abstraction properties discussed in Chapter 2.

3.2.1 Partitions

Let E be a convex, open, and strict subset of D. A *partition* of E, denoted by π, is a finite collection of non-empty subsets $\{q_i \subseteq E\}_{i \in Q}$ satisfying the conditions

$$(\forall i, j \in Q, i \neq j)\, q_i \cap q_j = \emptyset \tag{3.7}$$

$$E = \bigcup_{i \in Q} q_i, \tag{3.8}$$

where Q is the label set of the q_i's. Namely, a partition is made of mutually disjoint subsets (3.7) which together act as a cover for E (3.8). In the sequel we refer to those q_i's that have a nonempty interior in E as *partition cells* or *cells* for short. In Figure 3.2 a set E (defined by a solid line) and some cells, with label set $\{0, 1, 2, 3, 4, 5\} \subset Q$, are illustrated.

A boundary point p of a cell q_i with $i \in Q$, is a point whose neighborhoods contain a point in q_i and a point in q_i^c, the complement of q_i in D. The *boundary* of a cell q_i consists of the set of all boundary points of q_i and it is denoted by ∂^i. The closure of a cell q_i is defined as $\overline{q}_i := q_i \cup \partial^i$. In the case of Figure 3.2, if each boundary point in E is assigned to a unique cell, then $\{q_0, \ldots, q_5\}$ satisfies (3.7) and (3.8) and thus forms a partition of E. Unless stated otherwise, we assume that a partition is composed of cells only. Given a partition π of E, $\partial \pi := \bigcup_{i \in Q} \partial^i$ represents the set of

cell boundaries of π. In Figure 3.2, $\partial\pi$ corresponds to solid and dashed lines.

Given a partition cell q_i, its neighboring cells are those sharing boundary points with it. Formally the label set of neighboring cells of q_i is defined as

$$N_i := \{i' \in Q \setminus \{i\} \mid \partial^i \cap \partial^{i'} \neq \emptyset\} \subset Q. \tag{3.9}$$

For instance, in Figure 3.2 the cells neighboring q_0 are those given by the label set $N_0 := \{1, 2, 5\}$.
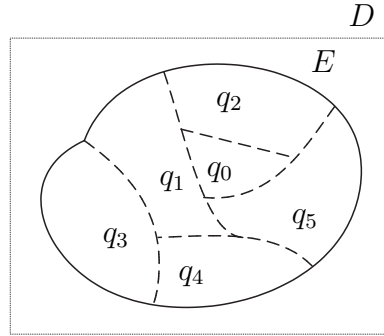
Figure 3.2: A set E and some partition cells

3.2.2 Abstractions of Controlled Switched Systems

A finite-state machine is a triple (Q, Σ, δ) where Q, Σ, and δ represent the finite set of discrete states, the alphabet, and the transition map, respectively. In contrast to an FSM, an FSM abstraction $\mathcal{A} := (Q, \Sigma, \delta)$ has its state set Q defined by a partition and its transition map δ determined by the partition, an underlying continuous system, and the event set Σ. That is, a partition π of $E \subset D$, a subset of the state space of a CSS, provides the state structure of the FSM abstraction. Thus a state $i \in Q$ of an FSM abstraction relates to a subset $q_i \subseteq E$ of the state space. In the case of a CSS, the FSM abstraction alphabet Σ coincides with the set of input values that are fed to the continuous system (ref. equation (3.2) on page 23).

An FSM transition map provides the state transitions under some input values. A generic description of this partial function[2] is given by $\delta : \Sigma \times Q \to 2^Q$, with 2^Q representing the set of all possible subsets of Q. Given an input value $\sigma_k \in \Sigma$ and a state $i \in Q$, if $\delta(\sigma_k, i) \neq \emptyset$ and $\#\delta(\sigma_k, i) = 1$, with $\#A$ representing the cardinality of set A, then $\delta(\sigma_k, i)$, the transition from state i under the input value σ_k, is said to be *deterministic*. By extension, an FSM transition structure is deterministic if all transitions are deterministic.

Let CSS_E^π denote a CSS defined on D and with a region $E \subset D$ partitioned by π. Then an FSM abstraction for such a CSS is defined as follows.

Definition 3.3 (FSM abstraction of a CSS_E^π) Consider a CSS_E^π whose partition results in a state set Q. A finite-state machine $\mathcal{A} := (Q, \Sigma, \delta)$ is an *FSM abstraction* of the CSS_E^π if for each pair $i, j \in Q$ and each input value $\sigma_k \in \Sigma$ satisfying $j \in \delta(\sigma_k, i)$,

(i) either $j = i$ and $(\exists p \in q_i) \, \phi_k(t, p) = p$ for all $t \in \mathbb{R}_{\geq 0}$, or $(\exists p \in q_i)$

$\phi_k(\beta T, p) = p$ for $T \in \mathbb{R}_{>0}$, any $\beta \in \mathbb{N}$, and $\phi_k(t, p) \in q_i$ for all $t \in \mathbb{R}_{\geq 0}$,

(3.10)

(ii) or $j \in N_i$ and $(\exists p \in q_i)(\exists p' \in \partial^i \cap \partial^j)(\exists t \in \mathbb{R}_{>0}) \, \phi_k^*([0, t), p) \in q_i$,

$\phi_k(t, p) = p'$, and $\phi_k(t^+, p) \in q_j$. $\qquad \qquad \diamond$

Condition $(3.10)(i)$ stipulates the case where a self-looping transition exists at state i. In particular, a self-loop occurs at state i if the cell q_i contains an equilibrium point or any periodic behaviour (as illustrated in cell q_i of Figure 3.3). Condition $(3.10)(ii)$ indicates that a transition departing from state i and leading to state j under σ_k exists if there is a trajectory initiated in q_i and transiting through a boundary point common to both q_i and q_j before reaching q_j, as shown in Figure 3.3.

---

[2] The function is *partial* since for some states in Q the function may be defined for a subset of Σ only. For instance, at some state $i \in Q$, an event $\sigma \in \Sigma$ may not be practically feasible.
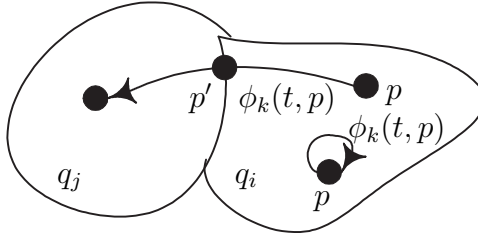
Figure 3.3: Trajectories inducing a discrete transition in an FSM abstraction

A few observations about Definition 3.3 are worth noting. First, condition (3.10)(i) is meant to emphasize the presence of particular behaviour for continuous trajectories in partition cells. A relaxation of condition (3.10)(i) allowing a self-looping transition based on the existence of any trajectory contained in q_i may result in an aggregation of continuous trajectories exhibiting distinct behaviour. Indeed, a self-loop could characterize any trajectory transiting through a cell as well as a trajectory reaching an equilibrium point or a periodic orbit, and thus never leaving the cell. Also, notice that condition (3.10)(ii) enforces a correspondence between a transition and the continuous behaviour that is not one-to-one since a family of trajectories may correspond to a discrete transition. Furthermore note that nondeterministic transitions occur, for instance, when a cell i has points satisfying condition (3.10)(i) and condition (3.10)(ii). Whenever clear from the context we will refer to an FSM abstraction of a CSS_E^τ simply as an FSM abstraction.

Remark 3.4 There are a few distinctions between the FSM abstractions of Definition 3.3 and some discrete-event system (DES) theories (for instance the one developed in (Ramadge and Wonham, 1987)). One notices the absence of ϵ, the "null-event", in the set of allowable sequences. This follows from the fact that, in general, in the continuous-time setup there exists no input value meaning "do nothing". Also, like a continuous system, the FSM abstraction can be initialized in any partition subset of E, which justifies the absence of an initial set Q_0, i.e., $Q_0 = Q$. At this stage,

all events in Σ are controllable, i.e., there are no uncontrollable events. Finally, the self-loops of an FSM abstraction have a precise dynamical meaning.⋄

So far we have provided formal definitions for the continuous dynamics and the FSM abstraction of an HCS. Prior to providing a problem definition, we use the next section to review some abstraction properties presented in Chapter 2.

3.2.3 Abstraction Properties

In this section we discuss three properties that are of interest. These are finiteness, transversality, and consistency.

Finiteness

Any partitioning of a state-space region results in subsets containing an infinite number of points. The *finiteness* property refers to the ability to fully characterize each partition cell by using only a finite number of points. Generally, this is the main challenge in obtaining the transition structure of an FSM abstraction. Indeed, the task must be completed in a finite number of operations despite the presence of an infinite number of points to analyze.

Transversality

Consider a partition π of a state-space region and let ∂ represent a cell boundary. Given a fixed input value $\sigma \in \Sigma$, a continuous trajectory, denoted here as a *c-path*, is characterized by a vector field whose evaluation at a point p, $f(x,\sigma)|_{x=p}$, indicates the local directional rate of change. The vector field $f(x,\sigma)$ is said to be *transversal* to a boundary ∂ at p if

$$N(\partial, x) \cdot f(x,\sigma)|_{x=p} \neq 0, \tag{3.11}$$

31

where $N(\partial, x)|_{x=p}$ stands for the normal to the boundary ∂ evaluated at p, and "$\cdot$" represents the inner product. If condition (3.11) holds for all $p \in \partial$, then we say that the vector field $f(x, \sigma)$ is transversal to ∂. Namely, a vector field is transversal to ∂ if it is nowhere tangent to ∂. In Figure 3.4 a boundary is represented as a line segment where the vector field and the normal are evaluated at two points, p and p'. In this case the vector field is not transversal at point $p' \in \partial$, therefore it is not transversal to ∂.
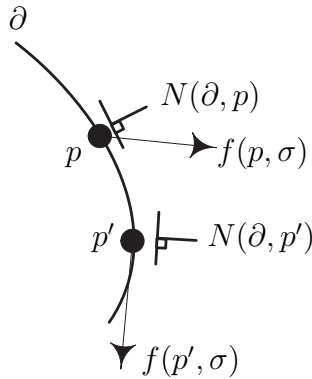
Figure 3.4: A vector field $f(x, \sigma)$ not transversal to a cell boundary ∂

The cell boundaries of an FSM abstraction act as sensors, i.e., the crossing of a boundary signals the traversal from one partition cell to another. Given an arbitrary partition and a boundary ∂, a non-vanishing c-path initiated at a point p and intersecting with ∂ can be: (a) tangent to ∂ at a point only, (b) transversal to ∂ at a point, or (c) "travelling along ∂", i.e., tangent to a connected subset of ∂, as represented in Figure 3.5.

A transversal situation is ideal in the sense that the c-path cuts clearly through a boundary to travel from one cell to another. The other types of c-paths are ambiguous because a small perturbation can lead to different cell-to-cell transitions depending on the direction of the perturbation. Thus transversality is a nice property since it provides a clear delineation of trajectories.
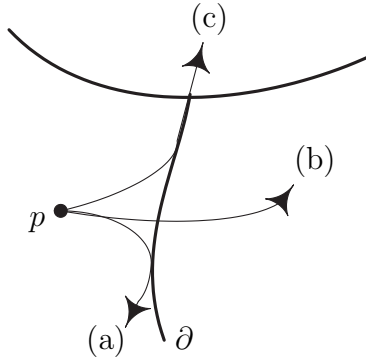
Figure 3.5: Possible intersections between c-paths and a cell boundary ∂

As transversality is a non-generic property of continuous systems with partitioned domains (Branicky *et al.*, 1998), one can either analyze where condition (3.11) holds or impose sufficient conditions enforcing it. For an arbitrary partition, the first approach possibly requires the computation of an infinite number of trajectories with distinct initial conditions thus leading to the finiteness phenomenon. In (Caines and Wei, 1998), the second approach is taken. It leads to sufficient conditions originating from controllability properties of the continuous system and the FSM abstraction. Both sufficient conditions rely on the class of admissible controls.

Deterministic Behaviour and Consistency

Usually one develops or classifies abstractions according to a property of interest. For instance, a correspondence between the abstracted and the original system based on a controllability property is developed in (Caines and Lemch, 1998). A different type of correspondence can be established by looking at the existence of c-paths, versus that of discrete paths, or *d-paths*, standing for discrete transitions of the FSM abstraction. As shown below, it turns out that such a correspondence has connections with the notions of deterministic transition structure, HIBC (Caines and Wei, 1998), and consistency.

Let a *simple d-path* be a sequence $i - \sigma - i'$, which translates a transition from a

state i to a neighbor state i' under an input value σ, that is $i \xrightarrow{\sigma} i'$. From an FSM abstraction point of view, the transition represented by a simple d-path $i - \sigma - i'$ exists if there is at least one c-path, induced by σ, initiated at some point p in the cell q_i, and connecting to some other point p' that belongs to cell $q_{i'}$. The bottom portion of Figure 3.6 represents three cells q_i, q_j, and q_k where two c-paths are illustrated by solid lines with an arrowhead. A c-path initiated at a point $p \in q_i$ and induced by input value σ_a leads to a point p' in the cell q_j. At the abstraction level the points of a cell are lumped and identified with a single discrete state (here we identify cell q_i with state i, cell q_j with state j, and so on). Consequently the previous c-path connecting q_i to q_j results in a simple d-path $i - \sigma_a - j$ whose corresponding transition is illustrated by the leftmost directed graph in the middle of Figure 3.6.
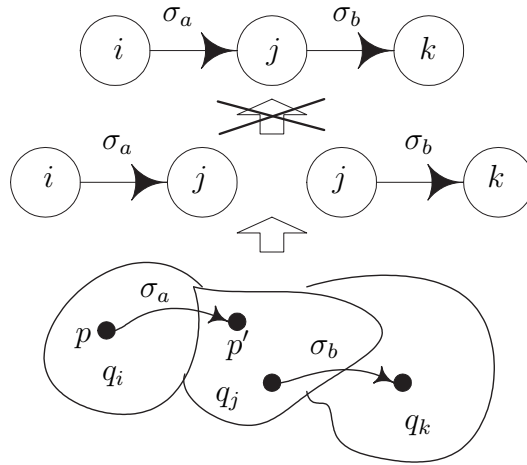
Figure 3.6: Example of a non-transitive general d-path

Whenever an FSM abstraction is used in an HCS setup, the abstraction serves as the base model to synthesize the controller which outputs a control sequence to the continuous system. The implementation of such a control sequence requires a correspondence between d-paths and c-paths. For this correspondence one needs to look at *general d-paths*, which are sequences of at least two consecutive simple d-paths.

The two simple d-paths $i-\sigma_a-j$ and $j-\sigma_b-k$, whose transitions are represented in the middle of Figure 3.6, is an example of a general d-path, which we write in a compact form as $i-\sigma_a-j-\sigma_b-k$. A general d-path is said to be *transitive* if there exists a c-path corresponding to the transitions captured by the general d-path. Unfortunately, the presence of two (or more) consecutive simple d-paths (see bottom directed graphs of Figure 3.6) does not necessarily imply the existence of a corresponding c-path (top directed graph of Figure 3.6). For instance, the two points (black dots) in q_j that induce transitions captured by the distinct single d-paths may not coincide. More generally, a c-path connecting those two points does not necessarily exist. Therefore, an additional condition is needed to ensure that general d-paths are transitive.

One sufficient condition for the transitivity of general d-paths is that for any input value all points of a cell visit only one neighboring cell. This condition implies a deterministic transition structure which almost certainly will not hold in the presence of dynamical singularities. Another sufficient condition is that for any two points of a cell, there exists a control sequence such that any point is reachable from the other. This corresponds exactly to the HIBC property (Caines and Wei, 1998) for which no partitioning technique is provided. Not surprisingly there exist continuous systems whose abstraction may have a deterministic transition structure without satisfying the HIBC property. An instance of such a system is the double-integrator controlled by piecewise-constant input signals in (Raisch, 1995). This example is considered later in order to explore the correspondence between d-paths and c-paths.

In comparison to existing notions of consistency, the transitivity of general d-paths is equivalent to the concept of r-consistency (with $r \to \infty$) developed in (Stursberg *et al.*, 2000), whereas it is weaker than the dynamical consistency defined in (Caines and Wei, 1998). Note that in the absence of dynamical singularities, a deterministic transition behaviour also implies dynamical consistency. A direct comparison with the consistency notion introduced in (Kokar, 1995) cannot be performed since it requires

an exact knowledge of initial conditions, which is usually lost due to the partition.

As seen above, consistency and transitivity of general d-paths are important properties because they allow one to focus on the transitions of FSM abstractions without worrying about the existence of corresponding c-paths. Conversely, the notion of completeness discussed in Chapter 2 ensures that each continuous trajectory is represented by a transition in the abstraction. In the next section we provide concepts of consistency and completeness tailored to FSM abstractions of CSSs.

3.2.4   Problem Statement

Consider an FSM abstraction of a CSS_E^π as in Definition 3.3 (page 29) that generates transitions resulting in a d-path $g := i_0 - \sigma_1 - i_1 \cdots i_{r-1} - \sigma_r - i_r$ with $r \geq 1$. A trajectory of the CSS_E^π and a d-path g are said to *coexist* if the cells intersecting with the trajectory correspond to the cells associated with the states of the d-path g. We now introduce notions of consistency and completeness tailored to an FSM abstraction and a CSS_E^π.

Definition 3.5 (Consistency) A CSS_E^π and an FSM abstraction of the CSS_E^π are *consistent* if for any d-path generated by the abstraction, there is a continuous trajectory induced by the CSS_E^π that coexists with the d-path.⋄

Definition 3.6 (Completeness) A CSS_E^π and an FSM abstraction of the CSS_E^π are *complete* if for each continuous trajectory induced by the CSS_E^π, there is a d-path generated by the abstraction that coexists with the trajectory.⋄

On one hand, an FSM abstraction as in Definition 3.3 is rarely complete in the sense of Definition 3.6. This follows from the fact that there may be no self-looping transition capturing those trajectories contained in each partition cell. Therefore the failure to satisfy the completeness property is inherent to our Definition 3.3. On the other hand, an FSM abstraction as in Definition 3.3 may not be consistent. For

instance, consider a subset of an FSM abstraction composed of two states $i, i' \in Q$ where an event σ leads to a self-loop transition at state i and also to a transition from state i to state i', as shown in Figure 3.7. The self-loop transition indicates the existence of a continuous behaviour that can remain forever in the cell q_i. Moreover the subset of the FSM abstraction provided in Figure 3.7 can presumably generate transitions resulting in the following d-path $i - \sigma - i - \sigma - i \cdots i - \sigma - i'$. That is, a large number of σ's may induce self-looping transitions while the last event σ leads to state i'. However any trajectory in q_i could have reached a singularity before the last event σ occurs. In this case, the last event σ could not induce a trajectory leading to cell $q_{i'}$, and consequently the FSM abstraction and the CSS would not be consistent.
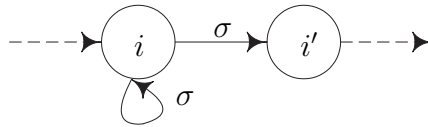
Figure 3.7: A subset of an FSM abstraction

A possible solution to circumvent the above difficulties could be to add to each transition a time range indicating the time period during which the transition is likely to occur. However in the context of partitions based on dynamical invariants, timing information is not readily available.

We denote the directed graph of Figure 3.7 as a *singularity* and the pair of state and event (i, σ) as a *singular pair*. Since the consistency property may fail in the presence of a singularity, we propose to satisfy the consistency property in a weaker sense, i.e., for a subset of general d-paths only. For this reason, we denote the general d-paths that do not contain any singular pair as *nonsingular d-paths*.

The previous definitions are now utilized in order to formulate the problem statement:

Given a CSS_E^π, determine the conditions under which an FSM abstraction of the CSS_E^π can be obtained in finite time, and such that the FSM abstraction and the CSS_E^π are consistent (ref. Definition 3.5) with respect to nonsingular d-paths.

The material to follow provides an answer to the above problem for a class of nonlinear continuous systems.

3.3   Toward an FSM Abstraction

Now that the HCS dynamical models (original and abstract) have been defined, one can begin to relate the continuous system to an FSM abstraction. Before entering into technical details we briefly summarize the present approach. First recall that the overall abstraction procedure is achieved in two steps comprising (i) the construction of a partition of a state-space region, and (ii) the analysis of the continuous trajectories of the underlying system with respect to the partition, resulting in the abstraction transition structure. The second step remains by far the main challenge for the construction of FSM abstractions. In this section we focus on the first step and provide a partitioning technique.

As shown in the literature review, the above abstraction steps (i) and (ii) are usually independent (except for a few techniques generating s-abstractions). A feature of the actual technique is that the two steps are made dependent, i.e., the partition is defined by surfaces that have a dynamical meaning. Indeed in Section 3.3.1 we introduce a subcategory of CSSs for which such surfaces exist. This requires an extension of the notion of integrability for dynamical systems. Then in Section 3.3.2 a partitioning technique using those dynamical surfaces is provided. The double-integrator system serves as an example to illustrate the approach.

3.3.1 A Subclass of Controlled Switched Systems

This section begins by providing some preliminary notions about first integrals and integrable systems. It is followed by an introduction to a notion of integrability tailored to the class of Controlled Switched Systems. This property is instrumental for the partitioning technique that follows since it provides the surfaces used to decompose a state-space region of a CSS. The reader is referred to Section A.5 (see page 149) for some basic notions from exterior calculus.

Definition 3.7 (First Integral) Let f be a vector field with domain $D \subset \mathbb{R}^n$. A C^k ($k \geq 1$) real-valued function $\gamma : D' \to \mathbb{R}$ defined on D', an open subset of D, is said to be a *time-independent C^k first integral* (or *first integral* for short) for the vector field f on D' if it satisfies

$$d\gamma(x) \cdot f(x)|_{x=p} = 0, \text{ for all } p \in D', \tag{3.12}$$

where $d\gamma := [\partial\gamma/\partial x_1, \ldots, \partial\gamma/\partial x_n].\diamond$

In general, there exists no procedure for extracting the first integrals of a nonlinear continuous system (Goriely, 2001). As illustrated by Figure 3.8, a geometrical interpretation of a first integral is a function with a preimage to which f is tangent. Other common names for first integrals include *conserved quantities*, *constants of motion*, *(dynamical) invariants*, and *potential functions*. A trivial or constant first integral is such that $d\gamma(x)|_{x=p} = 0$ for all $p \in D'$.

Throughout this section we adapt some notions related to first integrals to the class of CSSs. The first extension consists of the presence of the input variable u in the first integrals. Indeed for vector fields with an input argument u, a first integral has the additional requirement of being defined for all possible input values $u = \sigma \in \mathbb{R}^m$, thus leading to the mapping $\gamma : D' \times \Sigma \subset \mathbb{R}^m \to \mathbb{R}$. With this condition, the following
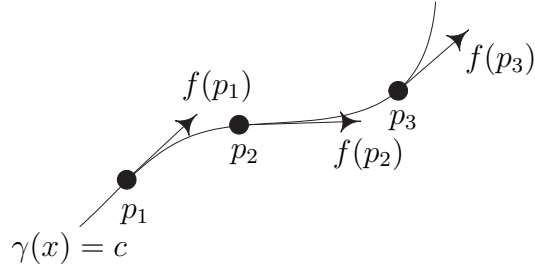
Figure 3.8: A first integral γ for a vector field f

development is independent of the input value set Σ defined in (3.2). Throughout the thesis, a "first integral" means a non-trivial first integral that is analytic on its domain. Whenever it is appropriate, we identify the necessity of the analyticity condition for first integrals.

A notion closely related to first integrals is that of "integrability". Various definitions of the notion of integrability exist and a discussion about them can be found in (Grammaticos and Ramani, 1996; Goriely, 2001). However, in the context of dynamical systems such as in (3.1), integrability usually refers to the solvability of the set of ODEs. A stronger notion, that of "complete integrability", requires a sufficient number of independent first integrals (see Definition A.11 on page 149). The precise meaning of "sufficient" depends upon the class of systems under study, i.e., nonlinear systems, Hamiltonian systems, etc. For general nonlinear systems, such as CSSs , complete integrability requires $n-1$ first integrals. As shown below, the Frobenius' Theorem provides necessary and sufficient conditions for the complete integrability of $r \in \mathbb{N}^+$ one-forms in a local sense, i.e., for some open subset of D.

Theorem 3.8 (Frobenius (Edelen, 1985))

Let C_r be a collection of r independent 1-forms $\{\omega_a(x), a = 1, \ldots, r\}$ defined on D', an open subset of D. The collection C_r is completely integrable over D', if and only if

$$\omega_1(x) \wedge \cdots \wedge \omega_r(x) \wedge d\omega_j(x)|_{x=p} = 0, \tag{3.13}$$

40

for all $j \in \{1, \ldots, r\}$ and $p \in D'$.$\diamond$

The above theorem stipulates that complete integrability is equivalent to saying that over D' each differential $d\omega_j$ can be expressed in terms of elements in the collection C_r. A geometric interpretation of complete integrability is provided later. A consequence of Theorem 3.8 in the presence of $r = n - 1$ first integrals is summarized as follows.

Corollary 3.9

Given a fixed $u = \sigma \in \Sigma$ and a vector field $f(x, u)$, assume that there exist $n - 1$ first integrals $\gamma_j(x, \sigma)$, $j \in \{1, \ldots, n-1\}$, defined on $D' \subset D$. Let C_{n-1} be composed of the one-forms $\omega_j(x, \sigma) = d\gamma_j(x, \sigma)$. The collection C_{n-1} is completely integrable over D' if the following linear independence condition holds

$$\omega_1(x, \sigma) \wedge \cdots \wedge \omega_{n-1}(x, \sigma)|_{x=p} \neq 0, \tag{3.14}$$

for all $p \in D'$.$\diamond$

Therefore a sufficient condition for the complete integrability of $n - 1$ one-forms $\omega_j(x, \sigma) = d\gamma_j(x, \sigma)$ is their linear independence. This follows from the number of first integrals and the closure of their differentials, which by definition satisfies (3.13) automatically (ref. §A.5 on page 149).

Complete integrability is a non-generic property of nonlinear continuous systems. Therefore a legitimate question is: *Why bother to study such systems?* Mainly, complete integrability allows one to characterize the behaviour of a continuous dynamical system without solving explicitly the original set of ODEs. Consequently, integrable systems are "nice" in the sense that their first integrals provide information about the dynamics. Furthermore this feature may enable the construction of Lyapunov functions (see Chetaev's method in (Rouche *et al.*, 1977)), and it may also lead to some stability results (Aeyels and Sepulchre, 1992; Salvadori and Visentin, 1999).

The next example shows the impact of input values on the complete integrability of first integrals for the class of CSSs and, it also provides a geometric interpretation of Theorem 3.8.

Example 3.10 (Triple-integrator) Consider the triple-integrator modeled by $\dot{x}_1 = x_2, \dot{x}_2 = x_3, \dot{x}_3 = u$ and defined over $D = \mathbb{R}^3$ with $u = \sigma \in \Sigma := \{0, a\}$ where $a \in \mathbb{R} \setminus \{0\}$. For $D' = D$, a set of first integrals is $\gamma_1(x, \sigma) = x_1 \sigma^2 - x_2 x_3 \sigma + x_3^3/3$ and $\gamma_2(x, \sigma) = x_2 \sigma - \frac{1}{2} x_3^2$. Let $\omega_1(x, \sigma) = d\gamma_1(x, \sigma)$ and $\omega_2(x, \sigma) = d\gamma_2(x, \sigma)$. If $\sigma = 0$ (resp., $\sigma = a$) then $\omega_1(x, \sigma) \wedge \omega_2(x, \sigma) = 0$ (resp., $\neq 0$) for all $p \in D'$ and the system fails to satisfy (resp., satisfies) condition (3.14) everywhere. Thus any input value $\sigma \neq 0$ leads to complete integrability which, in turn, allows the reconstruction of the trajectory space (a one-dimensional object) from the level surfaces corresponding to $\gamma_1(x, \sigma)$ and $\gamma_2(x, \sigma)$. This is illustrated in Figure 3.9(a) where two surfaces induced by $\gamma_1(x, \sigma)$ and $\gamma_2(x, \sigma)$ have distinct gray tone and where a trajectory initialized at the intersection of those surfaces is represented by a line with an arrowhead. For $\sigma = 0$, the surfaces reduce to planes in $x_1 - x_2$ such that our knowledge of the system trajectories (which are trivial) is that they live on a two-dimensional subspace of $\mathbb{R}^3$ (Figure 3.9(b)).●

The previous example demonstrates that the presence of the input argument u distorts the independence condition (3.14) between first integrals. Therefore, a notion of independence between a collection of first integrals with input values is required. For this one needs the $n + m$ dimensional space $D' \times (\sigma - \epsilon, \sigma + \epsilon)$ where $\sigma \in \Sigma$ and $(\sigma - \epsilon, \sigma + \epsilon) := (\sigma^1 - \epsilon, \sigma^1 + \epsilon) \times \ldots \times (\sigma^m - \epsilon, \sigma^m + \epsilon)$ with a small value $\epsilon \in \mathbb{R}_{>0}$. By definition, the first integrals exist for any value $\sigma' \in (\sigma - \epsilon, \sigma + \epsilon) \subset \mathbb{R}^m$, leading to the following notion of integrability.

Definition 3.11 (Near Integrability) A CSS with $n - 1$ first integrals $\gamma_j(x, u)$, $j \in \{1, \ldots, n-1\}$, is said to be *nearly integrable* over D' if for any fixed input value

(a) Case with $\sigma \neq 0$. (b) Case with $\sigma = 0$.
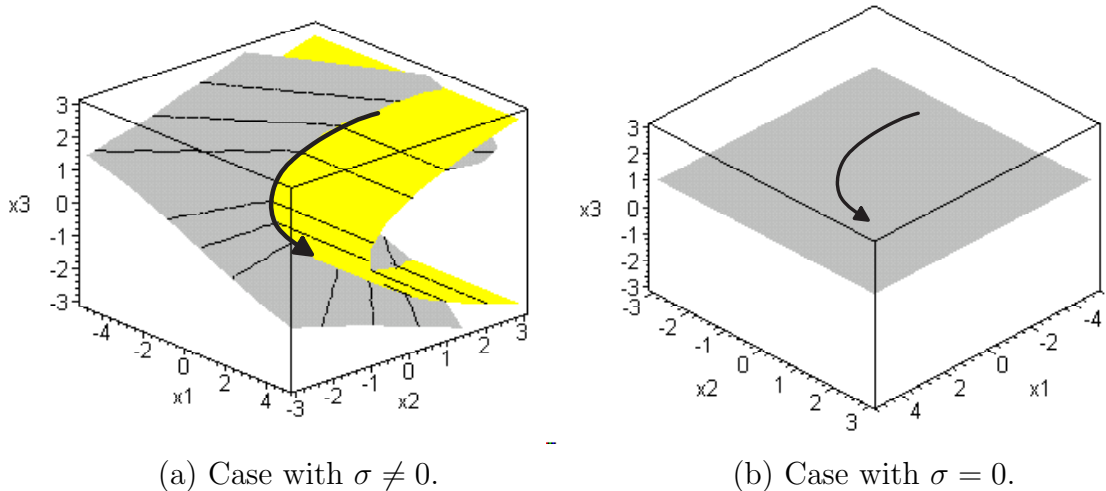
Figure 3.9: Geometric interpretation of complete integrability for Example 3.10

$u = \sigma \in \Sigma$ the independence condition (3.14) holds on an open and dense subset of $D' \times (\sigma - \epsilon, \sigma + \epsilon)$.$\diamond$

The preceding definition serves two purposes: (i) it removes sets of first integrals with differentials that are everywhere dependent on D' for any input value and, (ii) it enlarges the set of admissible inputs by allowing the violation of condition (3.14) for some values in $\mathbb{R}^m$. In order to illustrate point (i), consider a system defined over $D' \subset \mathbb{R}^3$ with two first integrals whose differentials satisfy $\omega_2(x, u) = \lambda \omega_1(x, u)$ for $\lambda \in \mathbb{R}$ and $u = \sigma \in \Sigma$. This system is not nearly integrable because $\omega_1(x, \sigma') \wedge \omega_2(x, \sigma')|_{x=p} = 0$ for all $p \in D'$ and any $\sigma' \in (\sigma - \epsilon, \sigma + \epsilon)$. Example 3.10 illustrates point (ii) because even with $\sigma = 0$ any small perturbation to σ is such that condition (3.14) holds on an open and dense subset (ref. §A.2.1 on page 145) of $D' \times (\sigma - \epsilon, \sigma + \epsilon)$. Given an input value $\sigma \in \Sigma$, we denote by G_σ the open and dense subset of $D' \times (\sigma - \epsilon, \sigma + \epsilon)$ satisfying the condition of Definition 3.11. For Example 3.10 the set G_σ with $\sigma = 0$ is represented as a hatched region in Figure 3.10, i.e., $G_\sigma := D' \times (-\epsilon, \epsilon) \setminus D' \times \{0\}$.

In the remainder of this section we identify some useful properties of nearly integrable CSSs. By definition, a nearly integrable CSS is such that each input value

43
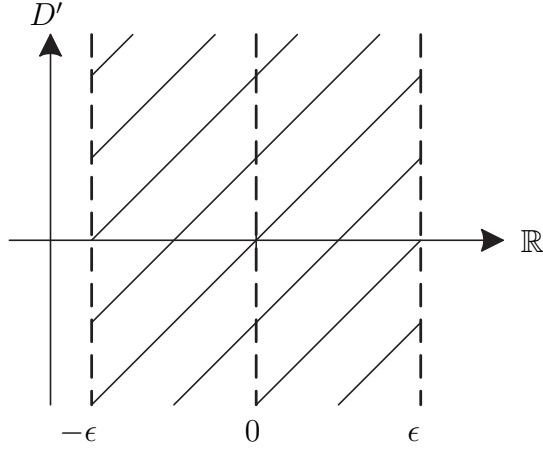
Figure 3.10: A representation of G_σ with $\sigma = 0$ for Example 3.10

$u = \sigma_k \in \Sigma$ induces a collection of $n - 1$ first integrals $\Gamma^k := \left\{ \gamma_1^k, \, \ldots, \gamma_{n-1}^k \right\}$ defined over D', where γ_j^k, $j \in \{1, \, \ldots, n-1\}$, is a compact representation for $\gamma_j(\cdot, \sigma_k)$. Consequently, one associates to Σ the set of first integrals

$$\Gamma := \{\Gamma^k \mid k \in \mathcal{I}_\Sigma\}, \tag{3.15}$$

composed of $(n - 1) \times (\#\Sigma)$ first integrals, where $\#\Sigma$ denotes the number of input values in Σ.

Let a point in $D' \times (\sigma - \epsilon, \sigma + \epsilon)$ be denoted by $h = (p', \sigma')$ where $p' \in D'$ and $\sigma' \in I_\sigma := (\sigma - \epsilon, \sigma + \epsilon)$. Given an input value $\sigma_a \in I_\sigma$, the projection over D' of the set of points in G_σ with coordinate σ_a is defined as

$$D'_{\sigma_a} := \{p' \in D' \mid h = (p', \sigma_a) \in G_\sigma\}. \tag{3.16}$$

This leads to the next result.

Proposition 3.12

Consider a nearly integrable CSS and an input value $\sigma \in \Sigma$. Let G_σ be the open and dense subset of $D' \times I_\sigma$ where condition (3.14) holds. Then there exists an input

value $\sigma_a \in I_\sigma$ such that D'_{σ_a} is nonempty and open in D'.⋄

Proof: Let $\sigma_b \in I_\sigma$ be an arbitrary input value. Then one of two cases is possible: (i) $D'_{\sigma_b} = \emptyset$ or, (ii) $D'_{\sigma_b} \neq \emptyset$. If case (i) holds then for any $h = (p', \sigma_b) \in D' \times I_\sigma$ it follows that $h \notin G_\sigma$. As G_σ is dense in $D' \times I_\sigma$ any neighborhood of h, N_h, is such that $N_h \cap G_\sigma \neq \emptyset$. Thus there exists in N_h some location $h' = (p'', \sigma'')$ such that $h' \in G_\sigma$. If we take σ_a as σ'' then one gets that $p'' \in D'_{\sigma_a}$, leading to case (ii).

Now assume that case (ii) holds and let $p \in D'_{\sigma_b}$ be an arbitrary point. Thus there is a point $h = (p, \sigma_b)$ belonging to G_{σ_b}. Since G_{σ_b} is open there exists an open neighborhood of h, say N_h, that is contained in G_{σ_b}. The topology on $D' \times I_\sigma$ implies that the set N_h contains a rectangular neighborhood of h whose projection over D' results into a set $(p_1 - \delta_1, p_1 + \delta_1) \times \cdots \times (p_n - \delta_n, p_n + \delta_n)$ where $\delta_1, \ldots, \delta_n \in \mathbb{R}_{>0}$. Therefore there is an open neighborhood of p in D'. Since this holds for any point in D'_{σ_b}, by taking the union of all such open sets one proves that D'_{σ_b} is an open set.□

Remark 3.13 In the presence of a connected set D' and analytic first integrals, one can show that D'_{σ_a} of Proposition 3.12 is also dense in D'. This follows from results on analytic (co)distributions (see §A.2.2 on page 145).⋄

From Proposition 3.12 a nearly integrable CSS is "near to complete integrability" in the sense that for each $\sigma_k \in \Sigma$ there exists an approximate input value $\sigma'_k \approx \sigma_k$ for which condition (3.14) is satisfied on an open subset of D'. In order to consider all input values in Σ we define the set

$$D'' := \bigcap_{k \in \mathcal{I}_\Sigma} D'_{\sigma'_k} \subseteq D', \tag{3.17}$$

where $D'_{\sigma'_k}$ represents the set of Proposition 3.12 characterized by the approximate input value σ'_k. Therefore D'' consists of the subset of D' where condition (3.14) holds for the input value set $\Sigma' := \bigcup_{k \in \mathcal{I}_\Sigma} \sigma'_k$. Whenever $\Sigma' \neq \Sigma$, the nearly integrable

CSS using Σ' instead of Σ is called an approximation. The next result provides some characteristics of the set D'', especially if the conditions in Remark 3.13 are satisfied.

Proposition 3.14

Let $A_1, A_2, \ldots, A_k$ be a finite collection of open and dense subsets of D'. Then $\bigcap_{i=1}^{k} A_i$ forms an open and dense subset of D'.$\diamond$

Proof: Initially we prove the claim for two sets of the collection A_a and A_b with $1 \leq a, b \leq k$. We first show by contradiction that $A_a \cap A_b \neq \emptyset$ holds. Assume that $A_a \cap A_b = \emptyset$, i.e., A_a and A_b are disjoint sets. Consequently any neighborhood $N \subset A_a$ of a point in A_a satisfies $N \cap A_b = \emptyset$. However this contradicts the fact that A_b is dense in D', therefore $A_a \cap A_b \neq \emptyset$ is true. The openness of $A_a \cap A_b$ follows from that of A_a and A_b.

Then we show that $A_a \cap A_b$ is dense in D'. If $p \in D'$ is such that $p \notin A_a \cap A_b$ then one needs to show that for any neighborhood of p, $N_p \subset D'$, one has $N_p \cap (A_a \cap A_b) \neq \emptyset$. Assume that there exists a neighborhood $N_p \subset D'$ such that $N_p \cap (A_a \cap A_b) = \emptyset$. One has that $N^* := N_p \cap A_a$ is nonempty since A_a is dense in D', and moreover N^* is open since both N_p and A_a are open. However by assumption one gets $N^* \cap A_b = N_p \cap A_a \cap A_b = \emptyset$, i.e., A_b and an open subset of D' do not have any common point. This contradicts the fact that A_b is dense in D', thus proving that $A_a \cap A_b$ is dense in D'.

Since the collection $\{A_1, A_2, \ldots, A_k\}$ is finite one can proceed as above to show that the intersection $\bigcap_{i=1}^{k} A_i$ leads to an open and dense subset of D'.$\square$

We conclude this section by defining a family of CSSs for which there exists a common subset of D' where complete integrability holds for all values in Σ'.

Definition 3.15 (ICSS) A Controlled Switched System that is nearly integrable over D' and such that $D'' \neq \emptyset$ is an *Integrable Controlled Switched System* (or ICSS).$\diamond$

The advantages of dealing with an ICSS, instead of a nearly integrable CSS, will become clearer in the next section and the next chapter. An instance of an ICSS consists of the system of Example 3.10 where $D'' = D'$.

In summary we have extended the notion of first integrals for the class of CSSs. Furthermore a concept of integrability for such first integrals was developed. More precisely this is an independence condition for first integrals with input arguments. The above development characterized the family of nearly integrable CSSs, which under an additional condition leads to the class of integrable CSSs.

3.3.2   Dynamical Partitions

In the previous section we defined a class of CSSs possessing a set of first integrals Γ that takes into account all input values in Σ. This section shows how elements in Γ can be used to partition the state-space region of a nearly integrable CSS in order to obtain the state structure of an FSM abstraction. However, prior to this we introduce the notion of a dynamical partition.

A *dynamical partition* is a special type of partition (ref. equations (3.7) and (3.8) on page 27) where the sets are defined by the vector field of a dynamical system. Another category of partitions consists of a *foliation*, which is a partition with connected subsets possessing a particular local parameterization (Abraham *et al.*, 1988). For the n-dimensional Euclidean space $\mathbb{R}^n$, a trivial k-dimensional foliation, $0 < k < n$, is

$$\mathbb{R}^n = \bigcup_{(p_{k+1},\ldots,p_n)\in\mathbb{R}^{n-k}} \mathbb{R}^k \times (x_{k+1} = p_{k+1},\ldots,x_n = p_n), \qquad (3.18)$$

for some constants $p_{k+1},\ldots,p_n \in \mathbb{R}$. Moreover a foliation may turn out to be a dynamical partition. Indeed, in the presence of a vector field $f(x,u)$ a sufficient condition for the existence of a local foliation for any $p \in O$, with O an open subset

of D', is that $f(x, u)|_{x=p}$ be nonsingular, i.e., $O \cap \mathcal{S}_u = \emptyset$, with $\mathcal{S}_u$ as defined in (3.3). If this condition holds everywhere then one obtains a foliation over D' (Tamura, 1992). In the next example, it is shown that the previous sufficient condition is not necessary for the existence of a local foliation in the presence of a vector field.

Example 3.16 (Two-tank linear model) Consider the two-tank linear system introduced in §1.1.1 with differential equations $\dot{h}_1 = F/A - \beta(h_1 - h_2)/A$, $\dot{h}_2 = \beta(h_1 - h_2)/A$ and with $D := \mathbb{R} \times \mathbb{R}$ and $D' := \mathbb{R}_{\geq 0} \times \mathbb{R}_{\geq 0}$. Assume that the input values are $F = 0$ and $\beta \neq 0$. In this case, the set of singularities for $f((h_1, h_2), (F, \beta))$ is $\mathcal{S}_{(F,\beta)} = \{(h_1, h_2) \mid h_1 - h_2 = 0\}$ as represented in Figure 3.11. With $\sigma = (F, \beta)$ the function $\theta(h_1, h_2) := -1 + h_1 + h_2$ results into a foliation where some of the subsets are shown in Figure 3.11. Also the flow direction under the input value σ is indicated with arrows.●
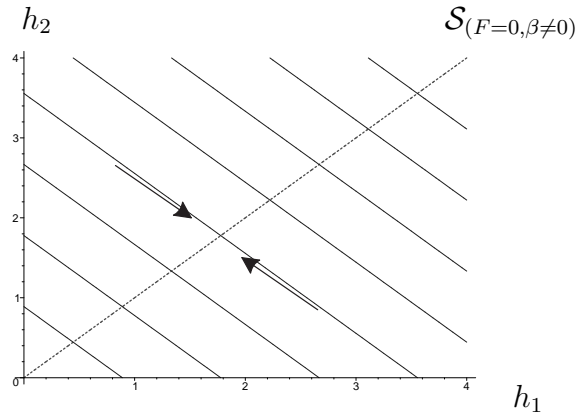
Figure 3.11: A foliation for the two-tank system

In order to explain the foliation of Example 3.16, the concept of submersion is introduced. Let M and N be differentiable manifolds. A smooth mapping $g : M \to N$ with a surjective derivative at p, i.e., with $rank(dg|_p) = dim(T_{g(p)=c}N)$ where $T_c N$ is the tangent space to N at c, is said to be a submersion at p. The mapping g is a *submersion* if it is a submersion for all $p \in M$, otherwise we say that the submersion

is local. Given a local submersion g and a value $c \in \{g(p) \mid p \in M\}$, the preimage of g is the set

$$g^{-1}(c) := \{p \in M \mid g(p) = c\}. \tag{3.19}$$

A point $c \in N$ is a *regular value* of the mapping g if $dg|_p$ is surjective for all values in $g^{-1}(c)$, otherwise c is a *critical value*. The set of regular values for g is denoted by $\mathcal{R}^g$.

Remark 3.17 While the set of critical values live in the range of the mapping g, its dual, the set of *critical points* sits in the domain of g. Namely, a point $p \in M$ is a critical point if $dg|_p$ is not surjective.$\diamond$

The interesting aspect about local submersions is that their preimage may form a submanifold. Indeed, by the Preimage Theorem (see §A.2.4 on page 147), if $c \in \mathcal{R}^g$ then $g^{-1}(c)$ forms a submanifold of M. For instance, in Example 3.16 the mapping θ is a submersion because $d\theta = [1, \; 1]$, thus leading to submanifolds that intersect with the set $\mathcal{S}_{(F=0, \beta \neq 0)}$. Notice that Sard's Theorem (see §A.2.5 on page 147) stipulates that the set of critical values of g has measure zero (ref. §A.2.1 on page 145).

We already have encountered candidate functions for local submersions, namely the collection of first integrals Γ of nearly integrable CSSs defined in (3.15). Notice that a first integral does not necessarily lead to a foliation. For instance, in Example 3.10 (see page 42) the preimages of the first integral γ_2^g with $\sigma = 0$ do not cover the whole of D' since no leaf exists on the plane $\{(x_1, x_2, x_3) \mid x_3 = 0\}$, and thus do not satisfy the property of a foliation. A first integral $\gamma_j^k : D' \to \mathbb{R}$, with $\sigma_k \in \Sigma$ and $j \in \{1, \ldots, n-1\}$, is a real function and its set of regular values, denoted by $\mathcal{R}^{j,k}$, is contained in $\mathbb{R}$. However, by definition $\mathcal{R}^{j,k}$ contains values without preimage in D'. Therefore we denote by $\widetilde{\mathcal{R}}^{j,k}$ the interior of the set of regular values that are in the range of γ_j^k. Given an input value $\sigma_k \in \Sigma$, a first integral $\gamma_j^k \in \Gamma$ defined on D',

and the open set $\widetilde{\mathcal{R}}^{j,k}$, we refer to the set of points

$$L_{j,k}^c := \{p \in D' \mid \gamma_j^k(x)|_{x=p} = c \in \widetilde{\mathcal{R}}^{j,k}\}, \tag{3.20}$$

as a *leaf* and the constant c is called a *first integral constant* (or FIC). As shown previously, a leaf $L_{j,k}^c$ may form a disconnected set in D'. By construction, a leaf is the preimage of a regular value and thus by the Preimage Theorem it qualifies as a submanifold of D'.

Remark 3.18 A benefit of dealing with leaves is that the conditions of the Implicit Function Theorem (see §A.2.3 on page 146) are automatically satisfied, thus ensuring a local characterization of the leaves.⋄

Remark 3.19 It can be shown that there exists no relationship between the existence of local submersions and the set of equilibrium points. Indeed an equilibrium point may or may not belong to a local submersion. Conversely a local submersion does not necessarily exist at some non-equilibrium point.⋄

Remark 3.20 For the special case where $D' \subseteq \mathbb{R}^2$, one notices that the locations where the linear independence condition (3.14) fails coincide with the region where a leaf does not exist. This is not the case in general. Indeed, in Example 3.10, if $u = \sigma = 0$ then $\omega_1(x,\sigma)|_{x=p} = 0$ and $\omega_2(x,\sigma)|_{x=p} = 0$ for $p \in \{(x_1, x_2, x_3 = 0)\}$ only whereas $\omega_1(x,\sigma) \wedge \omega_2(x,\sigma)|_{x=p} = 0$ for any $p \in D'$.⋄

For the remainder of this section, we show how first integrals and their leaves can be used to partition a state-space region of a nearly integrable CSS. The partition is restricted to E, a nonempty convex and open strict subset of $D' \subset D$ and the complement $D' \setminus E$ is lumped into one cell so that any control sequence leading to it is disabled (Hsu, 1987; Lunze *et al.*, 1999). For simplicity, the two-dimensional case is presented because of its reduced number of first integrals, i.e., only one first integral

per input value. In the sequel we keep the subscript j to indicate the impact of the choice of a first integral for higher-dimensional cases.

In order to partition $E \subset D'$ with leaves, the set of first integral constants (FICs) needs to be defined in an appropriate manner.

Definition 3.21 (FIC) Let $E \subset D'$ be a region that is to be partitioned and let $\gamma_j^k \in \Gamma$ be a first integral with input value $\sigma_k \in \Sigma$. The *first integral constants* (FICs) associated with γ_j^k and E take the form of a r-tuple $C_k^r := (c_{k,1}, \ldots c_{k,r})$, $r \in \mathbb{N}^+$, where each $c_{k,v}$, $v \in \{1, \ldots, r\}$, satisfies the following conditions

$$
\begin{aligned}
&\text{(i)} \quad c_{k,v} \in \widetilde{\mathcal{R}}^{j,k}, \\
&\text{(ii)} \quad c_{k,v} < c_{k,v'} \text{ for all } v < v' \text{ with } v, v' \in \{1, \ldots, r\}, \\
&\text{(iii)} \quad \exists p \in E \text{ such that } \gamma_j^k(x)|_{x=p} = c_{k,v}. \diamond
\end{aligned}
\tag{3.21}
$$

Let $\{C_k^r\}$ denote the set made of the elements of C_k^r and assume that $\{C_k^r\} \neq \emptyset$. Thus condition (3.21)(i) ensures that each element in $\{C_k^r\}$ has a preimage that is a submanifold while condition (3.21)(iii) guarantees that the preimage intersects with E. Condition (3.21)(ii) requires values in C_k^r to be given in an increasing order and elements of $\{C_k^r\}$ to be distinct. The above constraints ensure that each FIC value induces a distinct leaf. Therefore, the leaf corresponding to a constant $c_{k,v} \in \{C_k^r\}$, $v \in \{1, \ldots, r\}$, is defined as

$$
L_{j,k}^v := \{p \in E \mid \gamma_j^k(x)|_{x=p} = c_{k,v}\}.
\tag{3.22}
$$

Let $L_{j,k} := \{L_{j,k}^1, \ldots, L_{j,k}^r\}$ be the set of leaves associated with C_k^r. A schematic representation of a region E with a set of leaves $L_{j,k}$ is given in Figure 3.12.
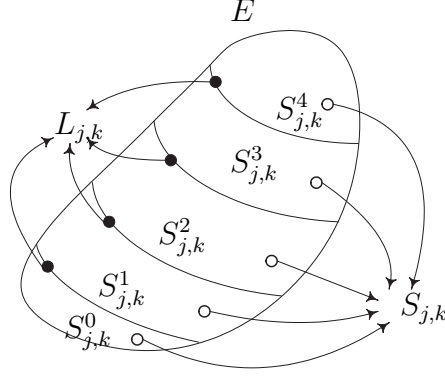
Figure 3.12: A region E partitioned by leaves $L_{j,k}$ and slices $S_{j,k}$

From Definition 3.21 the complement of $L_{j,k}$ in E is

$$S_{j,k}^0 := \{p \in E \mid \gamma_j^k(x)|_{x=p} < c_{k,1}\},$$

$$S_{j,k}^{v'} := \{p \in E \mid (r > 1,\, v' \in \{1,\, \ldots\, ,r-1\})\, c_{k,v'} < \gamma_j^k(x)|_{x=p} < c_{k,v'+1}\}, \quad (3.23)$$

$$S_{j,k}^r := \{p \in E \mid c_{k,r} < \gamma_j^k(x)|_{x=p}\},$$

The collection $S_{j,k} := \{S_{j,k}^w\}_{w \in \mathcal{I}_S}$ with index set $\mathcal{I}_S := \{0,\, \ldots\, ,r\}$, consists of the subsets of points in E that are delimited by $L_{j,k}$ and ∂E, the boundary of E as illustrated in Figure 3.12. The elements of $S_{j,k}$ are referred to as the *slices* of E. The following condition

$$\text{If } (\exists w \in \mathcal{I}_S)\, S_{j,k}^w = \emptyset \text{ then } S_{j,k} := S_{j,k} \setminus \{S_{j,k}^w\} \text{ and } \mathcal{I}_S := \mathcal{I}_S \setminus \{w\}, \quad (3.24)$$

is needed in order to guarantee the removal of any empty slice from $S_{j,k}$. We then show that the above construction leads to a partition of E.

Proposition 3.22

Let the input value $\sigma_k \in \Sigma$ be fixed. Assume that a set of FICs as in Definition 3.21 is provided and that the set $S_{j,k}$ satisfies condition (3.24). Then $L_{j,k} \cup S_{j,k}$ forms a partition of E, called a leaf-partition and denoted by π_k.$\diamond$

Proof: We must show that the conditions (3.7) and (3.8) are satisfied. First, Definition 3.21 and equation (3.22) imply that each leaf in $L_{j,k}$ is distinct and nonempty. Then (3.23) guarantees that $S_{j,k}$ is composed of disjoint sets complementing $L_{j,k}$ in E. Therefore the sets $L_{j,k}$ and $S_{j,k}$ are disjoint and such that $L_{j,k} \cup S_{j,k} = E$, thus satisfying (3.7) and (3.8). Finally, condition (3.24) guarantees that all elements in $S_{j,k}$ are nonempty. Therefore $L_{j,k} \cup S_{j,k}$ only contains nonempty sets, showing that $L_{j,k} \cup S_{j,k}$ is indeed a partition.□

Remark 3.23 From Definition 3.21, a foliation (from a submersion) corresponds to the special case where C_k^r has an infinite number of elements and all slices are empty.◇

Remark 3.24 On some occasions, the set of possible FICs can be quite large. In practice, some regions of the domain may be of special interest and should be enclosed by leaves as tightly as possible, thus determining a preferred set of FICs (see (Stiver *et al.*, 2000) for examples). Other constraints on FICs will be imposed in the next chapter.◇

Remark 3.25 The main advantage of dealing with an ICSS, instead of a nearly integrable CSS, is that for each input value the complete integrability of the collection of $n - 1$ first integrals holds over the subspace D'' defined in (3.17). Consequently each first integral can locally generate a foliation over D''.◇

From Proposition 3.22, a change of input value induces a different leaf-partition. Therefore the presence of P distinct input values induces a collection of leaf-partitions $\Pi := \{\pi_1, \ldots, \pi_P\}$. In order to consider all leaf-partitions in Π at the time one needs a rule that combines two (leaf-)partitions and results in to another (leaf-)partition. For this purpose we use an existing result (see §A.1 on page 144), which provides a technique to generate the coarsest refinement of any two partitions. Simply said the procedure amounts to superimposing the original partitions. The following corollary

captures the essence of an extension of the result in §A.1 to the set of leaf-partitions Π.

Corollary 3.26

Assume that $\Pi := \{\pi_1, \ldots, \pi_P\}$ is a finite collection of leaf-partitions over E. Then the composition $\pi_1 \star \cdots \star \pi_P$, with $\star$ as defined in §A.1, forms a partition over E, which we also denote by a leaf-partition.⋄

To summarize, we have provided a technique to construct the state structure of an FSM abstraction for nearly integrable CSSs. The approach proceeds by partitioning a region $E \subset D'$ with the leaves induced by the set of first integrals Γ (equations (3.21), (3.22), and (3.23)). Moreover it is possible to obtain a leaf-partition capturing the effect of all input values in Σ (Corollary 3.26). We complete this section by applying the above technique to an example.

Example 3.27 (Double Integrator) The double integrator is modeled by the following set of ODEs $\dot{x}_1 = x_2$, $\dot{x}_2 = u$ where $u = \sigma \in \Sigma$ and $D = \mathbb{R}^2$. The function $\gamma^\sigma(x) = \sigma x_1 - \frac{1}{2}x_2^2$ is a first integral defined over $D' = D$. If $\sigma \neq 0$ then $d\gamma^\sigma(x)|_{x=p} \neq 0$ for all $p \in D'$ whereas $\sigma = 0$ leads to $d\gamma^\sigma(x)|_{x=p} = 0$ for point in $\{(x_1, x_2) \mid x_2 = 0\}$, which is a subset with an empty interior. Consequently the double integrator is a nearly integrable CSS for any input value set Σ. Moreover notice that the double integrator is an ICSS on $D'' = D' \setminus \{(x_1, x_2) \mid x_2 = 0\}$.

For this example we select in an arbitrary manner a region $E := \{-2.1 < x_1 < 2.1, -2.1 < x_2 < 2.1\} \subset D'$, an input value set $\Sigma = \{-1, 1\}$ with $\sigma_1 = -1$ and $\sigma_2 = 1$ (in the future we will use the compact form $\Sigma = \{\sigma_1 = -1, \sigma_2 = 1\}$), and a set of FICs $C_1^4 = C_2^4 := (-1, 0, 1, 2)$. One can check that the conditions of Definition 3.21 are satisfied. With this setup one obtains the set of leaves shown in Figure 3.13. The orientation of the flow induced by Σ is indicated by lines with arrowhead.

The resulting leaf-partition contains sixteen cells whose interior is bounded by leaves. This leaf-partition provides the state structure Q of an FSM abstraction
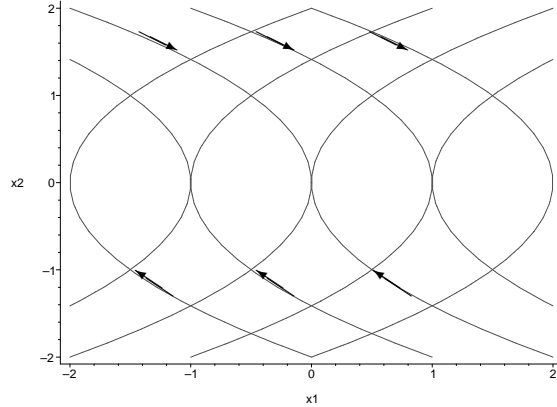
Figure 3.13: The set of leaves of Example 3.27

$\mathcal{A} := (Q, \Sigma, \delta)$ (ref. Definition 3.3 on page 29) for the double integrator over the region E defined above.•

3.4 Summary

In this previous sections, we have provided results on the class of Control Switched Systems (CSSs), which are continuous systems subject to piecewise-constant input signals. Initially, we have proposed a formal definition for an FSM abstraction of a CSS with a partitioned domain. It was followed by an exposition on some features of FSM abstractions, which has lead to the formulation of the problem of interest. Then we have identified a subclass of CSSs, called nearly integrable CSSs, and satisfying an integrability property over the domain of definition and for a given set of input values. Moreover we have demonstrated that a partitioning technique naturally arises in the presence of nearly integrable CSSs, thus providing a state structure for the FSM abstraction.

In order to define a transition map δ, one then needs to analyze how the continuous trajectories induced by the input value set Σ interact with the partition cells. This topic is covered in the following two chapters for the class of CSSs.

Chapter 4

Transversality and Consistency

In the previous chapter, we proposed a partitioning technique based on dynamical invariants. The next step in the construction of an FSM abstraction amounts to obtaining the transition structure induced by a leaf-partition and the continuous dynamics. Recall from §3.2.3 that the collapse of transversality indicates a qualitative change in the dynamical behaviour of continuous trajectories with respect to partition boundaries. Therefore the lack of transversality must be taken into account while evaluating the transition structure. For this reason we first investigate the transversality property while taking into account the specificities of leaf-partitions. Then we show how transversality impacts the consistency of the transition structure of an FSM abstraction.

In Section 4.1, results on the transversality of leaf-partitions are presented. Sufficient conditions for the existence of leaf-partitions with important transversality characteristics are provided. Distinct conditions are developed for the class of nearly integrable CSSs and ICSSs. The consistency property and its relationship with deterministic transition structures is then discussed in Section 4.2. Therein some benefits of transversality are shown.

4.1 Transversality for Leaf-Partitions

In the sequel the meaning of *well-conditioned transversality* for leaf-partitions consists of two pieces. First the locations where trajectories intersect non-transversally with leaves should be a submanifold of D'. Also we want to use this submanifold to "cut in a clean manner" any leaf of the partition. Such requirements are meant to divide a leaf into subleaves for which the transversality property of the flow is constant. We initiate the identification of conditions enforcing the above properties by defining transversality for leaf-partitions.

As seen previously, a vector field $f(x, u)$, with $u = \sigma_b \in \Sigma$, is transversal to a cell boundary ∂^i if

$$N(\partial^i, x) \cdot f(x, \sigma_b)|_{x=p} \neq 0, \text{ for all } p \in \partial^i. \tag{4.1}$$

Given a leaf-partition π, a partition cell boundary $\partial^i \subset \partial\pi$ contains a collection of subsets of leaves. Thus the normal to the boundary may locally take the form $N(\partial^i, x) = d\gamma_j^a(x)$ for some $\gamma_j^a \in \Gamma^a$ and $\sigma_a \in \Sigma$. In this context a general expression for the transversality between the trajectories induced by the input value σ_b and the leaves generated from the first integral $\gamma_j^a \in \Gamma^a$ becomes

$$d\gamma_j^a(x) \cdot f(x, \sigma_b) = \psi(x), \tag{4.2}$$

where the smoothness of the real-valued function $\psi : D' \to \mathbb{R}$ follows from that of γ_j^a and $f(x, \sigma_b)$. In this section we use equation (4.2) to characterize the transversality and non-transversality of leaf-partitions. This is done by first looking at a single pair of first integral and input value, followed by an extension to all first integrals and input values possibly involved in a leaf-partition.

4.1.1 Single First Integral - Single Input Value

In this section we treat the transversality between the trajectories defined by an input value σ_b and the single collection of leaves induced by some first integral $\gamma_j^a \in \Gamma^a$. As a reference, we recall in Figure 4.1 the possible intersections between trajectories and cell boundaries. Namely, a continuous trajectory initialized at p and intersecting with a boundary ∂^i can be: (a) tangent to ∂^i at a point only, (b) transversal to ∂^i at a point, or (c) tangent to a connected subset of ∂^i.
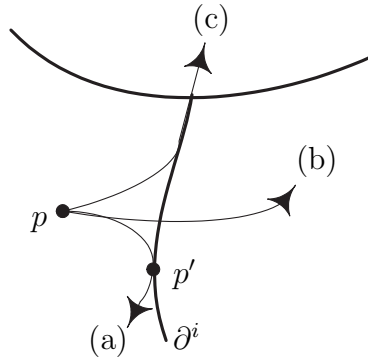
Figure 4.1: Intersections between a trajectory and a cell boundary

We first recall from the definition of a first integral (Definition 3.7 on page 39) that whenever $\sigma_b = \sigma_a$ in equation (4.2) one has $\psi(x)|_{x=p} = 0$ for all $p \in D'$. In other words, the vector field with an input value $\sigma_b = \sigma_a$ is everywhere tangent to the leaves defined by γ_j^a. Therefore a c-path initiated on a leaf induced by γ_j^a remains on that leaf as long as the input value σ_a is active. The following example provides a case where such a non-transversal behaviour occurs everywhere in D' even though $\sigma_b \neq \sigma_a$.

Example 4.1 Consider a three-dimensional system modeled by $\dot{x}_1 = x_2$, $\dot{x}_2 = x_3$, $\dot{x}_3 = u^2$ over $D' = \mathbb{R}^3$ and two first integrals $\gamma_1^u := x_1 u^4 - x_2 x_3 u^2 + x_3^3/3$ and $\gamma_2^u := -u^2 x_2 + \frac{1}{2} x_3^2$. With $\Sigma = \{\sigma_a = -1, \sigma_b = 1\}$ and $u = \sigma \in \Sigma$ one gets that $d\gamma_j^a(x) \cdot f(x, \sigma_b)|_{x=p} = 0$, for all $p \in D'$ and $j \in \{1, 2\}$. This phenomenon occurs

because γ_1^u and γ_2^u are both invariant to the sign of their input argument. Notice that any first integral resulting from a linear combination or a multiplication of functions of γ_1^u and γ_2^u leads to similar conclusions.●

In order to prevent this ambiguity about the effect of input values on first integrals and to pursue the characterization of transversality for leaf-partitions we require two conditions on the input value set Σ, that is, $\sigma_e \in \Sigma$ if

(i) $(\forall j \in \{1, \ldots, n-1\}) \, (\forall \sigma_d \in \Sigma \setminus \{\sigma_e\}) \, (\exists p \in D')$

$$d\gamma_j^e(x)|_{x=p} \not\equiv 0 \; \mathsf{mod}(\{d\gamma_1^d(x), \ldots, d\gamma_{n-1}^d(x)\}|_{x=p}), \text{ and} \qquad (4.3)$$

(ii) the singularity set $\mathcal{S}_e$ (ref. equation (3.3)) has a dense complement in D'.

Condition $(4.3)(i)$ is an independence condition among any first integral induced by input value σ_e and the set of $n-1$ first integrals defined by any other input value in Σ. Condition $(4.3)(ii)$ requires that the set of equilibrium points resulting from input value σ_e has an empty interior.

Conditions $(4.3)(i)$ and (ii) remove input values that may not induce any new dynamical behaviour on a subset of D'. Indeed, a violation of condition $(4.3)(ii)$ may lead to a situation where any trajectory generated by $\sigma \in \Sigma$ on an open subset of D is static, and thus does not enforce a discrete transition. Also, in the case of Example 4.1 condition $(4.3)(i)$ removes distinct input values leading to identical first integrals, thus reducing redundant dynamical behaviour. From now on, we assume that conditions $(4.3)(i)$ and (ii) are used to define an input value set Σ.

A first consequence of condition $(4.3)(i)$ on equation (4.2) is that the only first integrals for $f(x, \sigma_b)$ are those defined by the input value σ_b. Therefore the situation arising in case (c) of Figure 4.1 is partially characterized. That is, a trajectory remains on a leaf induced by some first integral $\gamma_j^b \in \Gamma^b$ as long as the input value equals σ_b. Conversely all trajectories induced by σ_b cannot stay for all times on a leaf defined

by an input value $\sigma_a \neq \sigma_b$.

In order to distinguish the non-transversal cases from the transversal ones, we identify conditions under which non-transversality arises by considering equation (4.2) with $\sigma_b \in \Sigma \setminus \{\sigma_a\}$. First notice that in general there exist points $p \in D'$ where non-transversality occurs, i.e., $\psi(x)|_{x=p} = 0$ or

$$d\gamma_j^a(x) \cdot f(x, \sigma_b)|_{x=p} = 0. \tag{4.4}$$

The points in D' where condition (4.4) holds may correspond to the location where (i) $f(x, \sigma_b)|_{x=p} = 0$ (or $p \in \mathcal{S}_b$), (ii) there is no leaf induced by γ_j^a, i.e., $d\gamma_j^a(x)|_{x=p} = 0$, or (iii) the vector field $f(x, \sigma_b)|_{x=p} \neq 0$ is non-transversal to the leaf with normal $d\gamma_j^a|_{x=p} \neq 0$ at p. An instance where case (iii) takes place consists of point p' of the c-path (a) of Figure 4.1.

Remark 4.2 Elements of $\mathcal{S}_b$ automatically satisfy (4.4) whereas they do not play a significant role in the existence of leaves (see Remark 3.19 on page 50).⋄

In order to achieve well-conditioned transversality, we first investigate if the object corresponding to $\psi^{-1}(0)$ forms a submanifold of D'. When this holds we denote $\psi^{-1}(0)$ by the *non-transversality submanifold* (NTSM). Such a requirement is motivated by the advantages of having $\psi^{-1}(0)$ taking the form of a reasonable geometric object in D'. After all, the points in $\psi^{-1}(0)$ correspond to locations around which the dynamical behaviour between a flow and any leaf induced by γ_j^a changes. Therefore the construction of the transition structure may benefit from some sort of characterization of $\psi^{-1}(0)$.

A sufficient condition for the existence of an NTSM is that $d\psi(x)|_{x=p} \neq 0$ for each point $p \in D'$ satisfying $\psi(x)|_{x=p} = 0$ (refer to the notion of a regular value on page 49). To verify this condition we define $\mathcal{C}$, the set of critical points of ψ in D' (ref.

Remark 3.17), and the set

$$\mathcal{E} := \{p \in D' \mid \psi(x)|_{x=p} = 0 \text{ and } d\psi(x)|_{x=p} = 0\}, \tag{4.5}$$

which results from the intersection between the set $\mathcal{C}$ and the zero-level set of ψ, thus leading to $\mathcal{E} \subseteq \mathcal{C} \cup \emptyset$. The set $\mathcal{E}$ represents a collection of "degenerate points" in the sense that if $\mathcal{E} \neq \emptyset$ the above sufficient condition for an NTSM does not hold. Conversely if $\mathcal{E} = \emptyset$ then an NTSM exists in D'.

We initiate a characterization of $\mathcal{E}$ for both classes of nearly integrable CSSs and ICSSs. We begin with the former.

Proposition 4.3

Consider a nearly integrable CSS with an analytic vector field and an input value set Σ. Let $\sigma_a, \sigma_b \in \Sigma$ be distinct input values and $\gamma_j^a \in \Gamma^a$ be an analytic first integral defined on D'. If D' is a connected set and $p \in D'$ is a point satisfying $d\psi(x)|_{x=p} = d(d\gamma_j^a(x) \cdot f(x, \sigma_b)) \neq 0$, then the set $\mathcal{E}$ is closed and has an empty interior.$\diamond$

Proof: If $\mathcal{E} = \emptyset$ then the above result holds. For $\mathcal{E} \neq \emptyset$ we use the fact that by construction the maps $\psi : D' \to \mathbb{R}$ and $d\psi : D' \to \mathbb{R}^n$ are analytic.

First we show that $\mathcal{E}$ is closed. For this recall that a map $h : A \subseteq \mathbb{R}^a \to B \subseteq \mathbb{R}^b$ is continuous if and only if for any closed set $b \subset B$ the preimage $h^{-1}(b)$ is a closed set in A (Kasriel, 1971). Since $\mathcal{E}$ consists of the intersection between preimages of closed sets, then $\mathcal{E}$ is closed in D'. Note that the preimage $(d\psi)^{-1}(0) := \{p \in D' \mid d\psi(x)|_{x=p} = 0\}$ is exactly the set of critical points $\mathcal{C}$.

We now prove that $\mathcal{E} \subset \mathcal{C}$ has an empty interior by showing that $\mathcal{C}$ has a dense complement in D'. We define the analytic codistribution $\Delta^\perp(x) := span\{d\psi(x)\}$ where $dim(\Delta^\perp(x)|_{x=p'}) \in \{0, 1\}$ for any p' in D'. From §A.2.2 (on page 145) the set of all regular points of maximal rank of an analytic codistribution forms an open and

dense set on the domain of definition. By assumption there is a point p satisfying $d\psi(x)|_{x=p} = a$ for some $a \in \mathbb{R}^n \setminus \{0\}$. Therefore $dim(\Delta^{\perp}(x)|_{x=p}) = 1$ and the set of regular points of $\Delta^{\perp}(x)$ with rank one is dense and open in D'. Consequently $\mathcal{C}$ has a dense complement in D', which completes the proof.□

Proposition 4.3 stipulates that under certain conditions the non-transversality between the leaves defined by γ_j^a and the trajectories induced by σ_b is such that $d\psi(x) \neq 0$ holds almost everywhere in D'. Consequently $\mathcal{E}$ is possibly nonempty, thus violating the sufficient condition for an NTSM.

Since ICSSs are a special class of nearly integrable CSSs, another set of conditions leads to a result similar to that of Proposition 4.3. Before proving this assertion we recall that for an ICSS there exist an open subset $D'' \subseteq D'$ and an approximate input value set Σ' where for each $\sigma \in \Sigma'$, the set of $n-1$ first integrals Γ^{σ} has linearly independent differentials on D''. We then show that given $\sigma_a, \sigma_c \in \Sigma'$, where σ_c is an approximate value for σ_b, equation (4.2) can be approximated by

$$d\gamma_j^a(x) \wedge (d\gamma_1^c(x) \wedge \cdots \wedge d\gamma_{n-1}^c(x)) = \widetilde{\psi}(x)\, dx_1 \wedge \cdots \wedge dx_n, \tag{4.6}$$

over D'' except in the presence of equilibrium points $\mathcal{S}_c$. Indeed, from Remark 3.19 it is possible, at least in principle, that some leaves defined by σ_c contain an equilibrium point p, thus satisfying condition $d\gamma_j^a(x) \cdot f(x, \sigma_c)|_{x=p} = 0$ while having $\widetilde{\psi}(x)|_{x=p} \neq 0$ in (4.6). The above development is captured by the following result.

Proposition 4.4

Consider an ICSS defined on $D'' \subseteq D'$ and with an input value set Σ'. Let $\sigma_a, \sigma_c \in \Sigma'$ be distinct input values. If $p \in D''$ and $p \notin \mathcal{S}_c$, then $\psi(x)|_{x=p} = d\gamma_j^a(x) \cdot f(x, \sigma_c)|_{x=p} = 0$ if and only if $\widetilde{\psi}(x)|_{x=p} = 0$.◇

Proof:($\Rightarrow$) Let p be such that $\psi(x)|_p = d\gamma_j^a(x) \cdot f(x, \sigma_c)|_{x=p} = 0$. Notice that $d\gamma_j^a(x)|_{x=p} \neq 0$ because for any $p \in D''$ the condition $d\gamma_1^a(x) \wedge \cdots \wedge d\gamma_{n-1}^a(x)|_{x=p} \neq$

0 leads to $d\gamma_j^a(x)|_{x=p} \neq 0$ for all $j \in \{1, \ldots, n-1\}$. Also $p \notin \mathcal{S}_c$ implies that $f(x, \sigma_c)|_{x=p} \neq 0$. From the near integrability of an ICSS, there exist $n-1$ first integrals γ_j^c, with $j \in \{1, \ldots, n-1\}$, defined in D' so that $d\gamma_j^c \cdot f(x, \sigma_c)|_{x=p'} = 0$ for all $p' \in D'$. Moreover, this set of $n-1$ first integrals $\gamma_1^c, \ldots, \gamma_{n-1}^c$ has linearly independent differentials over D'', thus at p. Therefore these differentials locally form a basis for an $n-1$ dimensional subspace which is orthogonal to $f(x, \sigma_c)$ at p. By assumption $d\gamma_j^a(x)$ is also orthogonal to $f(x, \sigma_c)$ at p. Thus $d\gamma_j^a(x)$ belongs to the space spanned by $d\gamma_1^c, \ldots, d\gamma_{n-1}^c$. Consequently $d\gamma_j^a(x) \wedge (d\gamma_1^c(x) \wedge \cdots \wedge d\gamma_{n-1}^c(x))|_{x=p} = 0$, leading to $\widetilde{\psi}(x)|_{x=p} = 0$.

($\Leftarrow$) Let p be such that $\widetilde{\psi}(x)|_{x=p} \, dx_1 \wedge \cdots \wedge dx_n = d\gamma_j^a(x) \wedge (d\gamma_1^c(x) \wedge \cdots \wedge d\gamma_{n-1}^c(x))|_{x=p} = 0$. Thus at p the differential of the first integral $\gamma_j^a(x)$ can be expressed as $d\gamma_j^a(x) = \alpha_1 d\gamma_1^c(x) + \cdots + \alpha_{n-1} d\gamma_{n-1}^c(x)$ for some real values α_i where $1 \leq i \leq n-1$. Consequently $d\gamma_j^a(x) \cdot f(x, \sigma_c)|_{x=p} = (\alpha_1 d\gamma_1^c(x) + \cdots + \alpha_{n-1} d\gamma_{n-1}^c(x)) \cdot f(x, \sigma_c)|_{x=p} = 0$ since $\gamma_1^c, \ldots, \gamma_{n-1}^c$ are first integrals for $f(x, \sigma_c)$. Therefore $\psi(x)|_p = 0$, proving the claim.$\square$

Let $\mathcal{E}'$ and $\mathcal{C}'$ denote the approximations of $\mathcal{E}$ and $\mathcal{C}$ with σ_c instead of σ_b, where $\sigma_c \approx \sigma_b$, $\sigma_c \in \Sigma'$, and $\sigma_b \in \Sigma$. Given the zero-level set of $\widetilde{\psi}$, that is,

$$\mathcal{F} := \{p \in D'' \mid \widetilde{\psi}(x)|_{x=p} = 0\}, \tag{4.7}$$

the following result provides a first characterization of $\mathcal{E}'$.

Proposition 4.5

Consider an ICSS defined on the open set $D'' \subseteq D'$ and with an input value set Σ'. Given distinct input values $\sigma_a, \sigma_c \in \Sigma'$ and a first integral $\gamma_j^a \in \Gamma^a$ defined on D', then either $\mathcal{E}' \cap D'' = \emptyset$ or $\mathcal{E}' \cap D'' \subset (\mathcal{F} \cup \mathcal{S}_c) \cap \mathcal{C}'.\diamond$

Proof: The case $\mathcal{E}' \cap D'' = \emptyset$ follows from $\mathcal{E}' = \emptyset$. Now let $p \in \mathcal{E}' \cap D''$ so that $\psi(x)|_p = d\gamma_j^a(x) \cdot f(x, \sigma_c)|_{x=p} = 0$, $p \in \mathcal{C}'$, and $p \in D''$. Thus at p one of the

following situation arises: (a) $d\gamma_j^a(x) \cdot f(x, \sigma_c)|_{x=p} = 0$ where $f(x, \sigma_c)|_{x=p} = 0$ (p is an equilibrium point), or (b) $d\gamma_j^a(x) \cdot f(x, \sigma_c)|_{x=p} = 0$ where $f(x, \sigma_c)|_{x=p} \neq 0$. Recall from Proposition 4.4 that $d\gamma_j^a(x)|_{x=p} = 0$ is not possible. If case (a) holds then $p \in \mathcal{S}_c$, and since $p \in \mathcal{C}'$ this leads to $p \in \mathcal{S}_c \cap \mathcal{C}'$. Considering that $\mathcal{S}_c \cap \mathcal{C}' \subset (\mathcal{S}_c \cap \mathcal{C}') \cup (\mathcal{F} \cap \mathcal{C}') = (\mathcal{F} \cup \mathcal{S}_c) \cap \mathcal{C}'$ one has $p \in (\mathcal{F} \cup \mathcal{S}_c) \cap \mathcal{C}'$. If instead case (b) holds then by Proposition 4.4 one gets $\widetilde{\psi}(x)|_{x=p} = 0$, which by equation (4.7) leads to $p \in \mathcal{F}$. Since p also belongs to $\mathcal{C}'$ one gets that $p \in \mathcal{F} \cap \mathcal{C}'$. The fact that $\mathcal{F} \cap \mathcal{C}' \subset (\mathcal{F} \cap \mathcal{C}') \cup (\mathcal{S}_c \cap \mathcal{C}') = (\mathcal{F} \cup \mathcal{S}_c) \cap \mathcal{C}'$ completes the proof.$\square$

Therefore in the presence of an ICSS the set $\mathcal{E}$ can be approximated by $\mathcal{E}'$ over D'' so that $\mathcal{E}'$ is either empty or bounded above by $(\mathcal{F} \cup \mathcal{S}_c) \cap \mathcal{C}'$. This leads to a result similar to that of Proposition 4.3 but for the class of ICSSs.

Proposition 4.6

Consider an ICSS defined over the open set $D'' \subseteq D'$, where all first integrals are analytic. Let $\sigma_a, \sigma_c \in \Sigma'$ be distinct input values and $\gamma_j^a \in \Gamma^a$ be a first integral. If D'' is connected and there exists a point $p \in D''$ satisfying $\widetilde{\psi}(x)|_{x=p} \neq 0$, then the set $\mathcal{E}'$ is closed and has an empty interior.$\diamond$

Proof: If $\mathcal{E}' = \emptyset$ then the above result holds. For $\mathcal{E}' \neq \emptyset$ we prove the claim by using the upper bound of $\mathcal{E}'$ in Proposition 4.5, i.e., we show that $\mathcal{F} \cup \mathcal{S}_c$ has a dense complement in D''. As condition (4.3)(ii) implies that $\mathcal{S}_c$ has an empty interior, thus on $D'' \subseteq D'$, we only need to show that $\mathcal{F}$ has a dense complement in D''. The closeness of $\mathcal{E}'$ follows from an argument similar to that of Proposition 4.3 for $\mathcal{E}$.

From the first integrals involved in equation (4.6) we define on D'' the matrix with lines $d\gamma_j^a(x), d\gamma_1^c(x), \ldots, d\gamma_{n-1}^c(x)$, and the codistribution $\Delta^\perp(x) := span\{d\gamma_j^a(x), d\gamma_1^c(x), \ldots, d\gamma_{n-1}^c(x)\}$ whose dimension at a point p is equal to the rank of the previous matrix. By construction, the codistribution $\Delta^\perp$ is analytic in x and satisfies $dim(\Delta^\perp(x)|_{x=p}) \in \{n-1, n\}$ over D''. By assumption there exists a point $p \in D''$ such that $\widetilde{\psi}(x)|_{x=p} = a \neq 0$, i.e., $dim(\Delta^\perp(x)|_{x=p}) = n$. Since D'' is connected, it

follows by §A.2.2 that the points in D'' where $\Delta^\perp(x)$ has rank n form an open and dense subset of D''. Consequently $\mathcal{F}$ has a dense complement in D'', which completes the proof.□

Proposition 4.6 stipulates that under certain conditions an ICSS can be approximated so that the non-transversality between the leaves induced by γ_j^a and the trajectories defined by σ_c is such that $d\psi(x) \neq 0$ almost everywhere in D''. Notice that Proposition 4.6 proceeds with a distinct upper bound for $\mathcal{E}'$ and that its sufficient condition involves $\widetilde{\psi}$, instead of the derivative of ψ as in Proposition 4.3. Also it can be shown that the sufficient condition of Proposition 4.6 on $\widetilde{\psi}(x)$ is automatically satisfied in the presence of a dense set D'' (ref. Remark 3.13 on page 45) and of condition $(4.3)(i)$.

Both Proposition 4.3 and Proposition 4.6 say that, in general, $\mathcal{E} \neq \emptyset$. Therefore, in the presence of leaf-partitions one cannot expect that a non-transversality submanifold (NTSM) exists in D' or D''. However this does not completely preclude a characterization of transversality.

As initially stated, the second requirement for a well-conditioned transversality necessitates that the set of points $\psi^{-1}(0)$ acts as a "cutting edge" to divide any leaf induced by the first integral γ_j^a. Since $\psi^{-1}(0)$ does not necessarily form a submanifold in D' we relax the investigation of the transversality property by considering a subset of leaves only. In this context a strong condition enforcing the second requirement is that *locally* a given leaf and the set $\psi^{-1}(0)$ be transversal. The main advantage of such an approach is that we transform the characterization of non-transversality between leaves and flow to a transversality problem, which is easier to handle since non-transversal sets may take rather intricate forms (see (Guillemin and Pollack, 1974) for some examples). In order to capture the locations where the transversality between

a leaf induced by a first integral $\gamma_j^a \in \Gamma^a$ and $\psi^{-1}(0)$ holds, we introduce the set

$$\mathcal{G} := \{p \in D' \mid \psi(x)|_{x=p} = 0 \text{ and } d\gamma_j^a(x) \wedge d\psi(x)|_{x=p} = 0\}. \tag{4.8}$$

The set $\mathcal{G}$, which by definition contains $\mathcal{E}$, captures the points in D' where the differentials of γ_j^a and ψ are linearly dependent. This leads to the following result.

Lemma 4.7 *Consider a nearly integrable CSS with an input value set Σ containing distinct input values σ_a and σ_b. Let $\gamma_j^a \in \Gamma^a$ be a first integral defined on D' and inducing a leaf $L_{j,a}^c$ for some regular value c. If $L_{j,a}^c \cap \mathcal{G} = \emptyset$, then for any point $p \in L_{j,a}^c \cap \psi^{-1}(0)$ the leaf $L_{j,a}^c$ can be locally divided in two regions R_1 and R_2 with opposite flow directions, that is,*

$$\begin{aligned} d\gamma_j^a(x) \cdot f(x, \sigma_b)|_{x=p \in R_1} &< 0, \\ d\gamma_j^a(x) \cdot f(x, \sigma_b)|_{x=p \in R_2} &> 0. \end{aligned} \tag{4.9}$$

$\diamond$

Proof: Since two-dimensional systems correspond to a special case, the proof splits in two parts, i.e., for systems where $n = 2$ and those where $n > 2$.

Let p be an arbitrary point of $L_{j,a}^c \cap \psi^{-1}(0)$. By assumption $p \notin \mathcal{G}$ so that $d\gamma_j^a(x) \wedge d\psi(x)|_{x=p} \neq 0$, that is, $d\gamma_j^a$ and $d\psi$ are linearly independent at p. By continuity, there exists a neighborhood of p in D', say N_p, where $d\gamma_j^a(x) \wedge d\psi(x)|_{x=p'} \neq 0$ for all $p' \in N_p$. Moreover since $d\psi(x) \neq 0$ over N_p, the Preimage Theorem (ref. §A.2.4 on page 147) implies that $\psi^{-1}(0)$ forms a submanifold in N_p.

For $n = 2$, the point p is completely characterized by γ_j^a and ψ. We claim that there exists a neighborhood where p is the unique intersection point between $L_{j,a}^c$ and $\psi^{-1}(0)$. We prove the claim by contradiction, that is, we assume that there is a neighborhood of p where $L_{j,a}^c$ and $\psi^{-1}(0)$ coincide and we denote by T the set of

points in $L_{j,a}^c \cap \psi^{-1}(0)$. Since $T \subset \psi^{-1}(0)$ then $\psi(x)|_{p'}$ is constant (and equals zero) for all $p' \in T$. Consequently at point $p \in T$ the differential of $\psi(x)$ equals zero, which, in turn, means that $p \in \mathcal{G}$, a contradiction. Since $L_{j,a}^c$ consists of a one-dimensional submanifold, the point p locally divides $L_{j,a}^c$ in two parts.

From the smoothness of $\psi(x)$ it follows that $d\psi(x)$ does not change sign on some neighborhood of the point p. Therefore a sufficiently small perturbation of p along $L_{j,a}^c$, say $p' \in L_{j,a}^c \setminus \{p\}$, leads to $\psi(x)|_{x=p'} \neq 0$. Indeed, since $\psi(x)|_p = 0$ and $d\psi(x)|_p \neq 0$, if a perturbation of p along $L_{j,a}^c$ leads to $\psi(x)|_{x=p'} > 0$ (resp., $\psi(x)|_{x=p'} < 0$) with $p' \in L_{j,a}^c \setminus \{p\}$ then a perturbation along $L_{j,a}^c$ in the opposite direction leads to $\psi(x)|_{x=p''} < 0$ (resp., $\psi(x)|_{x=p''} > 0$) with $p'' \in L_{j,a}^c \setminus \{p\}$.

For $n > 2$, we define a mapping $\beta : D' \to \mathbb{R}^2$ as $\beta(x) := [\gamma_j^a(x), \psi(x)]^T$. Since by assumption $L_{j,a}^c \cap \mathcal{G} = \emptyset$ then for any point $p \in L_{j,a}^c \cap \psi^{-1}(0)$ there exists a neighborhood of p, say N_p, where $rank(d\beta(x)|_{x=p'}) = 2$ for all $p' \in N_p$. Said otherwise, the point $(c, 0) \in \mathbb{R}^2$ is a regular value for $\beta(x)$ in N_p. Thus it follows by the Preimage Theorem that $\beta^{-1}(c, 0)$ forms a submanifold of N_p of dimension $n-2$, which we denote by S. Moreover the submanifold S locally represents the intersection points between $L_{j,a}^c$ and $\psi^{-1}(0)$. Similarly to the above development, in a neighborhood of p the submanifold S splits the leaf $L_{j,a}^c$ in two parts. Moreover a small perturbation along the leaf and away from S leads to the expected result, completing the proof.$\square$

From Lemma 4.7 a leaf without points in $\mathcal{G}$ is such that for each point $p \in \psi^{-1}(0)$ there is a submanifold, which locally delineates two regions with opposite flow directionality. If no point in $L_{j,a}^c$ belongs to $\psi^{-1}(0)$ then the flow does not change directionality with respect to the leaf. Consequently only one point of the leaf needs to be evaluated to obtain the directionality of the flow.

Remark 4.8 For the special case of $n = 2$, it can be shown that between any two consecutive points in $L_{j,a}^c \cap \psi^{-1}(0)$ the relative direction of the flow with respect to the leaf remains unchanged. In reference to Figure 4.1 (on page 58), the conditions of

Lemma 4.7 amounts to requiring that, whenever a trajectory and a leaf are defined by distinct input values, no intersection of type (c) occurs.⋄

The following result provides a sufficient condition so that there exists an open and dense subset of D' where the condition of Lemma 4.7 is satisfied.

Proposition 4.9

Consider a nearly integrable CSS with an analytic vector field and an input value set Σ containing two distinct input values σ_a and σ_b. Let $\gamma_j^a \in \Gamma^a$ be an analytic first integral defined on a connected set D'. If there exists a point $p \in D'$ satisfying $d\gamma_j^a \wedge d\psi(x)|_{x=p} \neq 0$, then the set $\mathcal{G}$ is closed and has an empty interior.⋄

Proof: Since both γ_j^a and $f(x, \sigma_b)$ are analytic then so is the codistribution $\Delta^\perp(x) := span\{d\gamma_j^a(x), d\psi(x)\}$. By definition one has that $dim(\Delta^\perp(x)) \in \{0, 1, 2\}$. Moreover, by assumption, the point p is such that $dim(\Delta^\perp(x)|_p) = 2$. From the connectedness of D' and §A.2.2, it follows that the points in D' where $\Delta^\perp(x)$ has rank two form an open and dense subset. Since this set of points is in the complement of $\mathcal{G}$ in D' then $\mathcal{G}$ has an empty interior. The closure of $\mathcal{G}$ follows from the fact that it consists of the intersection of two closed sets in D', proving the claim.□

This completes the characterization of non-transversality in the presence of a single collection of leaves defined by an input value and the flow of a vector field induced by a distinct input value. In the next section we perform a simple extension of the previous results for the case where multiple first integrals and input values are considered.

4.1.2   Multiple First Integrals - Multiple Input Values

Since $\mathcal{G}$ in equation (4.8) qualifies a first integral γ_j^a and a flow generated by σ_b, we denote it here by $\mathcal{G}_{j,a}^b$. In order to consider all input values in Σ that are distinct from

σ_a, we define the set

$$\mathcal{G}_{j,a}^{\Sigma} := \bigcup_{\sigma_b \in \Sigma \setminus \{\sigma_a\}} \mathcal{G}_{j,a}^b. \tag{4.10}$$

In particular, if each $\mathcal{G}_{j,a}^b$ is closed and has an empty interior then so is $\mathcal{G}_{j,a}^{\Sigma}$ (by using the complements and Proposition 3.14 on page 46). A similar procedure can be followed to scan through all first integrals in Γ, in order to lead to a subset of D' where all leaves have a well-conditioned transversality property. We complete the characterization of transversality for leaf-partitions by using an immediate extension of Lemma 4.7.

Corollary 4.10

Consider a nearly integrable CSS and a leaf-partition π generated from an input value set Σ and a set of first integrals Γ defined on D'. If for any $j \in \{1, \ldots, n-1\}$, $\sigma_a \in \Sigma$, and $\sigma_b \in \Sigma \setminus \{\sigma_a\}$ the set $\mathcal{G}_{j,a}^b$ does not intersect with leaves in π that are generated by γ_j^a, then each leaf containing a point $p \in \psi^{-1}(0)$ can be locally divided in two regions with opposite flow directionality.◇

Proof: This follows from Lemma 4.7.□

Remark 4.11 For two-dimensional systems Corollary 4.10 implies that the behaviour of continuous trajectories around a point of $\psi^{-1}(0)$ belonging to a leaf can be determined by selecting only two points of the leaf and on each side of $\psi^{-1}(0)$.◇

Remark 4.12 With respect to Remark 3.24 (on page 53), Corollary 4.10 imposes additional constraints on the selection of FICs (ref. Definition 3.21 on page 51).◇

4.1.3 Summary

Given a collection of leaves defined by an input value and trajectories induced by another input value, Proposition 4.3 (resp., Proposition 4.6) provides a first charac-

terization of the locations where non-transversal intersections (between trajectories and leaves) for a nearly integrable CSS (resp., an ICSS) do not define a submanifold. Furthermore, Lemma 4.7 gives conditions under which a leaf (defined by an input value) has a well-conditioned transversality property with respect to a flow (induced by another input value). Such a transversality property enables the identification of transitions simply by evaluating points in the neighborhood of $\psi^{-1}(0)$. In Corollary 4.10 a similar procedure is followed for all leaves generated by Σ and Γ, thus capturing all possible elements involved in a leaf-partition. In that sense Corollary 4.10 imposes additional constraints on leaf-partitions as it requires that no leaf in π intersects with some region in D'.

We conclude this section by illustrating the theory with two examples possessing an analytic vector field and analytic first integrals defined over a connected set D'.

Example 4.13 (Double Integrator) We pursue the double integrator example introduced in Chapter 3. In this example the vector field is $f = [x_2, u]^T$, and $\gamma_1^\sigma(x) = \sigma x_1 - \frac{1}{2}x_2^2$ is a first integral defined over $D' = D = \mathbb{R}^2$. As mentioned before, the system qualifies as both a nearly integrable CSS and an ICSS. Thus we assume $\Sigma := \{\sigma_a, \sigma_b\}$ with $\sigma_a, \sigma_b \in \mathbb{R} \setminus \{0\}$, $\sigma_a \neq \sigma_b$, and $\Gamma := \{\gamma_1^a, \gamma_1^b\}$. Notice that with such Σ and Γ conditions (4.3)(i) and (ii) are satisfied. Namely both $\mathcal{S}_a$ and $\mathcal{S}_b$ have an empty interior (as $\mathcal{S}_a = \mathcal{S}_b = \emptyset$), and thus satisfy condition (4.3)(ii). Also $d\gamma_1^a(x) \wedge d\gamma_1^b(x) = x_2(\sigma_a - \sigma_b)$ so that any point $(x_1, x_2 \neq 0) \in D'$ fulfills condition (4.3)(i).

Given the above first integral one gets $\psi(x) = d\gamma_1^a \cdot f(x, \sigma_b) = x_2(\sigma_a - \sigma_b)$, $d\psi(x) = (\sigma_a - \sigma_b)dx_2$ and $d\gamma_1^a(x) \wedge d\psi(x) = \sigma_a(\sigma_a - \sigma_b)dx_1 \wedge dx_2$. Therefore non-transversality occurs at points in $\{(x_1, x_2 = 0)\}$. Since $d\psi(x)|_{x=p} \neq 0$ for any $p \in D'$, Proposition 4.3 predicts a closed set $\mathcal{E}$ with an empty interior. Indeed one has $\mathcal{E} = \emptyset$ and the same result holds for the case of the ICSS since $D'' = D'$. Moreover one has that $\mathcal{G} = \mathcal{G}_{1,a}^b = \emptyset$. Consequently, Corollary 4.10 implies that a leaf-partition generated by

70

Σ and $\Gamma := \{\gamma_1^a, \gamma_1^b\}$ has well-conditioned transversality.●

Example 4.14 (Inverted pendulum) In Åström and Furuta (Åström and Furuta, 2000), an inverted pendulum is modelled by $\dot{x}_1 = x_2$, $\dot{x}_2 = \sin(x_1) - \cos(x_1)u/g$ over $D := S \times \mathbb{R}$ where x_1 and x_2 are the angle and angular velocity, respectively. Even though this system evolves on a cylinder D, which is not an open subset of $\mathbb{R}^3$, we restrict ourselves to the planar region $D := (0, 2\pi) \times \mathbb{R}$. Consider the first integral $\gamma_1^\sigma(x) = \frac{1}{2}x_2^2 + \cos x_1 + (\sin x_1)\sigma/g$ over $D' = \{0 < x_1 < 2\pi, x_2 \in \mathbb{R}\}$. Notice that the equilibrium point $(x_1 = \tan^{-1}(-\sigma/g), x_2 = 0)$ coincides with the location where $d\gamma_1^\sigma(x) = (-\sin x_1 + (\cos x_1)\sigma/g)d(x_1) + x_2 d(x_2)$ vanishes.
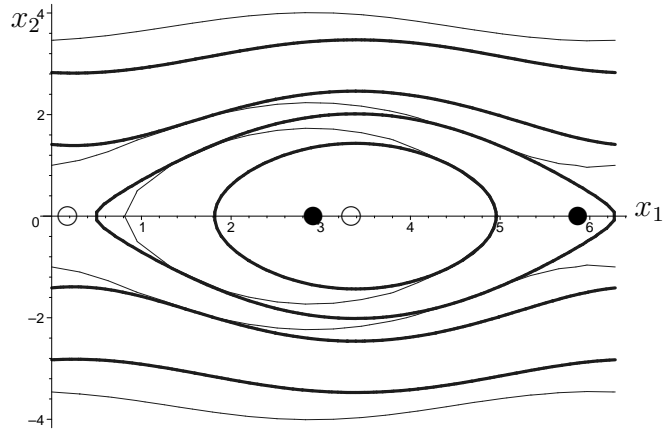
Figure 4.2: Level sets and equilibrium points for Example 4.14

Figure 4.2 shows the level sets of γ_1^σ for the input value set $\Sigma := \{\sigma_a = -0.25g, \sigma_b = 0.25g\}$ (thinner lines represent the input value $\sigma_a = -0.25g$) and the equilibrium points induced by Σ, which are represented by distinct circles for different input values. Since condition (3.14) holds over a dense subset of D', the system qualifies as a nearly integrable CSS. Moreover it is an ICSS over $D'' = D' \setminus \{(x_1 = \tan^{-1}(-0.25), x_2 = 0), (x_1 = \tan^{-1}(0.25), x_2 = 0)\}$.

Conditions (4.3)(i) and (ii) are satisfied as $\sigma_a \neq \sigma_b$. Given the above first integral one has $\psi(x) = d\gamma_1^a(x) \cdot f(x, \sigma_b) = x_2 \cos x_1(\sigma_a - \sigma_b)/g$ and $d\psi = (-x_2 \sin x_1 d(x_1) +$

$\cos x_1 d(x_2))(\sigma_a - \sigma_b)/g$. The set of non-transversal points $\psi^{-1}(0)$ is formed by the lines $x_1 = \frac{1}{2}\pi$, $x_1 = \frac{3}{2}\pi$ and $x_2 = 0$ (three of the locations where ψ vanishes are marked by an X in Figure 4.3). Also the critical points of ψ are $(x_1 = \frac{1}{2}\pi, x_2 = 0)$ and $(x_1 = \frac{3}{2}\pi, x_2 = 0)$ (represented by black dots in Figure 4.3).
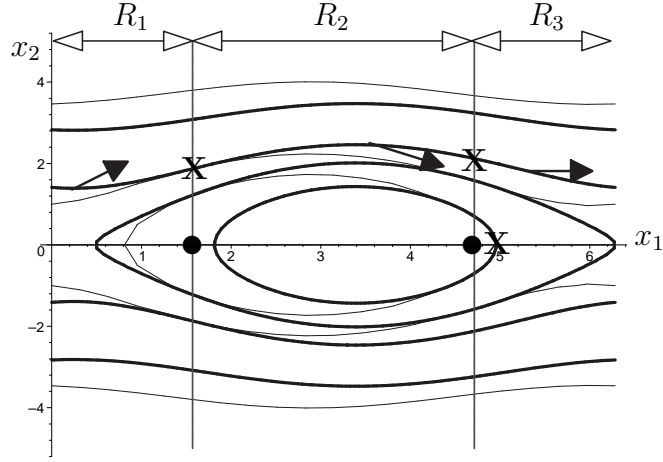
Figure 4.3: Critical points of $\psi(x)$ and set $\mathcal{E}$ for Example 4.14

Once again the conditions of Proposition 4.3 are satisfied and the set $\mathcal{E} = \{(\frac{1}{2}\pi, 0), (\frac{3}{2}\pi, 0)\}$ is closed and with an empty interior. Similarly the ICSS respects the conditions of Proposition 4.6 and $\mathcal{E}'$ has also an empty interior. Moreover, as $d\gamma_1^a(x) \wedge d\psi(x) = \frac{(\sigma_a - \sigma_b)}{g}[x_2^2 \sin x_1 - \sin x_1 \cos x_1 + \cos^2 x_1 \sigma_a/g]dx_1 \wedge dx_2$, one has that $\mathcal{G} = \mathcal{E} \cup \{(x_1 = \tan^{-1}(-\sigma_a/g), x_2 = 0)\}$. We then illustrate Remark 4.8. Namely three regions R_1, R_2, and R_3 with a fixed flow directionality are identified in Figure 4.3 for a leaf (the one represented by a thick line and with the two X's) that does not intersect with $\mathcal{G}$. The directionality of the vector field is indicated along the leaf. Notice that the leaves of the leaf-partition illustrated in Figure 4.3 do not encounter $\mathcal{G}$, thus satisfying the condition of Corollary 4.10.$\bullet$

The previous two examples illustrated how transversality may impact on the determination of the transition structure of an FSM abstraction. An important feature of a transition structure remains the presence of nondeterministic transitions. With

the next section, we initiate an analysis of the origin of those transitions for leaf-partitions.

4.2   Nondeterministic Transitions

In §3.2.3 we showed the strong relationship between deterministic transition structures and various notions of the consistency property. However, the partitioning of a state-space region of a continuous system usually leads to an abstraction with a nondeterministic transition structure. For this reason, this section aims at understanding the occurrence of nondeterministic transitions and their relationship with transversality. Since we focus on nonsingular d-paths, we consider leaf-partitions that do not contain any dynamical singularities. In this investigation we identify generic situations leading to nondeterministic transitions, and in parallel we assess techniques that are meant to reduce the number of such transitions.

In order to define scenarios where nondeterministic transitions arise we refer to a fictitious set of partition cells represented by simple two-dimensional rectangles as in Figure 4.4 where only the flow differentiates cases (a), (b), and (c). Figure 4.4(a) provides an example of deterministic transitions, i.e., the flows ϕ_k and $\phi_{k'}$ evolve unambiguously from one cell to another, $q_i \rightarrow q_l \rightarrow q_j$ and $q_l \rightarrow q_k$, respectively. The leaf-partition of the double-integrator presented in Figure 3.13 constitutes an example of a partition leading to a transition structure with deterministic transitions only. However a deterministic transition structure is not a generic property of abstractions based on leaf-partitions. For instance, in Figure 4.4(b) the orientation of the flow ϕ_k is slightly inclined so that it is no longer parallel to any boundary of the cells. In this situation the flow ϕ_k, when initiated in q_l, visits two neighbor cells q_j and q_k thus leading to a nondeterministic transition. Similarly, a slight perturbation of any of the leaves of Figure 3.13 immediately leads to a nondeterministic transition structure.

Indeed, in the leaf-partition of Figure 4.5(a), where all cells bounded by leaves are numbered, two trajectories initiated in the cell number 3 can reach the cells 2 and 9.

In the next sections we investigate two techniques in order to reduce the number of nondeterministic transitions arising in leaf-partitions.
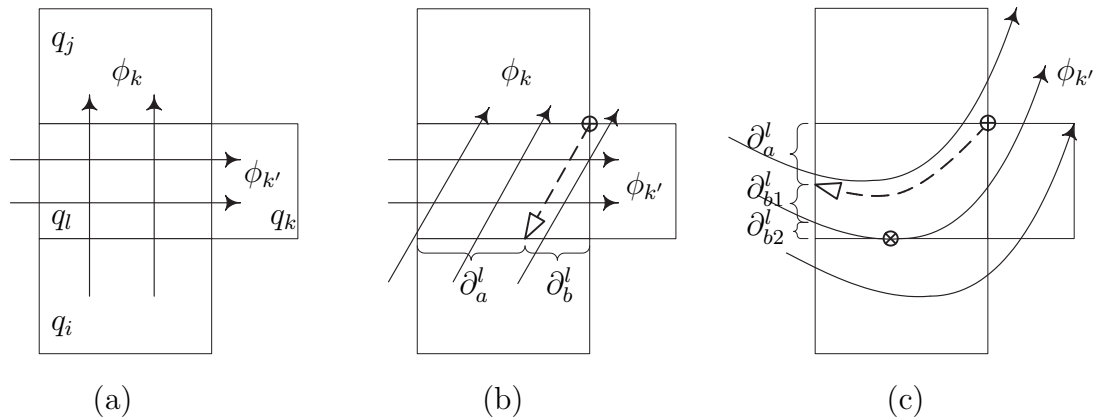
Figure 4.4: Some partition cells with three distinct flows

4.2.1 Subset Construction

Among the techniques to handle FSMs with a nondeterministic transition structure, one finds the method of *subset construction* (Hopcroft and Ullman, 1979). This approach enables one to find a deterministic FSM that recognizes the same language as the nondeterministic automaton. We now investigate the application of the subset construction technique to the double-integrator leaf-partition of Figure 4.5(a).

Given a source cell the subset construction groups all cells that are reached under the same input value. For instance, the nondeterministic transitions $\{3\} \rightarrow \{2\}$ and $\{3\} \rightarrow \{9\}$ shown in Figure 4.5(a) result in a deterministic transition $\{3\} \rightarrow \{2, 9\}$ where $\{2, 9\}$ forms a new state of the deterministic automaton. By performing this step for the whole leaf-partition, one obtains Table 4.1 whose columns contain the source cell as well as the target cells reached under distinct input values σ_1 and σ_2. The presence of – in columns of target cells indicates the disabling of an input value
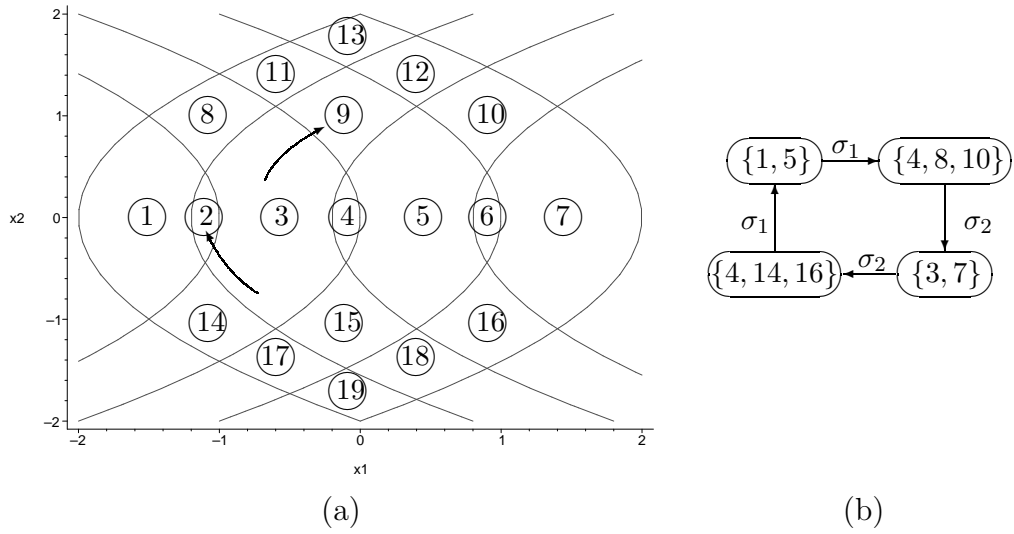
Figure 4.5: (a) A double-integrator leaf-partition, (b) Loop in the deterministic automaton

that leads outside the set of numbered cells. For instance, the set of cells numbered 1, 14, 17 and 19 can exit the leaf-partition under input value σ_2. Moreover, for an aggregated cell such as $\{4, 14\}$ the input value σ_2 is also disabled (see – in Table 4.1) because one of its elements, namely 14, exits the leaf-partition under the input value σ_2.

In Table 4.1 one notices a loop among some of the aggregated states, namely $\{1, 5\}$, $\{4, 8, 10\}$, $\{3, 7\}$, and $\{4, 14, 16\}$. Indeed the nondeterminism propagates in such a manner that wherever the leaf-partition of Figure 4.5(a) is initialized it may eventually reach the cyclic graph of Figure 4.5(b). Moreover, this phenomenon is invariant of the refinement, meaning that, in general, a finer/coarser partition leads to a similar conclusion.

From a continuous control perspective, the result depicted by the cyclic graph of Figure 4.5(b) is of limited use. Indeed one normally seeks to stabilize a continuous system in the vicinity of a point, i.e., in a set that is connected. However each aggregated state of Figure 4.5(b) forms a disconnected subset of the state space, so that a stabilization task as previously defined cannot take place. Consequently one

75

Source cell	Target cells $\sigma_1 = 1$	$\sigma_2 = -1$	Source cell	Target cells $\sigma_1 = 1$	$\sigma_2 = -1$
$\{1\}$	8	–	$\{16\}$	5	18
$\{2\}$	3	1	$\{17\}$	14	–
$\{3\}$	2,9	4,14	$\{18\}$	15	19
$\{4\}$	5	3	$\{19\}$	17	–
$\{5\}$	4,10	6,15	$\{2,9\}$	3,12	1,5
$\{6\}$	7	5	$\{4,14\}$	1,5	–
$\{7\}$	–	16	$\{4,10\}$	–	3,7
$\{8\}$	11	3	$\{6,15\}$	3,7	5,17
$\{9\}$	12	5	$\{3,12\}$	–	4,10,14
$\{10\}$	–	7	$\{1,5\}$	4,8,10	–
$\{11\}$	13	9	$\{3,7\}$	–	4,14,16
$\{12\}$	–	10	$\{5,17\}$	4,10,14	–
$\{13\}$	–	12	$\{4,10,14\}$	–	–
$\{14\}$	1	–	$\{4,14,16\}$	1,5	–
$\{15\}$	3	17	$\{4,8,10\}$	–	3,7

Table 4.1: Transition table for the leaf-partition of Figure 4.5(a)

requires a different technique to extract deterministic transitions out of leaf-partitions. This is the topic of the next section.

4.2.2 Back-propagation

In Figure 4.4(b) the location marked by $\oplus$ represents the junction of two boundary elements of ∂^l, the boundary of cell q_l. Let us assume that the input value is selected instantaneously when the flow encounters the boundary of a cell. Furthermore, we assume that the input value remains unchanged while the flow travels through a cell. In this case one can interpret a transition as the travelling between boundaries.

Remark 4.15 From an engineering point of view the above assumption about the absence of delay in the switching of input values is not realistic. This ideal scenario

is considered here for ease of treatment. However a generalization to a situation with delays needs to be developed.⋄

If the location corresponding to $\oplus$ on ∂^l is a submanifold, then it can be back-propagated with respect to the input value σ_k (illustrated by a dotted line with an arrowhead). If the back-propagation of $\oplus$ on ∂^l also results in a submanifold on ∂^l, then locally ∂^l can be divided in two subsets, say ∂_a^l and ∂_b^l as shown in Figure 4.4(b). In this case, if a trajectory enters cell q_l by intersecting with ∂_a^l (resp., ∂_b^l), then it will lead to cell q_j (resp., q_k), thus leading to deterministic transitions.

A more complex scenario is provided by Figure 4.4(c) where the flow initiated in q_l can lead to cell q_i, q_j, or q_k. In that situation, there is non-transversality between the flow $\phi_{k'}$ and the boundary ∂^l at the location marked by $\otimes$. Section 4.1 provides conditions under which the location marked by $\otimes$ is locally well-characterized. As in the previous situation if the back-propagation of locations marked by $\oplus$ and $\otimes$ on leaf segments leads to submanifolds on the boundary ∂^l, then it is possible to locally divide the cell boundary so that nondeterministic transitions induced by $\sigma_{k'}$ are eliminated. In the case of Figure 4.4(c) one could divide the boundary of q_l from which originates the flow leading to q_i, q_j, and q_k, into three regions ∂_a^l, ∂_{b1}^l and ∂_{b2}^l.

In principle, the back-propagation approach seems more appropriate than the subset construction for the removal of nondeterministic transitions induced by leaf-partitions. However this is done at the expense of requiring an analysis of the partition and of its transversality property. We postpone the details of an application of the back-propagation technique until Chapter 6.

Remark 4.16 In the ideal case the set of locations marked by $\oplus$ and $\otimes$ correspond to submanifolds. In the situation where $D \subseteq \mathbb{R}^2$ those objects often reduce to points and are, therefore, easier to back-propagate.⋄

4.3   Summary

This chapter depicts the importance of transversality for leaf-partitions of CSSs (both nearly integrable CSSs and ICSSs). First, we have provided a characterization of the locations where non-transversal intersections (between trajectories and leaves) do not define a submanifold. Also we have identified a transversality property that facilitates the analysis of transitions based on a reduced number of points in the neighborhood of non-transversal locations. Then we have investigated the occurrence of nondeterministic transitions resulting from leaf-partitions. It follows that some areas of partition cells are more likely to lead to such transitions. In order to perform the removal of nondeterministic transitions we have considered two different techniques, one of which relies on the transversality features of the leaf-partition.

The next chapter states a prerequisite in order to fully benefit from the transversality assessment of the leaf-partitions of CSSs.

Chapter 5

Bounded Leaf-Partitions

Chapter 4 provided a means of characterizing transitions through the leaves of a leaf-partition. This directly leads to a method for extracting transitions of partition cells whose boundary is made of subsets of leaves only. However there is no guarantee that such cells exist, thus rendering the analysis of transitions more intricate. For instance, a partition generated by the leaves of Example 3.10 with $\sigma = 0$ (see Figure 3.9(b) on page 43) has partition cells consisting of slices (see page 52) whose boundary points do not all belong to leaves. Furthermore even though a visual inspection is possible for systems in $\mathbb{R}^2$, the task of verifying the existence of such cells becomes complex for higher-dimensional systems. Another concern about the transition structure induced by a leaf-partition is the potentially large number of first integrals contained in Γ, which increases the burden of determining the transitions through leaves.

Motivated by the above reasons we undertake the identification of conditions under which a set of first integrals $\hat{\Gamma} \subseteq \Gamma$ defined in $D' \subset \mathbb{R}^n$ may lead to a partition made of cells whose interior is bounded by leaves. In Section 5.1 we introduce two notions of boundedness by leaves: L-boundedness and L$^\epsilon$-boundedness. In Section 5.2, we proceed with a characterization of those properties for nearly integrable CSSs. Namely, sufficient conditions for L-boundedness and L$^\epsilon$-boundedness are provided.

5.1 Boundedness by Leaves

The first notion to be introduced is that of "boundedness by leaves", or *L-boundedness* for short. A nonempty open set $P \subset D'$ is *L-bounded* if every boundary point in ∂P belongs to a leaf. An *L-partition* is a special type of leaf-partition for which the interior of each cell is L-bounded. In that case, one can interpret L-boundedness as a homogeneity requirement among the cells of a leaf-partition. A local version of L-boundedness is given next.

Definition 5.1 (L^ϵ-boundedness) Let P be an open subset of D'. A point $p \in P$ is L^ϵ-*bounded* if for any neighborhood of p, $N_p \subset P$, there exists an open subset of N_p containing p and whose boundary points belong to leaves.◊
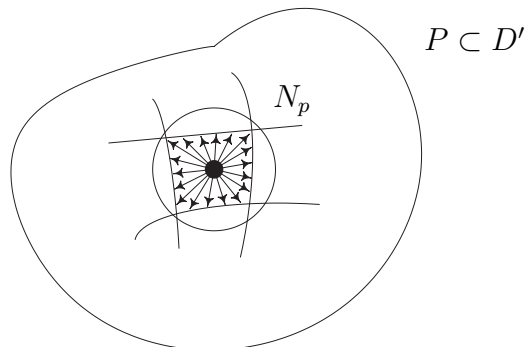
Figure 5.1: An L^ϵ-bounded point (black dot)

Therefore Definition 5.1 requires the existence of an L-bounded neighborhood of p. An example of an L^ϵ-bounded point is provided in Figure 5.1 where a point (black dot) is enclosed by four leaves that collectively define an open set contained in N_p (the circular set). Failure to satisfy the L^ϵ-boundedness property at a point says that, due to some obstruction, one cannot build an L-bounded neighborhood of arbitrary size around that point, thus indicating a limitation of the leaf-partition granularity.

In the following section, we define some relationships between L-boundedness and L^ϵ-boundedness.

5.2 L-boundedness for Nearly Integrable CSSs

In this section, we determine conditions under which the L-boundedness of a subset of D' is ensured. The overall approach uses the L^ϵ-boundedness in order to show that L-boundedness holds. For this reason we first provide a sufficient condition for the L^ϵ-boundedness, which is then relaxed. This is followed by a characterization of the L-boundedness property for nearly integrable CSSs.

As shown in Figure 5.1, if at a point p one looks in all possible directions and visually encounters a leaf, then intuitively p should be L^ϵ-bounded. The following proposition shows that this condition is indeed sufficient for the L^ϵ-boundedness of p.

Proposition 5.2

Consider an open subset $P \subset D'$ and a nearly integrable CSS with a collection of first integrals $\hat{\Gamma} \subseteq \Gamma$ defined on D'. A point $p \in P$ is L^ϵ-bounded if, for any non-trivial vector v in $\mathbb{R}^n$ there is a first integral γ in $\hat{\Gamma}$ with a leaf transversal to v at p, i.e.,

$$(\forall v \in \mathbb{R}^n \setminus \{0\}) \; (\exists \gamma \in \hat{\Gamma}) \;\; d\gamma(x) \cdot v|_{x=p} \neq 0. \diamond \tag{5.1}$$

Proof: The proof proceeds in two steps. First it is shown that at p there exist n first integrals with linearly independent differentials. Those first integrals are then used to construct a neighborhood of p bounded by leaves.

We show by contradiction that there are n first integrals with linearly independent differentials satisfying condition (5.1) at point p. Assume that $rank(d\hat{\Gamma}(x)|_{x=p}) = k$, with $k < n$ and where $d\hat{\Gamma}(x)$ represents the matrix formed of the differential of all first integrals contained in $\hat{\Gamma}$. Note that $k > 0$ otherwise $d\gamma \cdot v|_{x=p} = 0$ for all $\gamma \in \hat{\Gamma}$ and condition (5.1) is violated at p. Let $\gamma_1(x), \ldots, \gamma_k(x)$ be the set of k linearly independent first integrals at p. Also let us complete this set by $n - k$ smooth functions $\lambda_{k+1}(x), \ldots, \lambda_n(x)$ defined on D' so that $\alpha(x) = [\gamma_1(x), \ldots, \gamma_k(x), \lambda_{k+1}(x), \ldots, \lambda_n(x)]^T$

satisfies $rank(d\alpha(x)|_{x=p}) = n$. Therefore the map $\alpha : D' \to \mathbb{R}^n$ defines at p a local diffeomorphism, which, in turn, yields a local coordinate system $y = \alpha(x)$. Now let w be a nontrivial vector defined at $q = \alpha(x)|_{x=p}$ such that $w = [\underbrace{0, \ldots, 0}_{k}, \times, \ldots, \times]^T$ with $\times$ representing any nonzero value. Since $d\alpha|_x : \mathbb{R}^n \to \mathbb{R}^n$ is a linear map and $d\alpha|_p$ is non-singular it is thus possible to determine a unique vector v at p such that $d\alpha|_p v = w$. With the first k zero entries of w the vector v must annihilate the differential of each first integral $\gamma_1(x), \ldots, \gamma_k(x)$ at p, whereas the last $n - k$ nonzero values in w imply that $v \neq 0$. By assumption, any first integral γ in $\hat{\Gamma}$ can be expressed as a linear combination of $\gamma_1(x), \ldots, \gamma_k(x)$ at p. Therefore one gets $d\gamma \cdot v|_{x=p} = 0$ for all $\gamma \in \hat{\Gamma}$, contradicting condition (5.1). Consequently at p there is a collection of n first integrals $\gamma_1(x), \ldots, \gamma_n(x)$ with linearly independent differentials, i.e., $d\gamma_1(x) \wedge \cdots \wedge d\gamma_n(x)|_{x=p} \neq 0$.

If $d\gamma_1(x) \wedge \cdots \wedge d\gamma_n(x) = \beta(x) dx_1 \wedge \cdots \wedge dx_n$ then it follows from the smoothness of the first integrals that $\beta : D' \to \mathbb{R}$ is smooth. Moreover the restriction of β to the open set $P \subset D'$ is continuous. Given that $\beta(x)|_{x=p} = c$ for some $c \in \mathbb{R} \setminus \{0\}$, the continuity of β over P implies that for N_c, an open neighborhood of c in $\mathbb{R} \setminus \{0\}$, there exists a neighborhood of p, say $N_p \subset P$, such that $\beta(x)|_{x=p'} \in N_c$ for all $p' \in N_p$. Therefore $\gamma_1(x), \ldots, \gamma_n(x)$ form a collection of linearly independent first integrals everywhere in N_p. We then use each first integral $\gamma_i(x)$, $i \in \{1, \ldots, n\}$, to define a slice S_i. This can be done by a slight perturbation of the leaf induced by $\gamma_i(x)$ and defined at p. Let $\gamma_i(x)|_{x=p} = c_i$ for some $c_i \in \mathbb{R}$, an let ϵ_i be a small value so that $c_i - \epsilon_i < c_i + \epsilon_i$. Then a slice is defined as the set $S_i := \{p' \in N_p \mid c_i - \epsilon_i < \gamma_i(x)|_{x=p'} < c_i + \epsilon_i\}$. Thus a slice is an open subset of N_p containing p and bounded by two leaves and ∂N_p, the boundary of N_p. As $\beta(x)|_{x=p'} \in N_c$ for all $p' \in N_p$, it follows that $\gamma_i(x)$ has leaves defined everywhere in N_p. That is, ϵ_i can be made arbitrarily small so that the leaves of S_i are arbitrarily close to p. Therefore the collection of slices $S_1, \ldots, S_n$ forms a set $R_p := \bigcap_{i=1}^n S_i$, which by construction is open, contained in N_p, and contains p. It

remains to show that R_p has its boundary made of leaves only. This follows by the fact that the slices are mutually transversal in N_p and that R_p can be made arbitrarily small in N_p.□

Remark 5.3 It follows from Proposition 5.2 that R_p is diffeomorphic to an n-dimensional rectangle K^n. Given a set S and two points $p', p'' \in S$, if there exists a continuous map $h : [0,1] \to S$ such that $h(0) = p'$ and $h(1) = p''$ we say that a path in S joins p' to p''. If for any two points p' and p'' of S there is path joining p' to p'', we say that S is *path-connected* (Kasriel, 1971). The set $S = K^n$ is an example of a path-connected set. By using the map $h^* = \alpha^{-1} \circ h$, with α as defined in the first part of the previous proof, and a result on connected sets in §A.2.1 (see page 145), it can be shown that R_p is path-connected, and thus connected.◇

The sufficient condition of Proposition 5.2 refers to the notion of transversality previously defined. Indeed, Proposition 5.2 requires that locally there are mutually transversal leaves in sufficient number at p. Since the condition uses the differential of first integrals in $\hat{\Gamma}$, it characterizes all leaves that may be involved in further refinements or aggregations of the leaf-partition. We now present some closure property that L-bounded sets possess.

Proposition 5.4

Let R_a and R_b be L-bounded subsets of D'. Then $R_a \cup R_b$ forms an L-bounded set. Moreover if R_a and R_b are connected and $R_a \cap R_b \neq \emptyset$, then $R_a \cup R_b$ is connected.◇

Proof: If $p \in R_a \cup R_b$ then either $p \in R_a$ or $p \in R_b$. It follows from the openness of R_a and R_b that there exists a neighborhood of p, N_p, contained in R_a or R_b, i.e., $N_p \subset R_a \cup R_b$. Therefore the set $R_a \cup R_b$ is open and nonempty (since R_a and R_b are by definition nonempty).

Now we show that $\partial(R_a \cup R_b) \subset \partial R_a \cup \partial R_b$. Let $p \in \partial(R_a \cup R_b)$. Thus any neighborhood N_p of p intersects with both $R_a \cup R_b$ and $(R_a \cup R_b)^c$, the complement of

$R_a \cup R_b$ in D'. It follows that either $N_p \cap R_a \neq \emptyset$ or $N_p \cap R_b \neq \emptyset$. As $(R_a \cup R_b)^c \subset R_a^c$ and $(R_a \cup R_b)^c \subset R_b^c$, one gets that $N_p \cap (R_a \cup R_b)^c \neq \emptyset$ leads to $N_p \cap R_a^c \neq \emptyset$ and $N_p \cap R_b^c \neq \emptyset$. Consequently $p \in \partial R_a$ or $p \in \partial R_b$, i.e., $p \in \partial R_a \cup \partial R_a$, thus proving the claim. Therefore the open and nonempty set $R_a \cup R_b$ has it boundary made of the leaves of ∂R_a or ∂R_b, that is $R_a \cup R_b$ is L-bounded.

The connectedness of $R_a \cup R_b$ follows from $R_a \cap R_b \neq \emptyset$ and a byproduct of Theorem A.2 (page 145) which implies that the union of a collection of intersecting connected sets results in a connected set.$\square$

Among other things, Proposition 5.4 says that any two intersecting L-bounded sets can be "glued" together to form an L-bounded set. Moreover a collection of intersecting L-bounded sets can be combined so that it forms a larger L-bounded set. This feature is now exploited to show that condition (5.1) is not necessary for the L^ϵ-boundedness of a point.

Proposition 5.5

Assume that condition (5.1) of Proposition 5.2 holds for all points of the open set $O \setminus \{p\}$ where $O \subset P$ is a neighborhood of p. Then p is L^ϵ-bounded.◇

Proof: We first define an arbitrary open subset $O' \subset O$ containing p, and a n-dimensional empty sphere $\partial B_p^\delta \subset O'$ centered at p and of radius $\delta > 0$. Let p' be any point of ∂B_p^δ and select a neighborhood of p', $N_{p'} \subset O'$. By assumption p' is such that condition (5.1) holds. Therefore Proposition 5.2 implies that there exists an L-bounded set $R_{p'}$ containing p' and contained in $N_{p'}$. Now select any point p'' belonging to $\partial R_{p'} \cap \partial B_p^\delta$ so that there is an L-bounded set $R_{p''} \subset O'$ containing p'' and intersecting with $R_{p'}$ (see Figure 5.2(a)). Thus Remark 5.3 and Proposition 5.4 imply that $R_{p'} \cup R_{p''}$ forms an L-bounded set. Moreover one can repeat the above steps until the resulting set contains ∂B_p^δ. If R denotes the set thus constructed, then the boundary ∂R acts as an envelope for ∂B_p^δ as shown in Figure 5.2(b). Now let B_p^δ denote the n-dimensional open ball (a filled sphere without its boundary) centered

at p and of radius δ. Therefore the open set $R \cup B_p^\delta$ is connected (as $R \cap B_p^\delta \neq \emptyset$ and by Theorem A.2), contains p, and is bounded by leaves. Since O' and ∂B_p^δ are of arbitrary size, so is $R \cup B_p^\delta$, thus proving that p is L$^\epsilon$-bounded.□
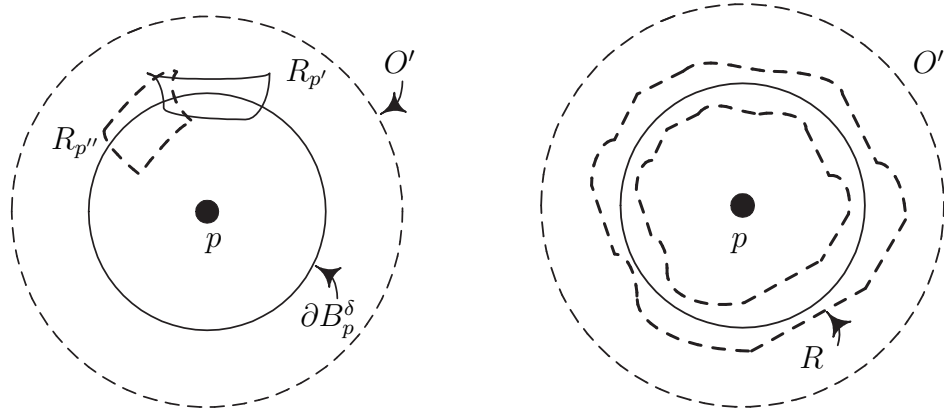
(a) Two intersecting L-bounded sets   (b) Resulting L-bounded set

Figure 5.2: Construction of an L-bounded set for a point p

The technique to construct an L-bounded set in Proposition 5.5 shows that the L$^\epsilon$-boundedness of every point of a subset of D' leads to an L-bounded set. However the condition of Proposition 5.5 is not necessary for L-boundedness of a subset of D'. For instance, consider a leaf-partition induced by a single first integral (such as in Figure 3.12 on page 52). In this situation L$^\epsilon$-boundedness does not hold for any point in D' because no leaves intersect anywhere in D'. This scenario includes the case of leaf-partitions made of compact leaves, which can lead to L-bounded sets. An example of such a partition consists of a finite collection of concentric annuli in $\mathbb{R}^2$.

To verify the L$^\epsilon$-boundedness of a point, condition (5.1) of Proposition 5.2 remains difficult to check due to the large number of vectors involved. An easier route may be to consider the information about the non-transversality of the first integrals of $\hat{\Gamma}$. Given a collection of first integrals $\hat{\Gamma} \subseteq \Gamma$, we define the set of points where non-transversality occurs as

$$\Omega(\hat{\Gamma}) := \{p \in D' \mid rank(d\hat{\Gamma}(x)|_{x=p}) < n\}, \qquad (5.2)$$

where $rank(d\hat{\Gamma}(x)|_{x=p})$ stands for the rank of the matrix formed by the differential of all first integrals in $\hat{\Gamma}$ evaluated at p. In general, the set $\Omega(\hat{\Gamma})$ may require as much analysis as D' does. For instance, this occurs whenever $\hat{\Gamma}$ is such that $\#\hat{\Gamma} < n$, leading automatically to $\Omega(\hat{\Gamma}) = D'$. Another scenario where $\Omega(\hat{\Gamma}) = D'$, despite the fact that $\#\hat{\Gamma} = n$, consists of the triple integrator of Example 3.10 (see page 42) with $\hat{\Gamma} := \{\gamma_1^\alpha, \gamma_2^\alpha, \gamma_1^\beta\}$, where $\alpha = 0$ and $\beta \neq 0$.

The following result shows that whenever $\Omega(\hat{\Gamma})$ satisfies some properties any subset P of D' has an L-bounded subset.

Proposition 5.6

Consider a nearly integrable CSS with a set of first integrals $\hat{\Gamma} \subseteq \Gamma$ and a non-transversality set $\Omega(\hat{\Gamma})$. If $\Omega(\hat{\Gamma})$ is closed and has a dense complement in D', then for any open set $P \subset D'$ there exists a connected L-bounded subset $P' \subset P$.$\diamond$

Proof: Since $\Omega(\hat{\Gamma})$ is closed and of measure zero then $P \setminus \Omega(\hat{\Gamma})$ is an open set where there are n first integrals with linearly independent differentials. As shown in Proposition 5.2 an arbitrary point p in $P \setminus \Omega(\hat{\Gamma})$ is L^ϵ-bounded, and is thus contained in an L-bounded set. A larger connected L-bounded subset $P' \subset P$ can then be obtained by taking the sequential union of intersecting L-bounded sets as in the proof of Proposition 5.5, which completes the proof.$\square$

In practice, various situations may lead to a set $\Omega(\hat{\Gamma})$ with the characteristics of Proposition 5.6. Indeed, in the presence of analytic first integrals defined over a connected set D', condition 4.3(i) (on page 59) implies that if $\hat{\Gamma}$ contains at least one set of n first integrals $\Gamma^a \cup \{\gamma_j^b\}$ for some $\sigma_a, \sigma_b \in \Sigma$ with $\sigma_a \neq \sigma_b$, then the set $\Omega(\hat{\Gamma})$ is guaranteed to be closed and to have an empty interior. In particular, this includes the case where $\hat{\Gamma} = \Gamma$ and $\#\Sigma \geq 2$.

In order to limit the number of vectors used to verify the L^ϵ-boundedness property, we restrict ourselves to vectors that are tangent to $\Omega(\hat{\Gamma})$ at a point. Notice that a closed set with an empty interior $\Omega(\hat{\Gamma})$ may fail to be convex (ref. the "++" shape

formed by $\{(x_1 \in \{\frac{1}{2}\pi, \frac{3}{2}\pi\}, x_2)\} \cup \{(x_1, x_2 = 0)\}$ in Figure 4.3 on page 72) and to have a well-defined tangent space. For this reason we define $H_{\Omega(\hat{\Gamma})}(p)$ as the set of vectors in $\mathbb{R}^n$ that are tangent to $\Omega(\hat{\Gamma})$ at p. More precisely a vector v belongs to $H_{\Omega(\hat{\Gamma})}(p)$ if

there exist a sequence p_i in $\Omega(\hat{\Gamma})$ converging to p, a sequence β_i in $(\infty, 0)$ decreasing to 0, and a sequence v_i converging to v such that $p_i + \beta_i v_i \in \Omega(\hat{\Gamma})$ for all i.

Note that the zero vector belongs to $H_{\Omega(\hat{\Gamma})}(p)$ for all $p \in \Omega(\hat{\Gamma})$ and that $H_{\Omega(\hat{\Gamma})}(p)$ is a relaxation of the notion of tangent cone provided in §A.3 (on page 148) and as developed in (Clarke, 1990).

By exploiting the knowledge about non-transversality among the leaves induced by $\hat{\Gamma}$, a sufficient condition for L^ϵ-boundedness can be written in the following manner.

Lemma 5.7 *Consider a set of first integrals $\hat{\Gamma}$ defined over D' such that the set $\Omega(\hat{\Gamma})$ is closed and has a dense complement in D'. Let p be an arbitrary point in $\Omega(\hat{\Gamma})$. The point p is L^ϵ-bounded if for each nontrivial vector $v \in H_{\Omega(\hat{\Gamma})}(p)$ there is a first integral $\gamma \in \hat{\Gamma}$ such that $d\gamma(x) \cdot v|_{x=p} \neq 0.\diamond$*

Proof: Let N_p be an arbitrary small neighborhood of p. For any point in the open set $N_p \setminus \Omega(\hat{\Gamma})$, there exists an L-bounded neighborhood (ref. Proposition 5.5). Let A denote all L-bounded sets contained in $N_p \setminus \Omega(\hat{\Gamma})$, and let $\overline{A}$ represent the union of the closure of elements in A. Since $\Omega(\hat{\Gamma})$ has a dense complement, any point in $N_p \cap \Omega(\hat{\Gamma})$ is arbitrarily close to A and contained in $\overline{A}$. Also N_p can be chosen so that A is arbitrarily close to p. If p is an isolated point in $\Omega(\hat{\Gamma})$, then the interior of $\overline{A}$ is an L-bounded set containing p. Assume that p belongs to a connected subset of $\Omega(\hat{\Gamma})$. By assumption, there are leaves transversal to $\Omega(\hat{\Gamma})$ at p. Consequently, for any point sufficiently close to p in $N_p \cap \Omega(\hat{\Gamma})$ a leaf is defined. Since any such leaf intersects with L-bounded sets in A, it is possible to form an L-bounded neighborhood for p. As N_p is of arbitrary size, the point p is L^ϵ-bounded, which completes the proof.$\square$

In words, Lemma 5.7 requires that $H_{\Omega(\hat{\Gamma})}$ is everywhere locally transversal to some leaves induced by the first integrals of $\hat{\Gamma}$.

In an attempt to characterize the existence of L-partitions on a subset of D', we have used two boundedness properties, a local one and a semi-global one. Sufficient conditions ensuring the two types of boundedness are given. However the proofs of sufficiency of L^ϵ-boundedness are based on the existence of local leaves, which is a more general approach than the construction of leaf-partitions as defined in §3.3.2. Therefore a necessity result is required in order to conclude if leaf-partitions generated from $\hat{\Gamma}$ fail to satisfy the L^ϵ-boundedness property. Also the use of L^ϵ-boundedness does not lead to a necessary condition for L-boundedness. Consequently, the local boundedness property cannot be used to conclude about the existence of L-partitions for leaf partitions as defined in §3.3.2.

Now we use a series of examples in order to illustrate the effect of the set of first integrals $\hat{\Gamma}$ and the choice of the region to partition on the sufficient conditions leading to the L^ϵ-boundedness property. We begin with the double integrator introduced in previous chapters.

Example 5.8 For the double integrator we consider the first integral $\gamma_1^\sigma(x) = \sigma x_1 - \frac{1}{2}x_2^2$ defined over $D' = D = \mathbb{R}^2$. Also we assume $\Sigma := \{\sigma_1, \sigma_2\}$ with $\sigma_1 \neq \sigma_2$ and $\hat{\Gamma} := \{\gamma_1^1, \gamma_1^2\}$. Therefore one gets $d\gamma_1^\sigma := [\sigma \quad -x_2]$ and $\Omega(\hat{\Gamma}) := \{(x_1, x_2 = 0)\}$. In this case, for any $p \in \Omega(\hat{\Gamma})$ the set $H_{\Omega(\hat{\Gamma})}(p)$ looks like $\{0_2, [\lambda \ 0]^T\}$ where $\lambda \in \mathbb{R} \setminus \{0\}$ and 0_2 represents the two-dimensional zero vector. Thus the condition of Lemma 5.7 is satisfied everywhere in D' because for $v := [\pm 1, 0]^T$ one has $d\gamma_1^\sigma \cdot v = \pm\sigma \neq 0$ for at least one σ in Σ (since both values cannot be equal to zero).●

The following example illustrates how the selection of $\hat{\Gamma}$ may lead to a violation of the sufficient condition of Lemma 5.7.

Example 5.9 Consider the triple-integrator (ref. Example 3.10, page 42) with the

first integrals $\gamma_1^k(x_1, x_2, x_3) = \sigma_k^2 x_1 - x_2 x_3 \sigma_k + x_3^3/3$ and $\gamma_2^k(x_1, x_2, x_3) = -x_2 \sigma_k + \frac{1}{2}x_3^2$

defined on $D' = D = \mathbb{R}^3$. Also assume that $\hat{\Gamma} := \{\gamma_1^{k1}, \gamma_1^{k2}, \gamma_1^{k3}\}$ with distinct input

values $\sigma_{ki} \in \Sigma$, $i \in \{1, 2, 3\}$. Then one has

$$d\gamma_1^k(x_1, x_2, x_3) = \begin{bmatrix} \sigma_k^2 & -x_3\sigma_k & (-x_2\sigma_k + x_3^2) \end{bmatrix}, \qquad (5.3)$$

so that

$$\Omega(\hat{\Gamma}) := \{(x_1, x_2, x_3 = 0)\}, \qquad (5.4)$$

where $rank(d\hat{\Gamma}) = 1$ for points in $\{(x_1, x_2 = 0, x_3 = 0)\}$ while $rank(d\hat{\Gamma}) = 2$ for points

in $\{(x_1, x_2 \neq 0, x_3 = 0)\}$. The set $\Omega(\hat{\Gamma})$ defines an $x_1 - x_2$ plane passing through the

origin. For any point $p \in \Omega(\hat{\Gamma})$, one has $H_{\Omega(\hat{\Gamma})}(p) = \{0_3, [\lambda \ \alpha \ 0]^T\}$ where $\lambda, \alpha \in \mathbb{R}$.

With the vector $v := [0; 1; 0]^T$ one gets $d\gamma_1^k(x) \cdot v|_{x=p} = 0$ for $p \in \{(x_1, x_2, x_3 = 0)\}$ and

any σ_k, thus violating the condition of Lemma 5.7. However, if $\hat{\Gamma} := \{\gamma_1^{k1}, \gamma_2^{k2}, \gamma_1^{k3}\}$

with $\sigma_{k2} \neq 0$ then

$$d\gamma_2^{k2}(x_1, x_2, x_3) = [0 \ -\sigma_{k2} \ x_3] \quad \text{and} \quad \Omega(\hat{\Gamma}) := \{(x_1, x_2 = 0, x_3 = 0)\}, \qquad (5.5)$$

so that $H_{\Omega(\hat{\Gamma})}(p) = \{0_3, [\lambda \ 0 \ 0]^T\}$ with $\lambda \in \mathbb{R} \setminus \{0\}$ and for any $p \in \Omega(\hat{\Gamma})$. Therefore

with $v := [1; 0; 0]^T$ one gets $d\gamma_1^k(x) \cdot v|_{x=p} = \sigma_k^2 \neq 0$ for some $\sigma_k \in \Sigma$ (since only one

input can equal zero) and for any $p \in D'$. Thus the set $\hat{\Gamma} := \{\gamma_1^{k1}, \gamma_2^{k2}, \gamma_1^{k3}\}$ defined

above is such that all points in D' satisfy the conditions of Lemma 5.7.$\bullet$

In the previous example, the transversality requirement among the leaves is sat-

isfied by introducing the second first integral, i.e., using both first integrals γ_1^k and

γ_2^k in $\hat{\Gamma}$. The next example demonstrates that a restriction on D' may be required in

order to satisfy the condition of Lemma 5.7.

Example 5.10 (Controlled predator-prey model with limited growth) The Lotka-Volterra model captures the dynamics of predator and prey populations. When limited growth is considered the model becomes

$$
\begin{aligned}
\dot{x}_1 &= (-Ax_1 - Bx_2 + \lambda)x_1 \\
\dot{x}_2 &= (Cx_1 - Fx_2 - \mu)x_2,
\end{aligned}
\tag{5.6}
$$

where x_1 and x_2 represent the prey and predator populations evolving on $D = \mathbb{R}^2$ and A, B, C, F, λ and μ are real positive constants (Hirsch and Smale, 1974). With $A = F = 0$ one obtains the classical Lotka-Volterra model for which infinite growth is possible. A controlled version of the above model is obtained if one considers $\lambda = \alpha_1 u$ and $\mu = \alpha_2 u$ for some $\alpha_1, \alpha_2 \in \mathbb{R}$ and an input value $u = \sigma \in \mathbb{R}$ (De Leenheer and Aeyels, 2000). An interesting and academic example is due to (Goriely, 2001) where $A = 1$, $B = 5$, $C = 1$, $F = -1$, $\alpha_1 = 3$ and $\alpha_2 = 1$. Figure 5.3 shows level curves of the first integral

$$
\gamma_1^\sigma(x_1, x_2) = x_1^3 x_2^3 - 6x_1^2 x_2^3 \sigma + 6x_1^2 x_2^4 + 9x_1 x_2^3 \sigma^2 - 18x_1 x_2^4 \sigma + 9x_1 x_2^5,
\tag{5.7}
$$

with $\sigma = 1$. The Jacobian of (5.7) gives

$$
\left[3x_2^3(-\sigma + x_1 + x_2)(x_1 - 3\sigma + 3x_2) \quad 3x_1 x_2^2(-3\sigma + x_1 + 5x_2)(x_1 - 3\sigma + 3x_2) \right]
\tag{5.8}
$$

The phase plane of Figure 5.3 is divided by three thick lines which are the zero-level sets of the expressions $J_1 = x_1$, $J_2 = x_2$, and $J_3 = x_1 - 3\sigma + 3x_2$. The quantities J_1, J_2 and J_3 correspond to local invariants. Indeed, one notices that $\dot{J}_i = \alpha J_i$, $i \in \{1, 2, 3\}$, where α is some polynomial in x_1 and x_2. Notice that the first integral in (5.7) is obtained by the product $\gamma_1^\sigma(x_1, x_2) = J_1 J_2^3 J_3^2$. Now consider $\Sigma = \{\sigma_a, \sigma_b\}$ with

90
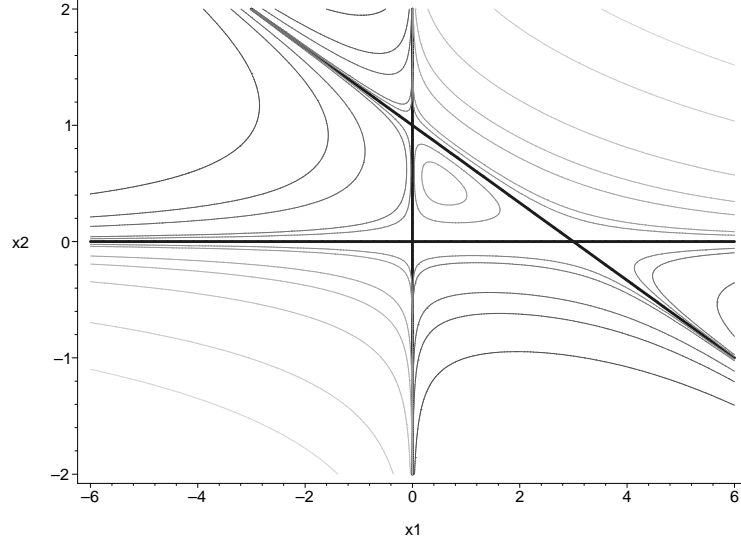
Figure 5.3: Level curves of first integral (5.7) with $\sigma = 1$

$\sigma_a \neq \sigma_b$, and $\hat{\Gamma} := \{\gamma_1^a, \gamma_1^b\}$. Therefore one gets

$$
\begin{aligned}
\Omega(\hat{\Gamma}) \quad := \quad & \{(x_1 = 0, x_2)\} \cup \{(x_1, x_2 = 0)\} \cup \{(x_1, x_2) \mid x_1 - 3\sigma_a + 3x_2 = 0\} \ldots \\
& \cup \{(x_1, x_2) \mid x_1 - 3\sigma_b + 3x_2 = 0\} \cup \{(x_1, x_2) \mid x_1 - x_2 = 0\}.
\end{aligned}
\tag{5.9}
$$

Consequently we have that

for $p \in \{(x_1 = 0, x_2)\}$ $\quad$ then $H_{\Omega(\hat{\Gamma})}(p) = \{0_2, [0 \ \lambda]^T\}$,

for $p \in \{(x_1, x_2 = 0)\}$ $\quad$ then $H_{\Omega(\hat{\Gamma})}(p) = \{0_2, [\lambda \ 0]^T\}$,

for $p \in \{(x_1, x_2) \mid x_1 - 3\sigma_a + 3x_2 = 0\}$ $\quad$ then $H_{\Omega(\hat{\Gamma})}(p) = \{0_2, [-3\lambda \ \lambda]^T\}$,

for $p \in \{(x_1, x_2) \mid x_1 - 3\sigma_b + 3x_2 = 0\}$ $\quad$ then $H_{\Omega(\hat{\Gamma})}(p) = \{0_2, [-3\lambda \ \lambda]^T\}$,

for $p \in \{(x_1, x_2) \mid x_1 - x_2 = 0\}$ $\quad$ then $H_{\Omega(\hat{\Gamma})}(p) = \{0_2, [\lambda \ \lambda]^T\}$,

where $\lambda \neq 0$. We then analyze the subsets comprising $\Omega(\hat{\Gamma})$ in order to detect if the conditions of Lemma 5.7 hold. In particular, those conditions are violated for vectors of the type $v := [\pm 1; 0]^T$ and $v := [0; \pm 1]^T$ along $\{(x_1, x_2 = 0)\}$ and $\{(x_1 = 0, x_2)\}$,

respectively. For the sets $\{(x_1, x_2) \mid x_1 - 3\sigma_a + 3x_2 = 0\}$ and $\{(x_1, x_2) \mid x_1 - 3\sigma_b + 3x_2 = 0\}$ the requirements are not satisfied at $(x_1, x_2) = (3\sigma, 0)$, and $(x_1, x_2) = (\frac{3}{4}\sigma, \frac{3}{4}\sigma)$ where $\sigma \in \Sigma$. Finally for the subset $\{(x_1, x_2 \mid x_1 - x_2 = 0)\}$ a pointwise failure occurs at $(x_1, x_2) = (0, 0)$, $(x_1, x_2) = (\frac{1}{2}\sigma, \frac{1}{2}\sigma)$ and $(x_1, x_2) = (\frac{3}{4}\sigma, \frac{3}{4}\sigma)$ where $\sigma \in \Sigma$.

By Proposition 5.5, L$^\epsilon$-boundedness holds at $(x_1, x_2) = (\frac{1}{2}\sigma, \frac{1}{2}\sigma)$ and $(x_1, x_2) = (\frac{3}{4}\sigma, \frac{3}{4}\sigma)$. Therefore if D' is restricted to $\mathbb{R}_{>0} \times \mathbb{R}_{>0}$ the sufficient conditions for L$^\epsilon$-boundedness are satisfied.●

In reference to a necessary condition for L$^\epsilon$-boundedness, we believe that the sufficient condition of Lemma 5.7 is conservative and that its relaxation may lead to the expected result. This position is supported by the following facts. First, it can be observed visually that a leaf-partition built with the first set of first integrals in Example 5.9 always has an aperture aligned with the x_2 axis. In the case of Example 5.10, the sufficient condition of Lemma 5.7 is violated at the locations corresponding to those local invariants that are independent of the input value. Therefore in both cases the violation of the condition of Lemma 5.7 indicates obstructions to form a cell whose interior is L-bounded.

5.3   Summary

In this chapter we have investigated the conditions under which a set of first integrals may generate a partition made of cells whose boundary points belong to leaves. For this purpose, we have proposed semi-global and local properties of boundedness by leaves. Then we have performed a characterization of these properties for nearly integrable CSSs and have suggested a set of sufficient conditions. Also we have demonstrated with examples that those conditions depend on the chosen set of first integrals and on the selection of the region to partition. The next chapter shows how to construct an FSM abstraction from a leaf-partition of a nearly integrable CSS.

Chapter 6

Two-dimensional Systems and Finiteness

In the last two chapters we discussed a transversality characteristic and a boundedness property for the leaf-partitions of a certain class of Controlled Switched Systems. In this chapter we exploit those notions in order to construct an FSM abstraction. We give sufficient conditions for the finiteness of computation of an FSM abstraction based on a leaf-partition with cells whose interior is L-bounded. Furthermore, we propose a technique for verifying the consistency property for some d-paths. The focus is on two-dimensional systems because (a) they represent a special case of the theory (ref. Remark 3.20, Remark 4.8 and Remark 4.16), and (b) such systems benefit from a visual support that is lost in higher dimensions.

In the next sections, we present a technique for synthesizing the state and transition structures of FSM abstractions based on leaf-partitions. First we provide a set of assumptions in Section 6.1. Then an algorithmic procedure is developed in Section 6.2. In Section 6.3 two case studies are presented. Section 6.4 closes the chapter with a summary.

6.1 Assumptions

This section introduces a set of assumptions related to the various elements of a nearly integrable CSS_E^π with a leaf-partition π. In the sequel, we refer to a nearly integrable CSS_E^π as a CSS_E^π. As a reminder, a leaf-partition π consists of a partition of a region $E \subset D' \subset D$, that is performed by using a subset of first integrals $\hat{\Gamma} \subseteq \Gamma$, an input value set Σ, and first integral constants or FICs (ref. pages 51 to 54). The first set of assumptions concerns the set $\hat{\Gamma}$, the space D, and the region E.

(H1) The set $\hat{\Gamma}$ is such that $\#\hat{\Gamma} \geq 2$.

(H2) The space D has a metric $\rho : D \times D \to \mathbb{R}_{\geq 0}$.

(H3) The region $E \subset D'$ is open, convex, and bounded.

The first assumption requires that $\hat{\Gamma}$ has enough elements so that intersection points between leaves exist. Assumption (H2) enables one to measure the distance between any two points in D whereas hypothesis (H3) asks that E be of finite dimension and in one piece.

The state structure resulting from a leaf-partition is built in a sequential manner by constructing objects of dimension zero (points), one (lines), and two (areas). Those points are determined by the intersection of leaves induced by the first integrals in $\hat{\Gamma}$ and the FICs. The following assumptions relate to the nature of such a set of points.

(H4) The set of all intersection points is nonempty, finite, and contained in E.

(H5) There exists an $\epsilon > 0$ such that an ϵ-neighborhood of any intersection point does not contain any other intersection point.

By the above hypotheses intersection points are finite in number and isolated in E. From the set of intersection points, one then defines line segments, which for two-dimensional systems consist of leaf segments, or subsets of leaves. The following assumptions pertain to the set of leaves and to the angle separating two vectors in D.

(H6) The space D is equipped with an inner product $\cdot : T_p D \times T_p D \to \mathbb{R}$ defined between vectors.

(H7) The set of leaves is finite.

We say that two leaf segments are *subsequent* if they share a common intersection point. The following step amounts to assembling subsequent leaf segments so that they form partition cells with an L-bounded interior. This collection of subsets of E forms the state structure of an FSM abstraction. Then one needs to determine the transition structure based on the leaf-partition and the continuous dynamics. The next hypotheses are relevant for this task.

(H8) The set of partition cells with an L-bounded interior is nonempty.

(H9) The conditions of Corollary 4.10 hold (see page 69).

(H10) The input value set Σ is finite and satisfies condition (4.3) of page 59.

Assumption (H8) requires that the leaf-partition π has some cells whose interior satisfies the L-boundedness property. Assumption (H9) is a transversality requirement whereas (H10) ensures an upper bound on the number of elements in Σ.

We briefly discuss the relative importance of some of the above assumptions. A necessary condition for hypothesis (H1) is that $\#\Sigma \geq 2$. This condition is always satisfied since with $\#\Sigma < 2$ one cannot talk about control, i.e., there is no choice of input values. Since we consider systems evolving on subsets of $\mathbb{R}^2$, assumptions (H2) and (H6) hold. As mentioned previously, assumption (H3) and the finiteness of the set Σ in (H10) are common in the context of HCSs. As for hypothesis (H5) the value ϵ can be evaluated in finite time due to (H4) and (H2). Notice that hypothesis (H7) could also be written in terms of a finite set of FICs. Overall, assumptions (H4) and (H9) are more restrictive and more difficult to check than the others.

The next section shows that, in the presence of a CSS_E^π, assumptions (H1) to (H10) are indeed sufficient conditions for obtaining an FSM abstraction for CSS_E^π in finite time.

6.2 Algorithmic Procedure

The previous section provided an overview of the technique used to extract an FSM abstraction of a CSS_E^π. Herein details are given and emphasis is put on the construction of leaf segments, partition cells, and the transition structure. Therefore the set of intersection points, obtained by solving sets of nonlinear equations, is assumed to be given and to satisfy assumption (H4).

6.2.1 One-dimensional objects

Given the intersection points, the leaf segments are first defined. This approach proceeds in two steps: first, we detect intersection points belonging to each leaf, then each leaf subset bounded by two consecutive intersection points is defined as a leaf segment. Since a leaf L is, in general, not completely contained in E, we call "branches" those sections of L that intersect with the interior of E. Figure 6.1 shows a rectangular region E and three branches of L with some intersection points represented by black dots.

The first result shows how consecutive intersection points can be determined.

Proposition 6.1

Consider a leaf-partition π and a CSS_E^π satisfying hypotheses (H2) to (H5). Let L be a leaf and $IP \neq \emptyset$ be the set of intersection points belonging to L. Then it is possible to determine the sequence of consecutive intersection points belonging to any branch of L in a finite number of steps.$\diamond$

Proof: Let $p \in IP$ be an arbitrary intersection point. Thus p belongs to a branch
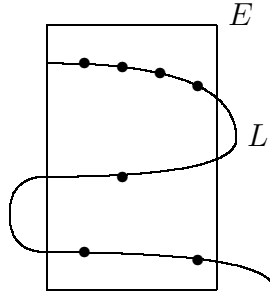
Figure 6.1: Example of a leaf L not contained in a region E.

of L, and the containment of all intersection points in E implied by assumption (H4) leads to $p \in E$.

Since FICs are regular values (see page 49), the Implicit Function Theorem (stated on page 146) enables one to determine a local characterization of the leaf L. With the metric of (H2), it is possible to depart from p and move along leaf L in a given direction (a few techniques are presented in Appendix B, on page 151). Also one can measure the distance between any two points of L, thus ensuring that each displacement along L is of magnitude $\beta\epsilon$, with $0 < \beta < 1$ and ϵ as defined in (H5). This guarantees that any intersection point on the branch of L containing p can be detected.

The above procedure can be repeated until (i) point p is reached (if the leaf loops back to p in E), or (ii) until it reaches the boundary of E. With the boundedness of E in (H3) it can be shown that there is a finite number of branches of L in E and that each branch is of finite length. Consequently one of the two scenarios described above will occur in a finite time. In case (ii) one can re-initiate the search of points from p in the opposite direction. Therefore all intersection points of the branch of L containing p are detected. The sequence of consecutive intersection points follows from their order of appearance and the search direction. Moreover, the sequence is finite since IP is a finite set by assumption (H4).

As p is chosen arbitrarily, the above procedure holds for any branch of L containing

97

an intersection point, which completes the proof.□

The finite number of leaves in assumption (H7) together with Proposition 6.1 imply that all sequences of consecutive intersection points are finite and can be determined in a finite time. Such sequences are then used to define leaf segments as those subsets of leaves bounded by two consecutive intersection points, which leads to a finite number of leaf segments. A generic representation of a leaf segment is provided in Figure 6.2 where the vector field tangent to the leaf at p is denoted by $f(p)$. Each leaf segment has two normal vectors (see $normal\_a$ and $normal\_b = -normal\_a$ in Figure 6.2) and thus contributes to the formation of at most two partition cells.
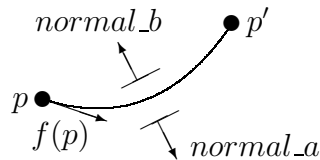
Figure 6.2: Representation of a leaf segment.

6.2.2 Two-dimensional objects

In order to benefit from the transversality property and determine transitions by investigating a reduced number of points, one needs to identify partition cells with an L-bounded interior. These sets are open subsets of E bounded by sequence(s) of leaf segments

(a) where each sequence of leaf segments loops back to a departing segment and thus forms a closed curve and,

(b) where the area delimited by the looping sequences does not contain any other leaf segment.

Figure 6.3 exhibits two distinct types of partition cells whose interior (the hatched region) is bounded by leaves. The cell of Figure 6.3(a) has a single closed curve as its boundary whereas that of Figure 6.3(b) is bounded by two closed curves made of leaf segments. Since the type of cells in Figure 6.3(a) is more frequent, the development to follow is restricted to such cells.

<div align="center">(a)   (b)</div>
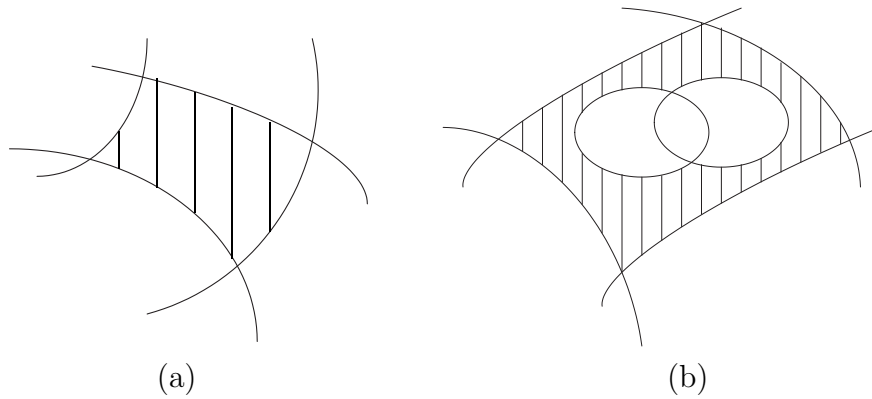
Figure 6.3: Partition cells: (a) made of one closed curve (b) made of two closed curves

Given an initial leaf segment L^a, we propose a procedure to detect the closest subsequent leaf segment. Initially the technique requires that one chooses a specific intersection point p and a normal to L^a, denoted by *normal*. Then the choice of the closest subsequent leaf segment is based on the vector field of all leaf segments intersecting at p and the angle they make with respect to $f(p)$, the vector field of L^a, and *normal*, both evaluated at p (and for each leaf segment we assume that the vector evaluated at p points toward the other extremity point). In essence, the above criterion (b) requires that one selects the leaf segment forming the minimum angle with respect to $f(p)$ whereas requirement (a) implies that leaf segments have their normal pointing toward a common interior region. Given a vector $f(p)$ and a normal N of L^a at p, we can classify a vector v as belonging to one of the eight sets illustrated

in Figure 6.4 (where N and $f(p)$ are represented) and defined as

Set 1: $v^T \cdot f(p) > 0$, $N \cdot v = 0$,   Set 5: $v^T \cdot f(p) < 0$, $N \cdot v = 0$,

Set 2: $v^T \cdot f(p) > 0$, $N \cdot v > 0$,   Set 6: $v^T \cdot f(p) < 0$, $N \cdot v < 0$,

Set 3: $v^T \cdot f(p) = 0$, $N \cdot v > 0$,   Set 7: $v^T \cdot f(p) = 0$, $N \cdot v < 0$,

Set 4: $v^T \cdot f(p) < 0$, $N \cdot v > 0$,   Set 8: $v^T \cdot f(p) > 0$, $N \cdot v < 0$,

and where v^T represents the transpose of vector v.
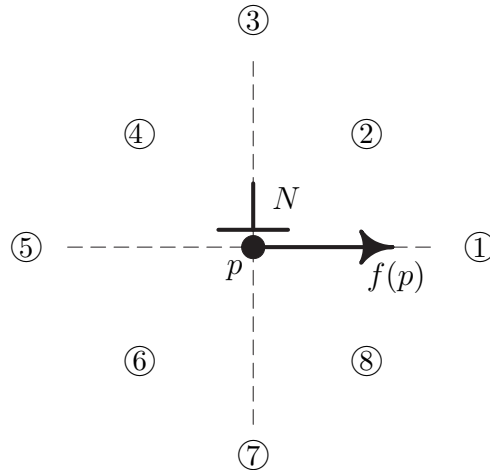
Figure 6.4: Sets with distinct inner products

The following four-step procedure, which we refer to as the "L-procedure", performs a search for a leaf segment whose tangent vector at p is encountered first if one rotates $f(p)$ around p in the direction of N.

1. For each leaf segment connected to p that differs from L^a, evaluate the vector field at p.

2. Compute the angle that each vector makes with respect to both $f(p)$ and N and determine the region of Figure 6.4 to which the vector belongs.

3. Search through the set of vectors and identify those belonging to the region with the lowest number. If this happens for regions 1 to 5 (resp., 6 to 8), then select the leaf segment whose vector forms the minimum absolute angle with respect to $f(p)$ (resp., $-f(p)$) and denote it by L^*.

4. If the region identified in the previous step belongs to $\{2, 3, 4\}$ (resp., $\{6, 7, 8\}$) then the normal to L^* is selected such that it makes an angle within $(-\frac{1}{2}\pi, \frac{1}{2}\pi)$ with respect to $f(p)$ (resp. $-f(p)$). Otherwise, the vector must be perturbed so that it belongs to a region in either $\{2, 3, 4\}$ or $\{6, 7, 8\}$.

For instance, if the above procedure is applied to the leaf segment bounded by points p and p' in Figure 6.5(b) with the indicated normal, then the segment $p - p''$ with its normal corresponds to the closest subsequent leaf segment.

If the solution obtained by the first three steps is unique, then the L-procedure can be used repeatedly until L^a is reached, or until no other subsequent leaf segment is found. Prior to showing the uniqueness of solution for the L-procedure, we illustrate how leaf segments may connect to a point $p \in E$.

Proposition 6.2

Let $\hat{\Gamma}$ be a set of first integrals satisfying (H1), and let $p \in E$ be an arbitrary point belonging to a leaf induced by an element of $\hat{\Gamma}$. Then

$$
p \in \Omega(\hat{\Gamma}) \Leftrightarrow \begin{array}{c} (\forall (\gamma^a, \gamma^b) \in \hat{\Gamma} \times \hat{\Gamma}, \ \gamma^a \neq \gamma^b, \ d\gamma^a(x)|_{x=p} \neq 0, \ d\gamma^b(x)|_{x=p} \neq 0) \\[2mm] \exists \lambda \in \mathbb{R}, \ d\gamma^a(x)|_{x=p} = \lambda d\gamma^b(x)|_{x=p} \end{array} \tag{6.1}
$$

$\diamond$

Expression (6.1) stipulates that a point p belonging to $\Omega(\hat{\Gamma})$, the set of points where there are fewer than n (here $n = 2$) first integrals in $\hat{\Gamma}$ with linearly independent differential (see page 85), is equivalent to saying that any pair of first integrals in $\hat{\Gamma}$ has linearly dependent differentials at p.

Proof: ($\Leftarrow$) Let $\hat{\Gamma}$ be represented by the following collection of first integrals $\{\gamma^1, \dots, \gamma^{\#\hat{\Gamma}}\}$. After some reordering, one gets $\gamma^{1,k} = \{\gamma^1, \dots, \gamma^k\} \subseteq \hat{\Gamma}$ with $1 \le k \le \#\hat{\Gamma}$, the set of first integrals with a non-trivial differential at p, i.e., $d\gamma^i|_p \ne 0$ for all $i \in \{1, \dots, k\}$. By assumption each pair of first integrals taken in $\gamma^{1,k}$ has linearly dependent differentials p. Thus for each $j \in \{1, \dots, k-1\}$ there exists an $\alpha_j \in \mathbb{R} \setminus \{0\}$ such that $d\gamma^j|_p = \alpha_j d\gamma^{j+1}|_p$. Consequently, at p a chain of linearly dependent differentials of first integrals can be created, thus leading to $rank([d\gamma^1, \dots, d\gamma^k]^T|_p) = 1$. The remaining first integrals in $\hat{\Gamma}$ do not have a leaf defined at p so that $rank([d\gamma^{k+1}, \dots, d\gamma^{\#\hat{\Gamma}}]^T|_p) = 0$. Therefore $rank([d\gamma^1, \dots, d\gamma^{\#\hat{\Gamma}}]^T|_p) = rank(d\hat{\Gamma}|_p) = 1$, which leads to $p \in \Omega(\hat{\Gamma})$.

($\Rightarrow$) By definition, p belongs to a leaf, i.e., $d\gamma^a|_p \ne 0$ for some $\gamma^a \in \hat{\Gamma}$. If there exists no other leaf defined at p and induced by a first integral in $\hat{\Gamma}$ then the right-hand side of (6.1) holds. Now assume that $\gamma^b \in \hat{\Gamma} \setminus \{\gamma^a\}$ is another first integral with a leaf defined at p, i.e., $d\gamma^b|_p \ne 0$, and denote the pair $\{\gamma^a, \gamma^b\}$ by $\widetilde{\Gamma}$. By assumption, $p \in \Omega(\hat{\Gamma})$, which leads to $rank(d\hat{\Gamma}|_p) < 2$. As $\{\gamma^a\} \subset \widetilde{\Gamma} \subseteq \hat{\Gamma}$ one gets that $rank(d\hat{\Gamma}|_p) \ge rank(d\widetilde{\Gamma}|_p) \ge rank(d\gamma^a|_p) = 1$, which leads to $rank(d\widetilde{\Gamma}|_p) = 1$. Consequently $d\gamma^b|_p = \lambda d\gamma^a|_p$ for some $\lambda \in \mathbb{R}$, i.e., the leaves induced by γ^a and γ^b are tangent (non-transversal) at p. As γ^a and γ^b are arbitrary first integrals, the previous result holds for any pair of leaves passing through p, which completes the proof.$\square$

Remark 6.3 The result of Proposition 6.2 is due to the fact that E is a subset of $\mathbb{R}^2$. In $\mathbb{R}^n$ with $n > 2$ two leaves may be transversal at p even though $p \in \Omega(\hat{\Gamma})$.$\diamond$

If p is an intersection point of leaves induced by first integrals in $\hat{\Gamma}$ then Proposition 6.2 stipulates that one of two possible situations holds: either $p \in \Omega(\hat{\Gamma})$ and all pairs of leaves defined at p are mutually non-transversal (as illustrated in Figure 6.5(a)), or $p \notin \Omega(\hat{\Gamma})$ and at least one pair of leaves is transversal at p (see Figure 6.5(b)). In any case some vector fields evaluated at point p may be indistinguishable, which

could compromise the uniqueness of solution for the L-procedure. A similar difficulty arises in the last step of the L-procedure whenever a leaf segment has a tangent vector in region 1 or 5. A solution to this problem consists of using the L-procedure with approximate tangent vectors. Notice that each of those vectors are required to have a distinct orientation in order to obtain a unique solution. The next result shows that it is indeed possible to find approximate vectors with the desired property.

(a) Case with $p \in \Omega(\hat{\Gamma})$ (b) Case with $p \notin \Omega(\hat{\Gamma})$
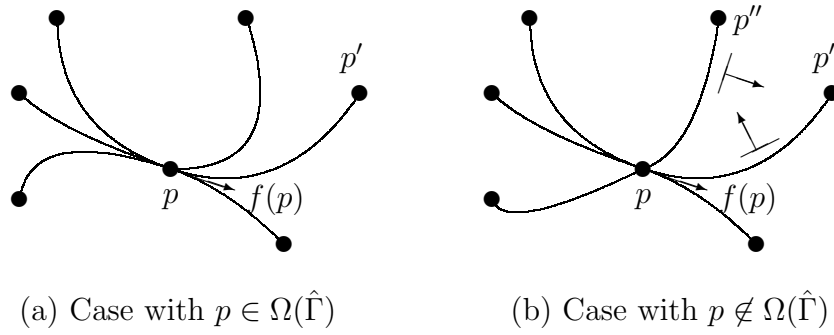
Figure 6.5: Possible configurations of leaf segments

Proposition 6.4

Consider a leaf-partition π and a CSS_E^{π} such that hypothesis (H5) holds and let $p \in E$ be an intersection point between leaves induced by a set of first integrals in $\hat{\Gamma}$. Then for each leaf segment defined at p there exists an approximate tangent vector at p with a unique orientation.⋄

    Proof: Let $\{L^a, L^b, \ldots\}$ represent the set of all leaf segments defined at p, that is, $dL^a|_p \neq 0$, $dL^b|_p \neq 0$, $\ldots$ where dL^a represents the differential of the first integral generating L^a. We begin by obtaining approximate vectors for two leaf segments that are non-transversal at p. Then we study the case of two transversal leaf segments. An extension to all leaf segments follows.

    For the first case we consider L^a an arbitrary leaf segment. Also let $L^b \neq L^a$ be any leaf segment such that $dL^a|_p = \alpha dL^b|_p$ for some $\alpha \in \mathbb{R} \setminus \{0\}$, i.e., dL^a and dL^b are dependent at p. Since $\partial L^a/\partial x_i|_p \neq 0$ for some $i \in \{1, 2\}$, it follows that

$\partial L^b/\partial x_i|_p \neq 0$. From the Implicit Function Theorem, there exists a smooth function $g^a : A_j^a \rightarrow A_i^a$ which locally characterizes L^a and where $A_i^a \in \mathbb{R}$ is a neighborhood of p_i, the ith coordinate of point p. A similar result holds for L^b since L^a and L^b share a common dependent variable at p. We then build approximate tangent vectors to L^a and L^b by determining two points $p^a \in L^a$ and $p^b \in L^b$ and connecting p to p^a and p to p^b. Given a $p_j^* \in A_j^a \cap A_j^b$ arbitrarily close to p_j and such that $p^a = (p_j^*, g^a(p_j^*)) \in L^a$ and $p^b = (p_j^*, g^b(p_j^*)) \in L^b$, assumption (H5) implies that $g^a(p_j^*) \neq g^b(p_j^*)$. Indeed if $g^a(p_j^*) = g^b(p_j^*)$ then $(p_j^*, g^a(p_j^*)) = (p_j^*, g^b(p_j^*))$, which contradicts the existence of an ϵ-neighborhood around p that contains no other intersection point of L^a and L^b. Consequently if $p^a = (p_j^*, g^a(p_j^*))$ and $p^b = (p_j^*, g^b(p_j^*))$ then the vector connecting p to p^a has an orientation distinct from the one joining p to p^b. If no such p_j^* can be found in an ϵ-neighborhood of p, the same conclusion is reached since L^a and L^b do not possess a second point with a common j coordinate. Since L^b is arbitrary, all leaf segments tangent to L^a at p have an approximate tangent vector with unique orientation.

Now consider two leaf segments L^a and L^b that are transversal at p, that is, $dL^a|_p \neq \alpha dL^b|_p$ for any $\alpha \in \mathbb{R}$. Let v^a and v^b be tangent vectors to L^a and L^b, respectively. Therefore $dL^a|_p \cdot v^a = 0$ and $dL^b|_p \cdot v^b = 0$ where $v^a \neq 0$ and $v^b \neq 0$. We show by contradiction that v^a and v^b have distinct orientations. Assume that $v^a = \beta v^b$ for some $\beta \in \mathbb{R} \setminus \{0\}$. Therefore $dL^a|_p \cdot v^b = 0$ and v^b is orthogonal to dL^a. Since v^b is also orthogonal to dL^b, then L^a and L^b must be non-transversal at p, which leads to a contradiction.

All sets of leaf segments that are mutually tangent at p can be treated as in the first case. Thus one is left with sets of leaf segments that are mutually transversal. Since the second case shows that such leaf segments have tangent vectors of distinct orientation, the proof is complete.□

The above development is summarized in the following result.

Proposition 6.5

Consider a leaf-partition π and a CSS_E^π for which hypotheses (H4) to (H7) hold. Let L^a be an arbitrary leaf segment given with its extremity point p and its normal. If there exist subsequent leaf segments then it is possible to identify the closest one and its normal in a finite number of steps.$\diamond$

Proof: The proof shows that the L-procedure outputs a unique solution in a finite number of steps. For each leaf segment defined at p, hypothesis (H5) together with Proposition 6.4 enable the computation of an approximate tangent vector at p. By assumption (H6), it is possible to compute the angle between any two vectors in E. Since assumptions (H4) and (H7) imply that the number of leaf segments connecting to p is finite, the computation of angles required in the L-procedure eventually terminates. The unique solution of the L-procedure is guaranteed by the unique orientation of each approximate tangent vector computed as in Proposition 6.4. Finally the normal to L^*, the closest subsequent leaf segment, can be obtained from the approximate tangent vector of L^* at p and the last step of the L-procedure, which completes the proof.$\square$

As mentioned before, cells with an L-bounded interior can be identified by applying the L-procedure repeatedly. Since the number of leaf segments is finite and each leaf segment possesses two normals then (a) the search for such cells can be completed in a finite number of steps, and (b) the set of cells with an L-bounded interior, whose label set is denoted by Q, is finite. This is summarized in the following result without proof.

Corollary 6.6

Consider a leaf-partition π and a CSS_E^π such that hypotheses (H4) to (H7) hold. Then one can determine the set Q in a finite number of steps.$\diamond$

Note that by assumption (H8) the set Q is nonempty. We recall from Chapter 3 that an element $i \in Q$ is referred to as a state to which corresponds a cell $q_i \subseteq E$.

Remark 6.7 For practical reasons we assume that for each leaf segment belonging to the boundary of a cell with an L-bounded interior, the normal to the leaf segment is recorded. By construction, this normal points towards the interior of the cell.⋄

6.2.3 Transition Structure

Given a collection of cells with label set Q the next task amounts to determining the cell-to-cell transitions induced by input values in Σ. These transitions are based on continuous trajectories defined by Σ and the way the trajectories intersect with the bounding leaf segments of each cell when leaving it. Figure 6.6 shows four distinct cells q_1, q_2, q_3, and q_4 defined by the points $a - b - f - c$, $a - c - d$, $c - e - f$ and $c - d - e$, respectively. Three trajectories initiated from q_1 and crossing its boundary (represented by solid lines) are shown in Figure 6.6. Two of those trajectories cut through the interior of leaf segments ($a - c$ and $c - f$) whereas another one goes through the extremity point c (also denoted an intersection point previously).
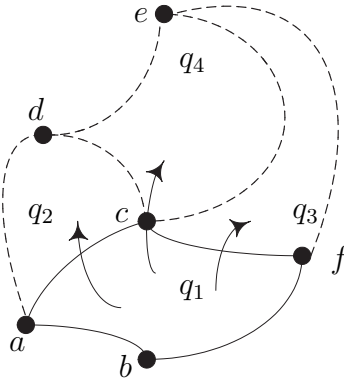
Figure 6.6: Transitions through the boundary of an L-bounded cell q_1

Given a cell with a label in Q, one compares the direction of the flow (that is, the vector field) induced by each input value $\sigma \in \Sigma$ with respect to the bounding leaf segments. The characterization of trajectories through the interior of leaf segments (that is, the leaf segment minus its extremity points) is facilitated due to assumption

(H9). Indeed this hypothesis implies that each leaf segment can be divided into subleaves where the transversality with the vector fields holds. By the boundedness of E in hypothesis (H3) and the smoothness of first integrals and vector fields it can be shown that there only exists a finite number of subleaves. In this case only one point in the interior of each subleaf needs to be evaluated in order to determine cell-to-cell transitions for each event in Σ.

Proposition 6.8

Consider a leaf-partition π and a CSS_E^π such that hypotheses (H3), (H6), (H8), (H9), and (H10) hold. Let L^a be a leaf segment belonging to the boundary of a cell q_i with $i \in Q$, and let Σ be the set of input values. Then it is possible to determine, in a finite number of steps, the state-to-state transitions departing from state i, induced by Σ, and based on continuous trajectories intersecting with the interior points of L^a in a transversal manner.◇

Proof: Since L^a is a leaf segment it is defined by an input value $\sigma_a \in \Sigma$ where σ_a only induces trajectories that evolve non-transversally with respect to L^a. Now consider an arbitrary input value $\sigma \in \Sigma \backslash \{\sigma_a\}$. Because of assumptions (H3) and (H9), L^a has a finite number of subleaves with well-determined transversality with respect to σ. For each subleaf one can determine an interior point by using the Implicit Function Theorem as performed in Proposition 6.4. By Remark 6.7 and hypothesis (H6) it is possible to evaluate at those points the direction of the vector field defined by σ with respect to the normal of L^a. Whenever the vector points outward from q_i then a search for the cells neighboring q_i is initiated. Since the set Q is finite, the search eventually terminates. If the vector points toward another cell q_j with $j \in Q$, then the discrete transition $i \xrightarrow{\sigma} j$ is recorded as an "enabled" state-to-state transition. Otherwise it is recorded as a "disabled" transition. Finally hypothesis (H10) guarantees that the loop over all elements in $\Sigma \setminus \{\sigma_a\}$ proceeds in finite time, which proves the claim.□

Cell-to-cell transitions through intersection points require more analysis than those through the interior of leaf segments. Indeed, transitions through a unique leaf segment can, at most, lead to one cell, whereas transitions through intersection points may lead to many cells. For instance in Figure 6.6 one could draw trajectories departing from cell q_1, going through intersection point c, and leading to cell q_2, q_3 or q_4. Given a fixed input value $\sigma \in \Sigma$, the conditions for having a transition from a "departure" cell q_d to an "arrival" cell q_a through an intersection point p are three-fold: (i) a vector field $f(x, \sigma)$ evaluated at $p \in \partial^d$ needs to point outward from q_d, (ii) the vector field $f(x, \sigma)|_{x=p}$ needs to point toward the interior of q_a, (iii) there must exist a point p' in the interior of q_d leading to the point p under input value σ. Since an intersection point may belong to a set of non-transversal leaf segments a procedure similar to the one developed in Proposition 6.4 can be applied to compute approximate vectors.

Remark 6.9 A necessary condition for the existence of cell-to-cell transitions through intersection points is that $\#\Sigma > 2$. Indeed an intersection point results from the encounter of two leaves induced by distinct input values, say σ_a and σ_b. If $\Sigma = \{\sigma_a, \sigma_b\}$ then any flow initiated from an intersection point will only travel along one of the two leaves, thus never reaching the interior of a cell.⋄

Since the procedure for transitions through intersection points is simple, we summarize the overall approach in the following result.

Corollary 6.10

Consider a leaf-partition π and a CSS_E^π for which hypotheses (H3), (H4), (H6), (H7), (H8), (H9), and (H10) hold. Let Q be the label set of cells in π and let Σ be the input value set. Then it is possible to determine, in a finite number of steps, the state-to-state transitions induced by Σ and based on continuous trajectories intersecting with the boundary points of cells in π in a transversal manner.⋄

Proof: Due to assumptions (H3), (H6), (H8), (H9), and (H10) Proposition 6.8 holds for any leaf segment bounding a cell with a label in Q. The finite number of leaf segments implied by (H4) and (H7) ensures that all cell-to-cell transitions based on trajectories intersecting transversally with the interior of leaf segments can be deduced in finite time. Moreover the finite number of intersection points required in (H4) enables the computation of transitions through intersection points in a finite number of steps, which completes the proof.□

Corollary 6.10 implies that enabled and disabled state-to-state transitions (induced by cell-to-cell transitions through leaf segments and intersection points) can be obtained by analyzing trajectories at the boundary of partition cells with an L-bounded interior. This leads to the main result.

Theorem 6.11

Consider a leaf-partition π and a CSS_E^π for which assumptions (H1) to (H10) hold. Then an FSM abstraction $\mathcal{A} := (Q, \Sigma, \delta)$ as in Definition 3.3 can be obtained in a finite number of steps.◇

Proof: The proof relies on previous results. Proposition 6.1 provides the leaf segments associated with the leaf-partition π. Proposition 6.5 allows the detection of the closest subsequent leaf segment, which, in turn, enables the construction of partition cells with an L-bounded interior in finite time (ref. Corollary 6.6). This provides the state set Q with the leaf segments bounding each cell q_i with $i \in Q$. Corollary 6.10 then stipulates that all state-to-state transitions based on the transversal crossing of leaf segments can be determined in a finite number of steps. This results in a transition map $\delta : \Sigma \times Q \rightarrow 2^Q$ capturing transitions from one state $i \in Q$ to states in $Q \setminus \{i\}$ under any input value in Σ.

If $\#Q = 1$ then there is no transition from one state to another, and consequently the triple (Q, Σ, δ) is an FSM abstraction for the CSS_E^π as stated in Definition 3.3 (page 29). A similar result holds with $\#Q > 1$ and a map δ without state-to-state

transitions. Now consider the case where $\#Q > 1$ and δ possesses state-to-state transitions. As per Corollary 6.10 a state-to-state transition $i \overset{\sigma_k}{\to} j$ with $i, j \in Q$, $i \neq j$, and $\sigma_k \in \Sigma$ occurs if there is a point p on the leaf segment(s) separating q_i from q_j such that the vector field $f(x, \sigma_k)|_{x=p}$ points away from q_i and toward q_j. If p is an intersection point between leaves then there exists another point in q_i leading to p under σ_k and such that $f(x, \sigma_k)|_{x=p}$ points toward the interior of q_j. Such a trajectory qualifies for condition (3.10)(ii) of Definition 3.3. Now assume that p is not an intersection point between leaves. Thus $f(x, \sigma_k)|_{x=p}$ is transversal to a leaf segment contained in the common boundary between q_i and q_j, i.e., in $\partial^i \cap \partial^j$, which has an empty interior. Since locally $f(x, \sigma_k)|_{x=p}$ approximates the trajectory defined by σ_k at p, it follows that $\phi_k(0^+, p) \in q_j$ and $\phi_k(0^-, p) \in q_i$. Once again this satisfies the condition (3.10)(ii) of Definition 3.3. Therefore all state-to-state transitions recorded in the transition map δ are such that the triple $\mathcal{A} := (Q, \Sigma, \delta)$ qualifies as an FSM abstraction for the CSS_E^τ, which proves the claim.$\square$

In reference to the problem definition provided in §3.2.4 (page 38), Theorem 6.11 addresses the finiteness of computation of an FSM abstraction of a CSS_E^τ.

As mentioned in §3.2.4 the completeness property as stated in Definition 3.6 may not hold for those trajectories evolving within partition cells. However a weaker notion of completeness that only involves trajectories intersecting with the partition boundary could be satisfied. For instance, the above construction (especially Corollary 6.10) detects all trajectories transiting through cell boundaries.

Verification of the consistency property

In order to handle the second part of the problem defined in §3.2.4, we must consider the dynamical singularities of the CSS_E^τ that are contained in E. Because of assumption (H10) there is a finite number of sets of equilibrium points. Moreover the first integrals defining the leaf segments can be used to detect (i) isolated equi-

librium points that are contained in the interior of a cell, or (ii) equilibrium points intersecting with a leaf. With the finite number of leaves, cells, and input values, and if only one equilibrium point is used to define a self-looping transition at a state, then the investigation terminates in finite time. Moreover if we add those transitions to the transition map δ obtained by the procedure of Theorem 6.11, the triple (Q, Σ, δ) remains an FSM abstraction for the CSS_E^π. For the detection of cyclic continuous trajectories contained in E, one can always check if the first integrals are proper functions, i.e., functions having compact sets as their preimages. Otherwise visual inspection is always possible for two-dimensional systems. Therefore we assume that all continuous singularities contained in the cells of the leaf-partition π over E are detected and that the transition map δ is extended by the addition of self-looping transitions.

We recall from §3.2.4 that a nonsingular d-path generated by an FSM abstraction is a general d-path that does not contain any singular pair of state and event (i, σ). Moreover the notion of consistency presented in Definition 3.5 (page 36) requires the existence of a continuous trajectory that coexists with the general d-path of interest. In the remainder of this section, we propose a technique to verify the consistency property of nonsingular d-paths based on the technique presented in §4.2.2 (see page 76).

To illustrate the approach, consider a partition cell q_i with $i \in Q$, and an input value $\sigma \in \Sigma$. Also assume that under σ there is a cell-to-cell transition exiting through a leaf segment L^a of ∂^i. We define a back-propagating flow of a point $p \in L^a$ under σ as the flow obtained by reversing the trajectory leading to p under input value σ. In essence we back-propagate the leaf segment L^a with respect to σ onto the other leaf segments bounding q_i. Figure 6.7 shows a cell q_i with a leaf segment L^a represented by a thicker line. Moreover we assume that under σ there is a trajectory exiting q_i through L^a. The back-propagation of L^a is illustrated at some locations by

streamlines (dashed lines with an arrowhead). The final step amounts to determining those subsets of leaf segments of ∂^i from which a forward flow induced by σ leads to L^a. In reference to Figure 6.7 those subsets correspond to the hatched regions of leaf segments L^1, L^3, L^4, and L^5.
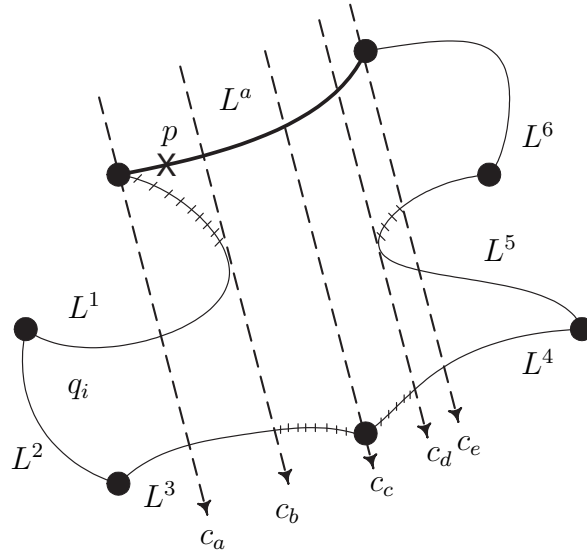
Figure 6.7: The back-propagation of a leaf segment L^a on other leaf segments of a cell q_i

Even though we referred to the back-propagation of a leaf segment the procedure to follow enforces the above steps in a different manner. Indeed the approach makes explicit use of first integral constants (FICs) related to the input value σ, called here σ-FICs. Notice that it is always possible to evaluate first integral constants everywhere in E. Without loss of generality, we assume that the interior of leaf L^a is transversal to the flow induced by the input value σ. Indeed due to assumption (H9) the leaf segment L^a can always be divided into subleaves whose interior is transversal to the trajectories generated by σ. Consequently an evaluation of σ-FICs at the extremity points of L^a provides the largest interval of σ-FIC values spanned by L^a, which we denote by $[c_{min}^\sigma, c_{max}^\sigma]$. Similarly one can get the σ-FIC values of the other leaf segments that belong to ∂^i and record those contained in the interval $[c_{min}^\sigma, c_{max}^\sigma]$ in order to form

S, an increasing sequence of σ-FIC values. In reference to the leaf segment L^a of Figure 6.7, one gets the sequence $S := [c^\sigma_{min} = c_a, c_b, c_c, c_d, c^\sigma_{max} = c_e]$, where c_a and c_e correspond to extremity points for L^a, c_b and c_d relate to non-transversality points between the flow induced by σ and leaves L^1 and L^5, respectively, while c_c takes into account the intersection point between leaves L^3 and L^4. Also an ordered sequence of leaves L_S whose σ-FIC interval contains values in S can be generated. This results in $L_S := [\{L^1, L^3\}, \{L^1, L^3\}, \{L^3, L^4\}, \{L^4, L^5\}, \{L^4, L^5\}]$ for the case illustrated in Figure 6.7. For instance both L^4 and L^5 have a σ-FIC interval that contains c_d and c_e.

For each interval bounded by two consecutive values in S, say $s := [S(k), S(k+1)]$, one must then identify which leaf segment in the kth and the $k + 1$th entries of L_S is encountered first by the back-propagation of L^a. This can be achieved by back-propagating a point of L^a whose σ-FIC value belongs to s (say the point p marked by an "X" in Figure 6.7 and belonging to the subinterval $s = [c_a, c_b]$) until an element of $L_S(k)$ or $L_S(k+1)$ is encountered (here L^1 is encountered before L^3). If L' corresponds to the closest leaf segment encountered then one identifies the subset of L' with the subinterval s. The above procedure can be repeated for any subinterval of S so that all subleaves of ∂^i leading to L^a under the input value σ are identified. Since the number of leaf segments contained in each cell is finite the above procedure terminates in finite time. The following result summarizes the approach.

Proposition 6.12

Consider a leaf-partition π and a CSS^π_E such that hypotheses (H1) to (H10) hold. Let q_i, $i \in Q$, be an arbitrary cell and let Σ be the set of input values. Then for each cell-to-cell transition induced by $\sigma \in \Sigma$ and starting at q_i, where q_i does not contain any dynamical singularity generated by σ, it is possible to extract the corresponding boundary-to-boundary transitions in a finite number of steps.$\diamond$

Proof: Assumptions (H1) to (H10) enable the identification of cell-to-cell transi-

tions leading outside of q_i under any input value. Because of the finite number of subleaves bounding q_i, the above procedure identifies boundary-to-boundary transitions under a given input value in finite time. As the number of input values is finite (ref. hypothesis (H10)), the overall procedure terminates in a finite number of steps. $\square$

In the presence of an FSM abstraction as built previously, Proposition 6.12 ensures that for every simple d-path $i - \sigma - j$ not containing a singular pair, it is possible to determine the subleaves of cell q_i through which a trajectory induced by σ must enter and exit in order to reach the cell q_j. Nonsingular d-paths are made of at least two such simple d-paths. Therefore in the presence of a nonsingular d-path one can construct a sequence of boundary-to-boundary transitions. Also with such a sequence it is possible to verify if the consistency property is satisfied by comparing the subleaves involved with two consecutive boundary-to-boundary transitions. In the following section we use an example to illustrate how the technique applies.

6.3   Examples of FSM Abstractions

In this section, leaf-partitions and FSM abstractions are obtained for the Lotka-Volterra system and the double integrator. The first system contains equilibrium points and is used to introduce the approach without the extra burden of back-propagation. The double integrator without equilibrium points is then used to illustrate the benefits of back-propagation. The following results are generated automatically by a program developed in ©Maple (see http://www.mapleapps.com). In §B.2 one can find the output of the program for the double integrator.

Example 6.13 (Lotka-Volterra) We begin by recalling from Example 5.10 (on page 90) the first integral of the Lotka-Volterra system

$$\gamma_1^\sigma(x_1, x_2) = x_1^3 x_2^3 - 6x_1^2 x_2^3 \sigma + 6x_1^2 x_2^4 + 9x_1 x_2^3 \sigma^2 - 18x_1 x_2^4 \sigma + 9x_1 x_2^5, \qquad (6.2)$$

defined on $D' := \mathbb{R}^2$ and its differential

$$\left[\; 3x_2^3(-\sigma + x_1 + x_2)(x_1 - 3\sigma + 3x_2) \quad 3x_1x_2^2(-3\sigma + x_1 + 5x_2)(x_1 - 3\sigma + 3x_2) \; \right] \quad (6.3)$$

For this system we consider the input value set $\Sigma := \{\sigma_1 = 1, \sigma_2 = 2\}$, the set $\hat{\Gamma} = \{\gamma_1^1, \gamma_1^2\}$, and the FICs $C_1^2 := (0.035, 0.5)$ and $C_2^2 := (0.5, 1.5)$. Therefore the system satisfies assumptions (H1) and (H7) automatically.

As per Example 5.10 we restrict E to belong to $\mathbb{R}_{>0} \times \mathbb{R}_{>0}$. For this reason we select $E := (0 < x_1 < 4) \times (0 < x_2 < 2)$, which by construction fulfills hypothesis (H3). One can verify that condition (4.3) of hypothesis (H10) is satisfied. From the leaf-partition associated with the above $\hat{\Gamma}$, Σ, and FICs one notices that the containment of all intersection points in E required in (H4) is respected (see Figure 6.8). By equation (6.3) the Lotka-Volterra system is a nearly integrable CSS on E. The non-transversality is characterized by $\psi(x_1, x_2) = -6x_1x_2^3(x_2 - x_1)(x_1 + 3x_2 - 3\alpha)(-\sigma_1 + \sigma_2)$ and $d\gamma_1^\alpha(x_1, x_2) \wedge d\psi(x_1, x_2) = 18x_1x_2^5(x_1 + 3x_2 - 3\alpha)(-x_2\alpha + 8x_1x_2 - 3x_1\alpha)(-\sigma_1 + \sigma_2)$ with $\alpha \in \{\sigma_1, \sigma_2\}$. Therefore assumption (H9) is satisfied since $\mathcal{G}_{1,2}^1 := \{(x_1, x_2) = (1, 1)\}$ and $\mathcal{G}_{1,1}^2 := \{(x_1, x_2) = (\frac{1}{2}, \frac{1}{2})\}$ of equation (4.8) do not intersect any leaf of the partition.

In Figure 6.8 the integers are meant to number the leaf segments whereas the circled integers stand for cell numbers. For clarity, some ells are not represented on the diagram. Those are given in (6.4) in the following format cell# = [leaf segment#, leaf segment#, ...] where numbers in the brackets correspond to the number of leaf segments bounding the cell

$$10 = [10, 14, 5, 19], \; 11 = [2, 21], \; 1 = [4, 16], \; 5 = [5, 15, 3, 20]. \quad (6.4)$$

For instance, the cell number 1 is bounded by the leaf segments number 4 and 16 (lower left corner of Figure 6.8). Overall there are eleven cells with an L-bounded inte-
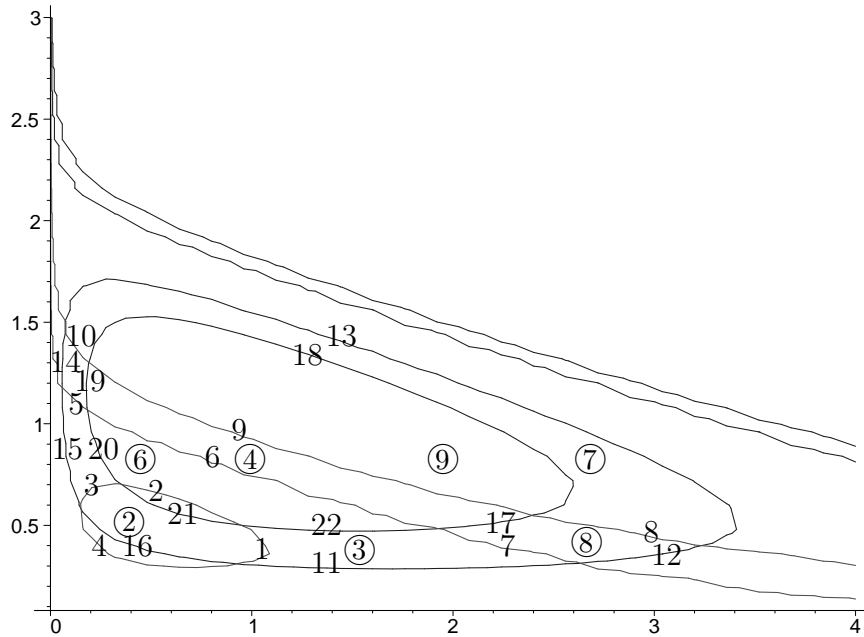
Figure 6.8: Leaf-partition for the Lotka-Volterra system

rior so that the state structure of the resulting FSM abstraction is $Q := \{1, 2, 3, 4, 5, 6,$ $7, 8, 9, 10, 11\}$. Moreover one notices that the Lotka-Volterra system possesses a distinct equilibrium point for each input value. For input value $\sigma_1 = 1$ (resp., $\sigma_2 = 2$) the equilibrium point is $(x_1, x_2) = (\frac{1}{2}, \frac{1}{2})$ (resp., $(x_1, x_2) = (1, 1)$) and is located in the cell number 2 (resp., 9).

The FSM abstraction for the Lotka-Volterra system is provided in Figure 6.9. Therein transition labels are given as pairs, (i_σ, i_L), where the argument i_σ is the index of the active input value whereas the second argument i_L captures the number of the leaf segment that is crossed under the flow induced by the input value with index i_σ. Transitions whose line terminates with a square captures disabled transitions, namely $(2, 4)$, $(1, 13)$, $(1, 14)$ and $(1, 15)$, are forbidden because they lead outside of the L-bounded region formed by the union of all cells with an L-bounded interior. The self-looping transitions due to equilibrium points are represented by dotted lines at cell 2 and 9. Notice that nondeterministic transitions arise at states 2, 4, 6, 7, and 9 because there is more than one transition induced by the same input value. For

116

instance, one finds transitions (1,16) and (1,21) leaving state 2.•
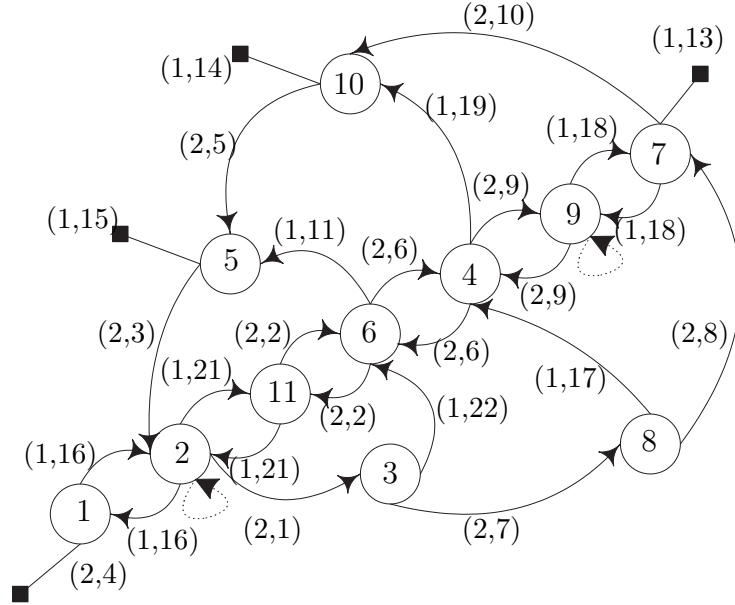
Figure 6.9: FSM abstraction for the Lotka-Volterra system

The following example illustrates the removal of nondeterministic transitions.

Example 6.14 As mentioned previously the double-integrator has a first integral $\gamma_1^\sigma := -\sigma x_1 + \frac{1}{2}x_2^2$ defined on $D' := \mathbb{R}^2$. We assume we have the following set of input values $\Sigma := \{\sigma_1 = 1, \sigma_2 = -1, \sigma_3 = 2\}$, of first integrals $\hat{\Gamma} := \{\gamma_1^1, \gamma_1^2, \gamma_1^3\}$, and of first integral constants $C_1^3 := (-2, 1, 3)$, $C_2^3 := (-4, 0, 5)$, and $C_{\sigma_3}^3 := (-8, -4, 8)$. We also consider a subset of $\mathbb{R}^2$ that is defined as $E := (-5 < x_1 < 11) \times (-6 < x_2 < 6)$. Consequently, assumptions (H1), (H3), and (H7) are satisfied. As shown in Example 3.27 the double-integrator as defined above qualifies as a nearly integrable CSS and an ICSS over $D'' = D'$. Moreover, Example 4.13 demonstrates that hypotheses (H9) and (H10) hold. Notice that no dynamical singularity is induced by Σ over the region E.

Figure 6.10 illustrates the leaf-partition that is generated from Γ, Σ and the above

set of FICs. One notices that assumption (H4) is satisfied. For clarity, Figure 6.10 only shows some leaf segment numbers (there are 39 of them in total) whereas all partition cells possess a circled number. Consequently the state structure of the FSM abstraction is $Q = \{1, 2, 3, 4, 5, 6, 7, 8, 9, 10, 11, 12, 13, 14, 15, 16, 17\}$.
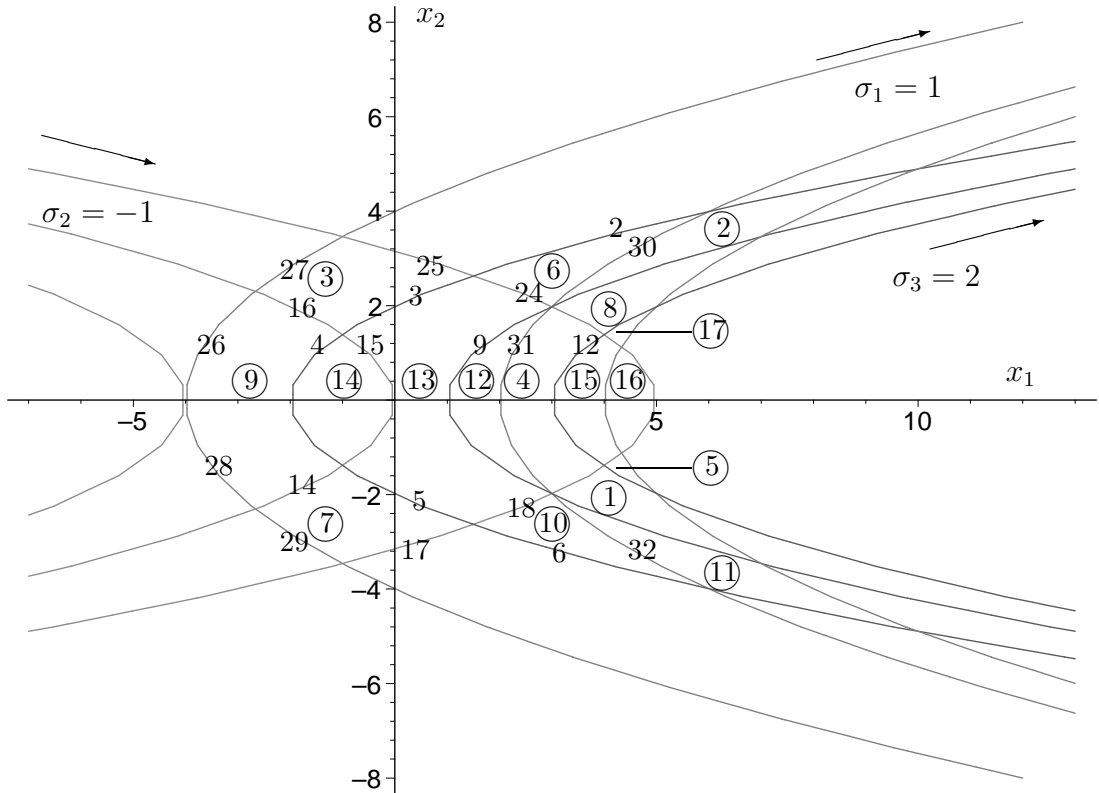
Figure 6.10: A leaf-partition for the double-integrator

Overall, sixty state-to-state transitions are enabled, and 24 are disabled. Since the FSM abstraction cannot be illustrated in its entirety, Figure 6.11 provides a schematic of the transition structure where each line with an arrowhead represents (possibly many) enabled transitions and any line terminated with a square captures (possibly many) disabled transitions. The full details of the transition structure can be found in §B.2 on page 153.
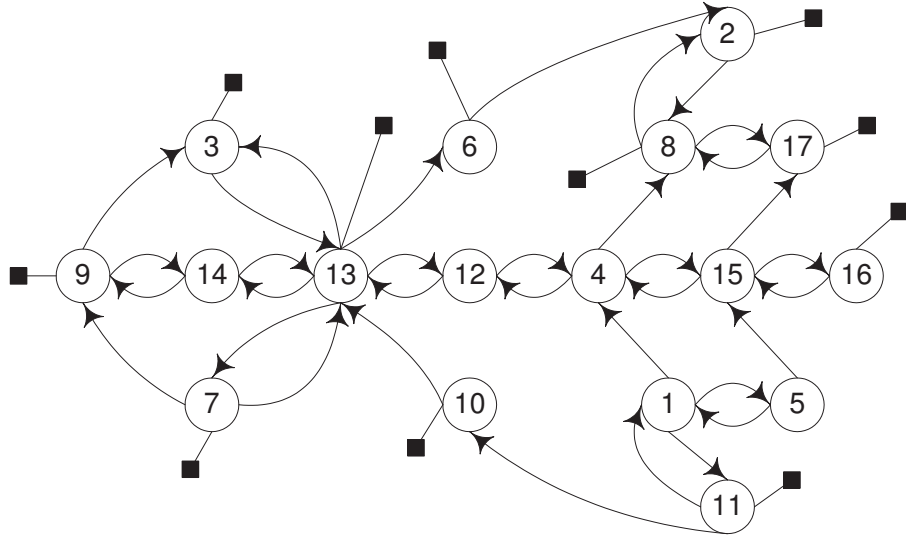
Figure 6.11: An FSM abstraction for the double-integrator

In order to explain how the boundary-to-boundary transitions can serve to verify the consistency property, we focus on enabled transitions exiting partition cell number 13, i.e.,

$$(13, 1, 15, 14), \quad (13, 1, 24, 6), \quad (13, 2, 5, 7), \quad (13, 2, 9, 12),$$

$$(13, 3, 9, 12), \quad (13, 3, 15, 14), \quad (13, 3, 24, 6), \quad (13, 3, 3, 3),$$

with the format (departure cell #, input value index, exiting leaf segment #, arrival cell #). From the previous set of transitions one notices that under the input value σ_1 partition cells number 14 and 6 can be reached. A similar phenomenon occurs with σ_2 and cells $(7, 12)$, and input σ_3 and the cells $(3, 6, 12, 14)$. Therefore once in cell 13 any input value leads to more than one possible partition cell.

A preliminary step toward the construction of boundary-to-boundary transitions under input value σ consists of dividing the leaf segments of cell 13 into subleaves that are transversal to the flow defined by σ. This is illustrated in Figure 6.12 where leaf segments 15 and 9 are partitioned into subleaves 15000, 15001, 9000, and 9001.

With respect to those subleaves the above set of cell-to-cell transitions is extended to a set of boundary-to-boundary transitions

$$(13, 1, \mathbf{18}, 15, 14), \quad (13, 1, \mathbf{15001}, 24, 6), \quad (13, 1, \mathbf{18}, 24, 6), \quad (13, 2, \mathbf{3}, 5, 7),$$

$$(13, 2, \mathbf{9001}, 5, 7) \quad (13, 2, \mathbf{3}, 9, 12), \qquad\quad (13, 3, \mathbf{18}, 9, 12), \quad (13, 3, \mathbf{5}, 15, 14),$$

$$(13, 3, \mathbf{18}, 15, 14), \quad (13, 3, \mathbf{15001}, 24, 6), \quad (13, 3, \mathbf{9000}, 24, 6), \quad (13, 3, \mathbf{15001}, 3, 3),$$

where numbers in bold represent the leaf segment leading to the exiting transition. For example the transition $(13, 1, 24, 6)$ is extended in two boundary-to-boundary transitions $(13, 1, 15001, 24, 6)$ and $(13, 1, 18, 24, 6)$. Therefore if a trajectory enters cell 13 through leaf segment 15001 (or leaf segment 18) and that the input value σ_1 is selected, then the leaf segment number 24 is reached, thus leading to partition cell number 6. One can observe that these subdivisions do not remove nondeterminsitic transitions as seen by transitions $(13, 3, 15001, 24, 6)$ and $(13, 3, 15001, 3, 3)$, i.e., if subleaf 15001 is hit and the input value is σ_3 then leaf segments 3 or 24 can be reached, thus leading to cell 3 or 6.
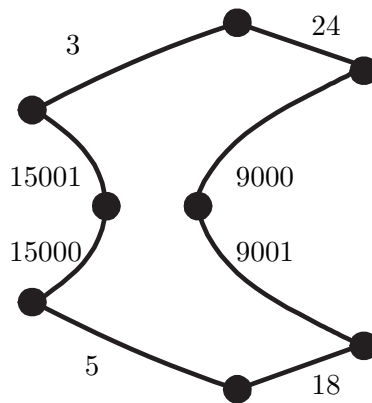
Figure 6.12: Partition cell number 13

One can remove nondeterministic transitions by referring to the σ_3-FIC intervals. Indeed the σ_3-FIC interval for the whole subleaf 15001 is $[-1.5, 0]$, whereas the

transitions $(13, 3, 15001, 24, 6)$ and $(13, 3, 15001, 3, 3)$ occur on the σ_3-FIC subintervals $[-0.25, 0]$ and $[-1.5, -0.25]$, respectively. Therefore whenever the subleaf 15001 is encountered under a flow induced by σ_3 the σ_3-FIC value is used to determine to which subintervals, $[-0.25, 0]$ or $[-1.5, -0.25]$, it belongs. This, in turn, provides the leaf segment that will be reached while exiting cell 13 under input value σ_3. If the σ_3-FIC value equals -0.25 then the intersection point of leaf segments 3 and 24 is reached. For this example, the overall set of boundary-to-boundary transitions is formed from a total of 93 transitions.

We now consider nonsingular d-paths. From §B.2 one finds the transitions $(7, 3, 5, 13)$, $(7, 3, 14, 9)$, $(13, 3, 3, 3)$ and $(13, 3, 24, 6)$. Therefore, the following general d-path $7 - \sigma_3 - 13 - \sigma_3 - 3$ qualifies as a nonsingular d-path that can be generated by the FSM abstraction. Figure 6.13 captures the portion of the FSM abstraction, which contains the above nonsingular d-path. The boundary-to-boundary transitions of interest for cell 13 under input value σ_3 are $(13, 3, 5, 15, 14)$ and $(13, 3, 15001, 3, 3)$, and those for the cell 7 under σ_3 are $(7, 3, 17, 5, 13)$ and $(7, 3, 17, 14, 9)$. Consequently the only boundary-to-boundary transition leading to cell 13 while departing from cell 7 is $17 \overset{\sigma_3}{\to} 5$. However the boundary-to-boundary transition departing from cell 13 and reaching cell 3 under σ_3 is $15001 \overset{\sigma_3}{\to} 3$. Therefore the leaf segment number 5 in cell 7 does not lead, under the input value σ_3, to a leaf segment shared by cell 3. Moreover, the transition $(13, 3, 5, 15, 14)$ indicates that any point departing from leaf segment 5 only reaches leaf segment 15 before attaining cell 14. Indeed the σ_3-FIC interval of leaf segment 5 is $[-1.5, -0.25]$ whereas that of leaf segment 15 is $[-1.5, 0]$, meaning that a back-propagation of leaf segment 15 under σ_3 completely covers leaf segment 5. Therefore no trajectory entering cell 13 through the leaf segment 5 can reach the cell 3, proving that the d-path $7 - \sigma_3 - 13 - \sigma_3 - 3$ violates the consistency property.●
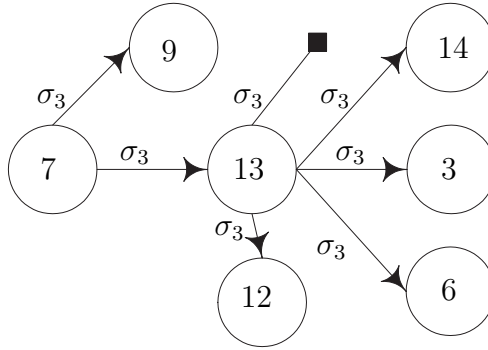
Figure 6.13: A nonsingular d-path

6.4 Summary

In this chapter, we have provided both a set of sufficient conditions (Section 6.1) and an algorithmic procedure (Section 6.2) to construct an FSM abstraction for a two-dimensional CSS_E^π where π is a leaf-partition. Moreover we have demonstrated that the computation of such an FSM abstraction terminates in finite time. In Section 6.3 we have applied the technique to two examples, each of which shows that, like other partition techniques, one generally obtains an FSM abstraction with nondeterministic transitions. Also we have proposed techniques for removing nondeterministic transitions and for verifying the consistency property of nonsingular d-paths generated by the FSM abstraction. The second example has shown that the transition structure of an FSM abstraction generated by the proposed procedure can violate the consistency property. We have also suggested a weaker notion of completeness that can be achieved by the present approach.

On one hand, the proposed algorithmic procedure is limited to cells whose interior is L-bounded. Since the nature and the number of such cells depend on the leaf-partition π over E, it generally happens that the collection of cells with an L-bounded interior forms a strict subset of E (see Example 6.13 and Example 6.14). On the other hand, the sequential use of the L-procedure provides a sufficient condition for the

existence of cells with an L-bounded interior. Therefore one could use the algorithm to insert additional leaves and see if a satisfactory subset of E is covered by cells with an L-bounded interior. Moreover, the technique for checking the consistency property suggests that if additional boundary information is embedded in the transition map of an FSM abstraction one can possibly satisfy the consistency property.

In the following chapter, we extend the material of the previous chapters to another class of nonlinear systems.

Chapter 7

Extension to Lyapunov Functions

In practice, many industrial processes do not have any first integrals. In this situation one could always seek approximate first integrals with a common local domain (Blouin *et al.*, 2003). One can also look at another concept of local submersions that is of great use in modern control theory of continuous systems, that of *Lyapunov functions*. In the next section we compare the characteristics of Lyapunov functions with that of first integrals and we discuss an extension of the previous material to Lyapunov functions. We conclude this chapter by applying the approach to two case studies in chemical engineering.

7.1 Lyapunov Functions

In this section, we extend the material of the previous chapters by using Lyapunov functions for generating FSM abstractions for the class of Controlled Switched Systems. Namely, we present a method for constructing the state set and the transition structure of an abstraction from Lyapunov functions. While introducing the technique, we discuss the resemblances and distinctions between first integrals and Lyapunov functions.

We denote by Λ a system modeled by a set of ODEs defined over a region D and

with an equilibrium point x_{eq}. A Lyapunov function for Λ is defined as follows.

Definition 7.1 (Lyapunov Function (Khalil, 1992)) A continuously differentiable mapping $V : D \rightarrow \mathbb{R}$ is a *Lyapunov function* for Λ if it satisfies the following conditions (i) $V(x)|_{x=p} > 0$ for all $p \in D \setminus \{x_{eq}\}$, (ii) $V(x)|_{x=x_{eq}} = 0$, and (ii) $dV(x(t))/dt|_{x=p} \leq 0$ for all $p \in D. \diamond$

In general, there exists no useful technique for constructing Lyapunov functions for a continuous system with nonlinear dynamics. For systems such as those modeled in (3.1) with a vector field $f(x, u)$, the time derivative of a Lyapunov function becomes

$$dV(x)/dt = dV/dx \cdot dx/dt = dV/dx \cdot f(x, u).$$

Given a Controlled Switched System (ref. Definition 3.2 on page 26) one must find, for each fixed input value $u \in \Sigma$, a corresponding Lyapunov function V_u (for $u = \sigma_k$ we use the compact representation V_k). Thus a Lyapunov function V_u is a local submersion except at those locations where $dV_u(x)/dx$ vanishes. Furthermore, V_u is a local submersion on $D \setminus \{x_{eq}^u\}$ if $dV_u(x)/dt|_{x=p} < 0$ for all $p \in D \setminus \{x_{eq}^u\}$, where x_{eq}^u denotes the equilibrium point associated with the input value $u \in \Sigma$. In this case, any element of $\mathbb{R}_{>0}$ is a regular value of the function V_u.

We now provide a method for obtaining the state set of an FSM abstraction by partitioning a region of the state space with the level sets of Lyapunov functions. As seen above, Lyapunov functions are similar to first integrals in the sense that their preimage may form a submanifold of D (ref. §A.2.4 on page 147). Since the partitioning technique presented in §3.3.2 (see page 47) also relies on submersion properties, it can be extended to Lyapunov functions. Indeed, by considering V_k instead of γ_j^k in Definition 3.21, equation (3.22), and equation (3.23), then Proposition 3.22 and Corollary 3.26 apply. A difference when using Lyapunov functions is that for each input value there is only one submersion, compared to $n - 1$ in the case of

first integrals.

The main distinctions between first integrals and Lyapunov functions lie in the transversality features of the partitions generated by their level sets. From a continuous trajectory point of view, Lyapunov functions (resp., Lyapunov level sets) can be seen as the dual of first integrals (resp., leaves). Indeed recall from Chapter 4 that the trajectories induced by an input value $\sigma_a \in \Sigma$ are non-transversal to the leaves of first integrals defined by σ_a (ref. equation (3.12) on page 39). In contrast, the trajectories resulting from the input value σ_a are transversal to the level sets of the corresponding Lyapunov function wherever $dV_a(x)/dt$ is distinct from zero. If $dV_a(x)/dt|_{x=p} < 0$ for all $p \in D \setminus \{x^a_{eq}\}$, then the equilibrium point x^a_{eq} is the only location where the transversality property collapses. Moreover, unlike first integrals, the transversality (resp., non-transversality) of Lyapunov level sets does not imply the transversality (resp., non-transversality) of trajectories. This is because continuous trajectories are constrained to evolve on leaves, whereas they are not in the case of Lyapunov level sets. Consequently the non-transversality locations between Lyapunov level sets do not necessarily coincide with a change in the behaviour of continuous trajectories.

We now illustrate how one derives the transition structure of an abstraction based on Lyapunov functions. Similar to first integrals, the non-transversality between the surfaces defined by a Lyapunov function $V_a(x)$ and a vector field $f(x, \sigma_b)$ corresponds to the locations where the function

$$\beta(x) := dV_a(x) \cdot f(x, \sigma_b) \tag{7.1}$$

equals zero. Equation (7.1) is the analog of (4.2) (page 57) in the presence of a Lyapunov function V_a instead of the first integral γ^a_j. In that sense, a development similar to that of §4.1 with $\beta(x)$ instead of $\psi(x)$ can be undertaken. Indeed if one considers $V_a^{-1}(c)$ instead of the leaf $L^c_{j,a}$, where c is a regular value, then Lemma

4.7 and Corollary 4.10 can be utilized to check for a well-conditioned transversality property. In the special case of two-dimensional systems such as those presented in the next section, one can detect the non-transversality between a Lyapunov level set induced by the input value σ_a and trajectories enforced by input value σ_b by monitoring the sign of $\beta(x)$ while searching for intersection points along Lyapunov level sets.

Throughout the thesis we have singled out results pertaining to analytic vector fields. If in addition such a vector field has an Hurwitz Jacobian at an equilibrium point, the technique in (Kazantzis *et al.*, 2002) enables the construction of local candidate Lyapunov functions. The approach amounts to constructing a Taylor series for a Lyapunov function $V_u(x)$ based on the expansion of the series for $f(x, u)$ and a positive real analytic function $Q(x)$ around an equilibrium point x_{eq}^u such that $dV_u(x) \cdot f(x, u) = -Q(x) < 0$ holds. The coefficients for the Taylor series for $V_u(x)$ are then obtained in a recursive manner by progressively increasing the series truncation order. Consequently the local nature of the candidate Lyapunov function dictates the characteristics of the region that can be partitioned.

7.2 Case Studies

In this section we briefly illustrate the approach with Lyapunov functions for the class of CSSs by using two industrial applications. Both examples possess analytic vector fields.

Example 7.2 (Nonisothermal Continuous Stirred Tank Reactor) The first example to consider is a nonisothermal continuous stirred tank reactor (CSTR) shown in Figure 7.1, in which a first order and irreversible chemical reaction $A \rightarrow B$ takes place (Ogunnaike and Ray, 1994).

A reactant A is fed into the tank at a given flowrate F_{in}, concentration c_{in}, and
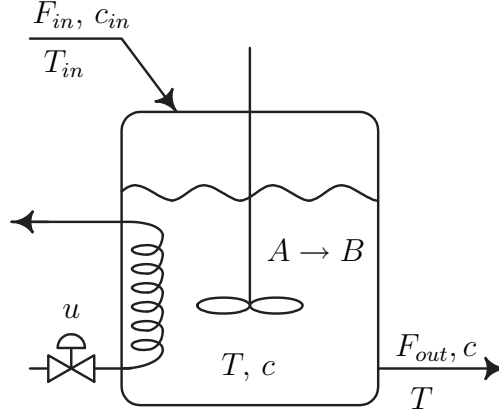
Figure 7.1: A nonisothermal continuous stirred tank reactor

temperature T_{in}. The conversion of reactant A into product B is governed by a reaction constant k_0 and it depends on the temperature and the concentration of the mixture in the tank. Under a well-mixed assumption, the liquid in the tank is homogeneous in T, the temperature, and c the concentration of A. Heat can be transferred (either added or removed) to the mixture via the coil. In the presence of a constant hold-up, i.e., $F_{in} = F_{out}$, and by assuming constant density and heat capacity ($Joule/(^\circ C\ kg)$) of the reacting material, the reactor dynamics are described by the following set of ODEs

$$
\begin{aligned}
\frac{dc}{dt} &= -Dc - k_0 e^{(-E/RT)}c + Dc_{in}, \\
\frac{dT}{dt} &= -DT + \beta k_0 e^{(-E/RT)}c + DT_{in} - u.
\end{aligned}
\tag{7.2}
$$

The input variable u corresponds to the heat transferred to the mixture. For the simulation the following parameters are used: $k_0 = 1.287 \times 10^{12}\ h^{-1}$, $E/R = 9758.3\ ^\circ C$, $\beta = 1.4936\ ^\circ C\ L/mole$, $D = 14.19\ h^{-1}$, $c_{in} = 0.5\ mole/L$ and $T_{in} = 100\,^\circ C$. We assume the input variable can take two distinct values, i.e., $\Sigma := \{-50, 50\}$, for which the equilibrium points are $(c_0, T_0)_{u=-50} = (0.5, 103.52)$ and $(c_0, T_0)_{u=50} = (0.5, 96.48)$. By using the technique presented in (Kazantzis *et al.*, 2002) with a truncation order

of two, one obtains the following local candidate Lyapunov functions

$$V(c,T)_{u=-50} \;=\; 0.0514\,T^2 - 10.6454\,T + 20.5661\,c\,(c-1) + 556.1652, \quad (7.3)$$

$$V(c,T)_{u=50} \;=\; 0.0361\,T^2 - 6.9745\,T + 14.4585\,c\,(c-1) + 340.0527. \quad (7.4)$$

Both (7.3) and (7.4) are Lyapunov functions for the nonisothermal reactor over the region $E := \{(c,T) \in (0,1) \times (60,130)\}$. Notice that $dV(c,T)_{u=-50}$ and $dV(c,T)_{u=50}$ are linearly dependent along the line $\{(c=0.5,T)\}$ only.

Then level sets for the Lyapunov function (7.3) are obtained for the constants 0.1, 0.5, 1.2, and 2, whereas we associate the constants 0.1, 0.4, 0.9, and 1.5 to the Lyapunov function (7.4). The resulting partition is provided in Figure 7.2, where one-dimensional objects are numbered by integers and two-dimensional objects by circled integers.
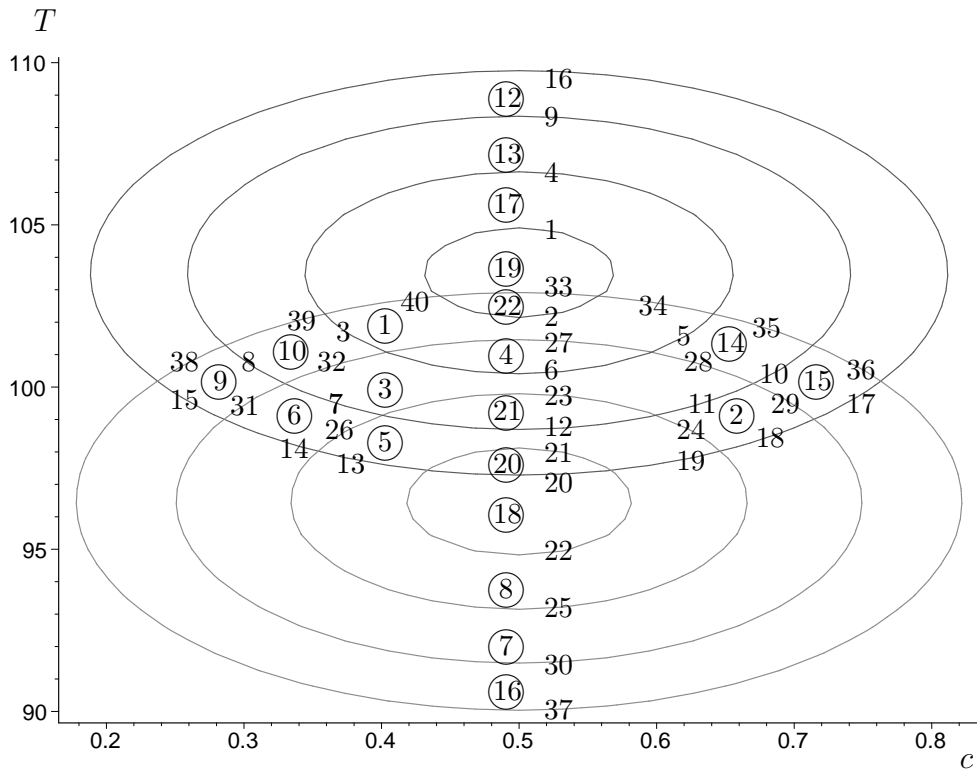
Figure 7.2: A partition for the nonisothermal reactor

129

The algorithmic procedure presented in §6.2 (see page 96) was modified to accommodate the treatment of Lyapunov functions. In the present context the displacement along level sets can only be performed by using Method (II) given in appendix §B.1 (on page 151). Consequently a schematic representation of the FSM abstraction induced by the partition of Figure 7.2 and the ODEs (7.2) is shown in Figure 7.3. Note that lines with arrowheads may represent many transitions. The detailed transition map, which contains 90 transitions, can be found in appendix §B.3 (page 159). In Figure 7.3 one notices the self-loops at state 18 and 19 that are induced by the equilibrium points under distinct input values.●
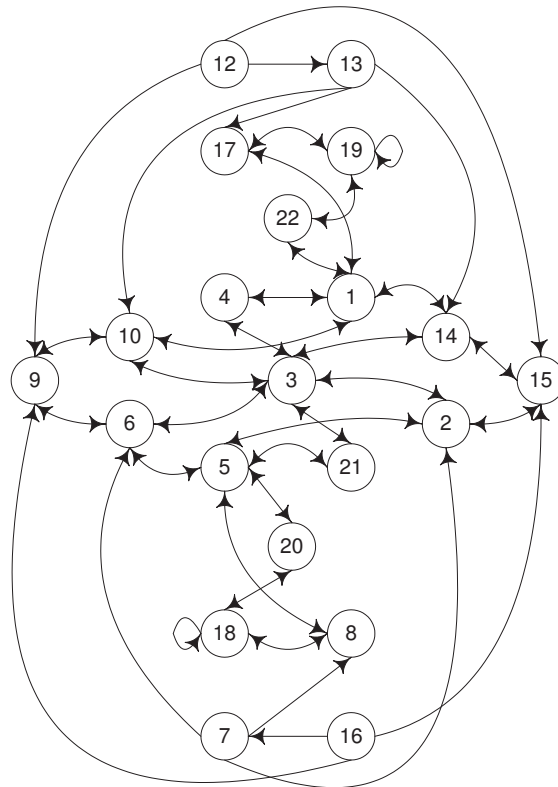
Figure 7.3: An FSM abstraction for the partition of Figure 7.2

Example 7.3 (Mixing Tank) The second example consists of a mixing tank first introduced in (Stursberg *et al.*, 2000) and illustrated in Figure 7.4. This process has been utilized to synthesize timed FSM abstractions by using two static partitioning

130

techniques. The system has two controlled inlet streams F_1 and F_2 (m^3/s) with distinct concentrations c_1, c_2 ($mole/L$) of a dissolved substance, and a free outlet stream F of concentration c. It is assumed that the tank is well-mixed so that c is uniform throughout the volume of the tank, and that the densities are constant and similar, i.e., $\rho_1 \approx \rho_2 \approx \rho$. The state variables of the system are the height of liquid h (m), and the concentration c.

A mass balance performed on the tank provides the following set of differential equations.

$$\frac{dh}{dt} = \frac{F_1 + F_2 - k_2\sqrt{h}}{k_1}$$

$$\frac{dc}{dt} = \frac{F_1(c_1 - c) + F_2(c_2 - c)}{k_1 h}$$
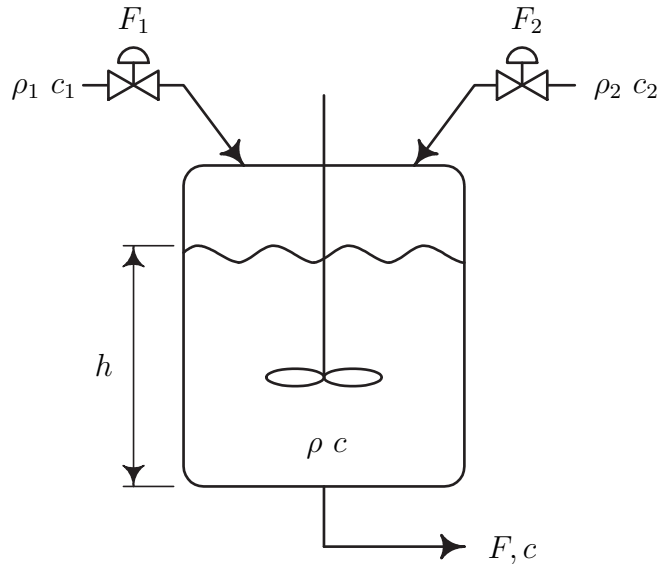
Figure 7.4: A mixing tank

The parameters k_1 and k_2 and the inlet concentrations are: $k_1 = 1\ m^2$, $k_2 = 0.02$ $m^{2.5}/s$, $c_1 = 1\ mole/L$, $c_2 = 2\ mole/L$. Unlike the previous system the input variable for the mixing tank consists of a pair of values, i.e., $u = (F_1, F_2)$. Given an

input value set $\Sigma := \{\sigma_1, \sigma_2, \sigma_3\}$ where $\sigma_1 = (0.0184, 0.0046)$, $\sigma_2 = (0.0158, 0.0158)$, $\sigma_3 = (0.0046, 0.0184)$, the resulting equilibrium points are $(h_0, c_0)_1 = (1.3225, 1.2)$, $(h_0, c_0)_2 = (2.5, 1.5)$, and $(h_0, c_0)_3 = (1.3225, 1.8)$. Once again the method in (Kazantzis *et al.*, 2002) is used to build the following local Lyapunov functions

$$V(h, c)_1 = 716.43\, c^2 - 1719.44\, c + 3537.76 + 1432.87\, h^2 - 3789.93\, h, \qquad (7.5)$$

$$V(h, c)_2 = 4316.36\, c^2 - 12949.09\, c + 63666.35 + 8632.73\, h^2 - 43163.63\, h, \quad (7.6)$$

$$V(h, c)_3 = 1305.43\, c^2 - 4699.53\, c + 8795.98 + 2610.85\, h^2 - 6905.71\, h. \qquad (7.7)$$

The functions (7.5), (7.6), and (7.7) are Lyapunov functions over the region $E := \{(h, c) \in (1, 5) \times (1, 5)\}$. The constants associated to input values σ_1, σ_2, and σ_3 are chosen arbitrarily to be $(50, 700, 2200)$, $(1400, 5000, 12000)$, and $(80, 1400, 3800)$, respectively. The corresponding partition is shown in Figure 7.5, whereas the complete FSM abstraction is shown in Figure 7.6. In this case there exist more than 160 transitions (not provided here).●

7.3 Summary

In this chapter, we have proposed an extension of the results in the previous chapters to a class of systems for which Lyapunov functions can be determined. Since Lyapunov functions are also local submersions most of the results apply almost directly. The algorithm that computes FSM abstractions of two-dimensional systems in finite time has been altered to treat systems with Lyapunov functions. Two industrial processes illustrate the type of abstractions that can be obtained.
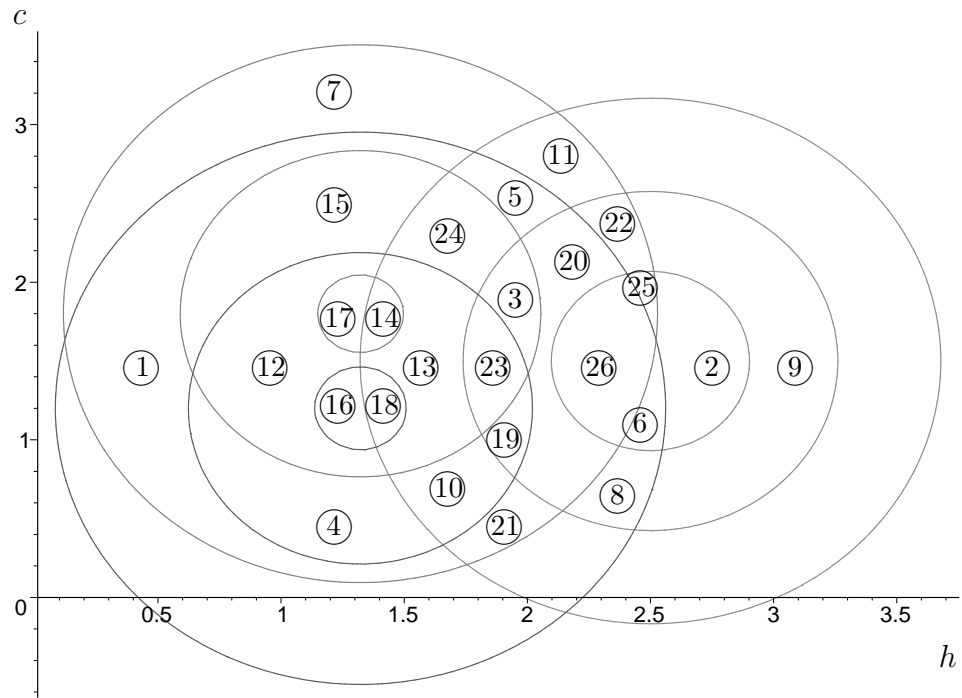
Figure 7.5: A partition for the mixing tank
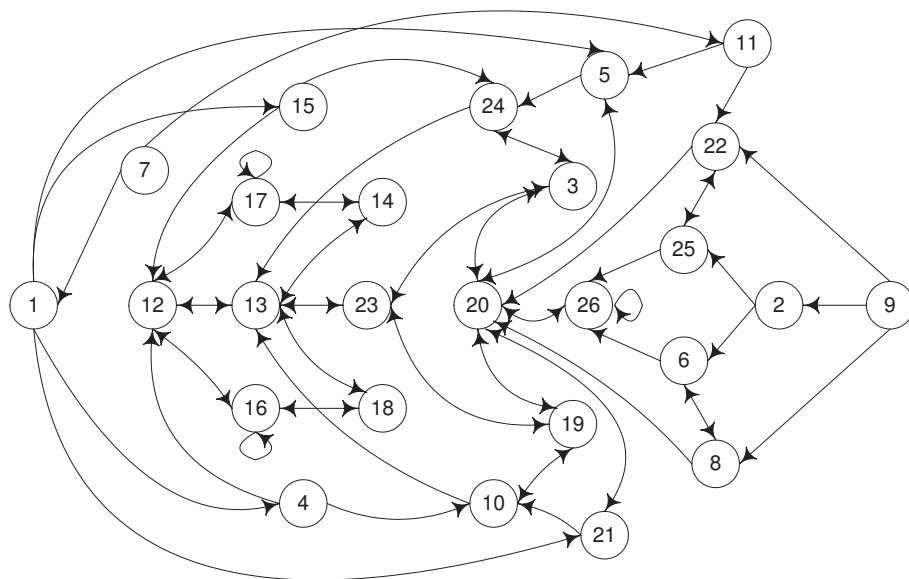
Figure 7.6: An FSM abstraction for the mixing tank

133

Chapter 8

Conclusions

The design of abstractions for continuous systems is an active research field spanning many areas such as verification, model validation, hierarchical control, and supervisory control. The construction of an abstraction is also a preliminary step to synthesizing a controller for those systems equipped with continuous and logical control objectives. In particular, abstractions can be utilized for the high-level control of complex chemical engineering processes.

In this thesis a framework was developed for the generation, in finite time, of finite-state machine abstractions for planar continuous systems. A particular emphasis was put on a class of nonlinear continuous systems satisfying an integrability property, called nearly integrable controlled switched systems. A dynamical equivalence between the abstract system and the original one was formulated in terms of consistency and completeness. Consistency ensures that given a sequence of discrete transitions generated by the abstraction, the existence of a corresponding trajectory induced by the continuous system is guaranteed. On the converse, completeness ensures that a trajectory induced by the continuous system has a corresponding sequence of discrete transitions generated by the abstraction.

The procedure that was chosen is comprised of two sequential steps. The state

structure of the abstraction is first determined, then followed by the construction of the transition structure of the abstraction. Given a state-space region of a nearly integrable controlled switched system, dynamical invariants are used to decompose the region into subsets, which act as the discrete states of the abstraction. Unlike other partitioning techniques (Zhao, 1994; Lunze *et al.*, 1999; Stursberg *et al.*, 2000; Stiver *et al.*, 2001; Bernard and Gouzé, 2002), the present procedure is model-based, independent of any specification, and it results in a single partition capturing the effect of a set of input values. Such abstractions are attractive since they can be used to achieve control tasks on continuous processes (such as hierarchical control, verification, and logical control), to validate dynamical models, and to perform process design.

An approach was then proposed to construct the transition structure of the finite-state machine abstraction. The procedure relies on the analysis of a transversality property that qualifies the dynamical behaviour of continuous trajectories with respect to partition boundaries. Moreover, a notion of well-conditioned transversality was introduced. This property facilitates the analysis of continuous trajectories that intersect with the partition boundary in a transversal manner. In particular, the property enables the characterization of such trajectories by analyzing a reduced number of points in the region. It was also demonstrated that, in general, nearly integrable controlled switched systems do not satisfy the well-conditioned transversality property. Consequently, sufficient conditions were provided in terms of constraints on the objects used to partition the state-space region. Furthermore, it was shown that a well-conditioned transversality property permits the removal of nondeterministic transitions.

In order to fully benefit from well-conditioned transversality, the method was further specialized to those partitions whose subsets have boundary points defined by dynamical invariants only. In an attempt to characterize the existence of such

partitions, local and semi-global boundedness properties were defined. Semi-global boundedness aims at detecting subsets with a boundary characterized by dynamical invariants, whereas local boundedness provides insight into the capability of forming subsets of arbitrary size. Sufficient conditions for both categories of boundedness were given for a generalized partitioning with invariants. However, necessary conditions are required in order to determine the violation of a boundedness property for the proposed type of partitions. A discussion about such conditions was provided.

An algorithm exploiting the above properties was developed in order to generate finite-state machine abstractions for two-dimensional systems. In particular, the algorithm provides a method for detecting partition subsets satisfying the semi-global boundedness property. Sufficient conditions were given in order to ensure the finiteness of computation. Also, simulation results have demonstrated that, like other partitions, one generally obtains a finite-state machine abstraction with nondeterministic transitions. In addition, it was shown that a weak notion of completeness can be achieved by the present algorithm. The verification of the consistency property for a continuous system and one of its abstractions was then undertaken. In general, it turns out that consistency does not hold unless more information is added to the abstraction transition map. Identification of the hyperplanes involved in the transitions as well as the time period during which a transition can take place were recommended as additional transition map arguments.

In the last chapter, the theory and the algorithmic procedure were extended to a class of systems for which Lyapunov functions can be determined. Such functions are advantageous because they relate directly to a wide spectrum of methods for synthesizing controllers. The above procedure was utilized to obtain finite-state machine abstractions for two chemical processes with actuators operating in finite modes ("on", "off", etc.). A potential application for the present research is the synthesis of a supervisory controller for such processes.

In a global sense, this thesis extends and generalizes verification techniques based on dynamical invariants, such as those developed in (Broucke, 1998; Stiver *et al.*, 2001). To the best of our knowledge, there exist only two other specification-independent strategies for generating abstractions of continuous systems with nonlinear dynamics (Stursberg *et al.*, 2000; Bernard and Gouzé, 2002). In comparison to those approaches, this research contributes in providing an in-depth analysis of the transversality of trajectories with respect to partition boundaries. Also the development of boundedness properties has provided indications about possible obstructions that may arise during the design of partitions using surfaces that are dynamically meaningful such as the level sets of a Lyapunov function.

This thesis offers many possible avenues for future research projects. On one hand, many useful results still need to be developed in order to fully benefit from the present construction of abstractions. First, a necessary condition for the local boundedness property of an abstraction is required. Also, it would be beneficial to have a sufficient condition for the semi-global boundedness that does not require the construction of lower dimensional objects (such as intersection points and leaf segments). In addition, finite-machine abstractions with a transition map that incorporates time and boundary information would enable one to satisfy stronger notions of completeness and consistency. With such finite-state machine abstractions, one then needs to develop a control theory for synthesizing a discrete supervisor.

On the other hand, the present results can be generalized in different directions. The major generalizations consist of extending the algorithm for treating higher-dimensional systems ($n > 2$) as well as developing a theory that considers larger classes of systems. By the latter, we consider systems that evolve on more general spaces than on an open subset of an Euclidean space, and also hybrid systems. In both cases the present material may still be useful. In particular, the hybrid model for the two-tank system can be analyzed by neighboring partitions of two subsets of

an Euclidean space. Similarly, the transversality analysis of the inverted pendulum could be performed even though the system evolves on a submanifold of the three-dimensional Euclidean space.

Bibliography

Abraham, R., Marsden, J. E. and Ratiu, T. (1988), *Manifolds, Tensor Analysis, and Applications*, Vol. 75 of *Applied Mathematical Sciences*, Springer-Verlag.

Aeyels, D. and Sepulchre, R. (1992), 'Stability for Dynamical Systems with First Integrals: A Topological Approach', *Systems & Control Letters* **19**, 461–465.

Alur, R., Henzinger, T., Lafferriere, G. and Pappas, G. (2000), Discrete Abstractions of Hybrid Systems, *in* 'Proceedings of the IEEE', number 88, pp. 971–984.

Artstein, Z. (1996), Examples of Stabilization with Hybrid Feedback, *in* Springer-Verlag, ed., 'Hybrid Systems III. Verification and Control.', number 1066 *in* 'Lecture Notes in Computer Science', pp. 173–185.

Åström, K. J. and Furuta, K. (2000), 'Swinging up a Pendulum by Energy Control', *Automatica* **36**, 287–295.

Bernard, O. and Gouzé, J.-L. (1995), Robust Validation of Uncertain Models, *in* 'Proceedings of the 3rd European Conference on Control', pp. 1261–1266.

Bernard, O. and Gouzé, J.-L. (1999), 'Non-linear Qualitative Signal Processing for Biological Systems: Application to the Algal Growth in Bioreactors', *Mathematical Biociences* (157), 357–372.

Bernard, O. and Gouzé, J.-L. (2002), 'Global Qualitative Description of a Class of Nonlinear Dynamical Systems', *Artifical Intelligence* (136), 29–59.

Blouin, S., Guay, M. and Rudie, K. (2001), An Application of Discrete-Event Theory to Truck Dispatching, *in* 'Proceedings of the 40th American Control Conference', pp. 2315–2320.

Blouin, S., Guay, M. and Rudie, K. (2003), 'Discrete Control of Nearly Integrable Two-dimensional Systems', To appear in *ADCHEM International Symposium on Advanced Control of Chemical Processes* .

Boothby, W. M. (1986), *An Introduction to Differentiable Manifolds and Riemannian Geometry*, Academic Press.

Branicky, M. (1995), Studies in Hybrid Systems: Modeling, Analysis, and Control, PhD thesis, Massachussetts Institute of Technology.

Branicky, M. S., Borkar, V. S. and Mitter, S. K. (1998), 'A Unified Framework for Hybrid Control Model and Optimal Control Theory', *IEEE Transactions on Automatic Control* **43**, 31–45.

Broucke, M. (1998), A Geometric Approach to Bisimulation and Verification of Hybrid Systems, *in* 'Proceedings of the 37th IEEE Conference on Decision and Control', pp. 4277–4282.

Caines, P. E. and Lemch, E. S. (1998), On the Global Controllability of Hamiltonian and Other Nonlinear Systems: Fountains and Recurrence, *in* 'Proceedings of the 37th IEEE Conference on Decision and Control', pp. 3575–3580.

Caines, P. E. and Wei, Y. J. (1998), 'Hierarchical Hybrid Control Systems: A Lattice Theoretic Formulation', *IEEE Transactions on Automatic Control* **43**(4), 501–508.

Clarke, F. H. (1990), *Optimization and Nonsmooth Analysis*, Philadelphia, SIAM.

Cuadrado, J. (1994), 'Teach Formal Methods', *BYTES* p. 292.

De Leenheer, P. and Aeyels, D. (2000), Accessibility Properties of Controlled Lotka-Volterra Systems, *in* 'Proceedings of the 39th IEEE Conference on Decision and Control', pp. 3977–3981.

Edelen, D. G. B. (1985), *Applied Exterior Calculus*, John Wiley & Sons.

Elkin, V. I. (1999), *Reduction of Nonlinear Control Systems*, Kluwer Academic Publishers.

Goriely, A. (2001), *Integrability and Nonintegrability of Dynamical Systems*, World Scientific.

Grammaticos, B. and Ramani, A. (1996), Integrability - and How to Detect It, *in* Springer, ed., 'Integrability of Nonlinear Systems, Lecture Notes in Physics, Proceedings of the CIMPA School Pondicherry University, India', pp. 30–94.

Guillemin, V. and Pollack, A. (1974), *Differential Topology*, Prentice-Hall.

Hirsch, M. W. and Smale, S. (1974), *Differential Equations, Dynamical Systems and Linear Algebra*, Academic Press.

Hopcroft, J. E. and Ullman, J. D. (1979), *Introduction to Automata Theory, Languages and Computation*, Addison-Wesley.

Hsu, C. S. (1987), *Cell-to-Cell Mapping: A Method of Global Analysis for Nonlinear Systems*, Vol. 64 of *Applied Mathematical Sciences*, Springer-Verlag.

Isidori, A. (1995), *Nonlinear Control Systems*, Springer-Verlag, Second Edition.

Kasriel, R. (1971), *Undergraduate Topology*, Vol. 71 of *Translations of Mathematical Monographs*, W.B. Saunders Company.

Kazantzis, N., Kravaris, N., Tseronis, C. and Wright, R. (2002), Optimal Controller Tuning for Nonlinear Processes, *in* 'Proceedings of the 15th IFAC World Congress'.

Khalil, H. K. (1992), *Nonlinear Systems*, Macmillan Publishing Company.

Kokar, M. (1995), 'On Consistent Symbolic Representations of General Dynamic Systems', *IEEE Transactions on Systems, Man and Cybernatics* **25**(8), 1231–1241.

Lefebvre, M.-A., Guéguen, H. and Buisson, J. (2002), Structured Hybrid Abstraction of Continuous Systems, *in* 'Proceedings of the 15th IFAC Triennal World Congress'.

Lemch, E. S. and Caines, P. E. (1999), Hybrid Partition Machines with Disturbances: Hierarchical Control via Partition Machines, *in* 'Proceedings of the 38th IEEE Conference on Decision and Control', pp. 4909–4914.

Liberzon, D. (2002), Stabilization by Quantized State or Output Feedback: A Hybrid Control Approach, *in* 'Proceedings of the 15th IFAC World Congress'.

Liberzon, D. and Morse, A. S. (1999), 'Basic Problems in Stability and Design of Switched Systems', *IEEE Control Systems Magazine* **19**, 59–70.

Lunze, J. (1992), 'Qualitative Modelling of Continuous-variable Systems by means of Non-deterministic Automata', *Intern. J. Intelligent Systems Engineering* **1**(1), 22–30.

Lunze, J. (1994), 'Qualitative Modelling of Linear Dynamical Systems with Quantized State Measurements', *Automatica* **30**(3), 417–431.

Lunze, J. (1995), 'Stabilization of Nonlinear Systems by Qualitative Feedback Controllers', *Int. J. Control* **62**(1), 109–128.

Lunze, J. (1998), 'Qualitative Modelling of Dynamical Systems: Motivation, Methods and Prospective Applications', *Mathematics and Computers in Simulation* **46**, 465–483.

Lunze, J., Nixdorf, B. and Schroder, J. (1999), 'Deterministic Discrete-event Representation of Linear Continuous-variable Systems', *Automatica* **35**, 395–406.

Nijmeijer, H. and van der Schaft, A. J. (1990), *Nonlinear Dynamical Control Systems*, Springer.

Ogunnaike, B. A. and Ray, W. H. (1994), *Process Dynamics, Modelling, and Control*, Oxford University Press.

Pappas, G. and Simic, S. (2002), 'Consistent Abstractions of Affine Control Systems', *IEEE Transactions on Automatic Control* **47**(5), 745–756.

Raisch, J. (1995), Control of Continuous Plants by Symbolic Output Feedback, *in* Springer, ed., 'Hybrid Systems II', number 999 *in* 'Lecture Notes in Computer Science', pp. 371–390.

Raisch, J. (2000), 'Discrete Abstractions of Continuous Systems - an Input/Output Point of View', *Mathematical and Computer Modelling of Dynamical Systems* **6**(1), 6–29. Special issue on Discrete Event Models of Continuous Systems.

Raisch, J. and O'Young, S. (1996), A DES Approach to Control of Hybrid Dynamical Systems, *in* Springer, ed., 'Hybrid Systems III: Verification and Control', number 1066 *in* 'Lecture Notes in Computer Science', pp. 563–574.

Raisch, J. and O'Young, S. (1998), 'Discrete Approximation and Supervisory Control of Continuous systems', *IEEE Transactions on Automatic Control* **43**(4), 569–573.

Ramadge, P. J. and Wonham, W. M. (1982), Supervision of Discrete Event Processes, *in* 'Proceedings of the IEEE Conference on Decision and Control', Vol. 3, pp. 1228–1229.

Ramadge, P. J. and Wonham, W. M. (1987), 'Supervisory Control of a Class of Discrete Event Processes', *SIAM Journal of Control and Optimization* **25**(1), 206–230.

Rosen, K. (2003), *Discrete Mathematics and its Applications, Fifth Edition*, McGraw Hill.

Rouche, N., Habets, P. and Laloy, M. (1977), *Stability Theory by Lyapunov's Direct Method*, Springer-Verlag.

Salvadori, L. and Visentin, F. (1999), 'First Integrals and Stability Properties', *Math. Japonica* **1**, 1–7.

Stiver, J. A. and Antsaklis, P. J. (1993), On The Controllability of Hybrid Control Systems, *in* 'Proceedings of the 32nd IEEE Conference on Decision and Control', pp. 294–299.

Stiver, J. A., Antsaklis, P. J. and Lemmon, M. D. (1995*a*), Hybrid Control System Design Based on Natural Invariants, *in* 'Proceedings of the 34th IEEE Conference on Decision and Control'.

Stiver, J. A., Antsaklis, P. J. and Lemmon, M. D. (1995*b*), Interface and Controller Design for Hybrid Control Systems, *in* Springer-Verlag, ed., 'Hybrid System II', number 999 *in* 'Lecture Notes in Computer Science', pp. 462–493.

Stiver, J. A., Koutsoukos, X. D. and Antsaklis, P. J. (2000), An Invariant Based Approach to the Design of Hybrib Control Systems, Technical Report ISIS-2000-001, ISIS Group, University of Notre-Dame,IN, U.S.A.

Stiver, J. A., Koutsoukos, X. D. and Antsaklis, P. J. (2001), 'An Invariant Based Approach to the Design of Hybrid Control Systems', *International Journal of Robust and Nonlinear Control* **11**(5), 453–478.

Stursberg, O., Kowalewski, S. and Engell, S. (2000), 'On the Generation of Timed Discrete Approximations for Continuous Systems', *Mathematical and Computer Modelling of Dynamical Systems* **6**(1), 51–70. Special issue on Discrete Event Models of Continuous Systems.

Tamura, I. (1992), *Topology of Foliations: An Introduction*, Vol. 97 of *Translations of Mathematical Monographs*, American Mathematical Society.

Willems, J. C. (1991), 'Paradigms and Puzzles in the Theory of Dynamical Systems', *IEEE Transactions on Automatic Control* **36**(3), 259–294.

Wonham, W. M. (1999), *Lecture Notes of DES class ECE1636F and ECE1637S*, University of Toronto, available at: http://www.control.utoronto.ca/people/profs /wonham/wonham.html.

Yang, X., Lemmon, M. D. and Antsaklis, P. J. (1995), 'On the Supremal Controllable Sublanguage in the Discrete-event Model of Nondeterministic Hybrid Control Systems', *IEEE Transactions on Automatic Control* **40**(12), 2098–2103.

Zhao, F. (1994), 'Extracting and Representing Qualitative Behaviors of Complex Systems in Phase Space', *Artificial Intelligence* **69**(1-2), 51–92.

Appendix A

Cited Results

The purpose of this appendix it to present results used throughout the thesis.

A.1 Algebra

Let X be a set. A binary relation $\leq$ is a *partial order* on X if it is reflexive, transitive, and antisymmetric. Two elements of a partial order need not be comparable, i.e., $(x, y \in X)$ $x \not\leq y$ and $y \not\leq x$ is possible. The pair $(X, \leq)$ is called a *poset*.

For a poset $(X, \leq)$ an element $l \in X$ is a meet (or greatest lower bound) for $x, y \in X$ if and only if

$$l \leq x \text{ and } l \leq y \text{ and } (\forall a \in X)\, a \leq x \text{ and } a \leq y \Rightarrow a \leq l. \tag{A.1}$$

The meet of x and y is denoted by $x \star y$. Let R be an equivalence relation on X. For xRx' we also write $x \equiv x' \,(\text{mod } R)$. As shown in (Rosen, 2003), a partition of a set induces an equivalence relation and an equivalence relation induces a partition.

Let $\mathcal{E}(X)$ be the collection of all equivalence relations over X. A partial order on $\mathcal{E}(X)$ is defined as

$$(\forall R_1, R_2 \in \mathcal{E}(X))\, R_1 \preceq R_2 \text{ iff } (\forall x, y \in X)\, xR_1y \Rightarrow xR_2y, \tag{A.2}$$

where R_1 is said to be "finer" than R_2.

Proposition A.1 ((Wonham, 1999))

In the poset $(\mathcal{E}(X), \preceq)$, the meet $R_1 \star R_2$ of elements $R_1, R_2 \in \mathcal{E}(X)$ defined as

$$(\forall x, x' \in X)\, x \equiv x'\, (mod\, R_1 \star R_2)\ \text{iff}\ x \equiv x'\, (mod\, R_1)\, \&\, x \equiv x'\, (mod\, R_2), \quad \text{(A.3)}$$

always exists.⋄

Consequently $R_1 \star R_2$ is the coarsest partition that is finer than both R_1 and R_2.

A.2 Differential Geometry and Topology

A.2.1 Measure Zero Sets, Dense Sets, Connected Sets

A subset $A \subset \mathbb{R}^n$ is of *measure zero* (also called *Lebesgue measure zero*) if, for every $\epsilon > 0$, there is a countable covering of A by open rectangles U_i such that the sum of the volumes of U_i is less than ϵ (Boothby, 1986).

A subset $A \subset B$ is *dense* in B if the closure of A coincides with B, that is, $\overline{A} = B$, or said otherwise, if for any point $p \in B$ every neighborhood of p, N_p, is such that $N_p \cap A \neq \emptyset$ (Abraham *et al.*, 1988). Notice that the complement of a dense set is of measure zero.

Theorem A.2 ((Kasriel, 1971))

Suppose K is a collection of connected subsets of B such that if $C_1 \in K$ and $C_2 \in K$, then $\bar{C}_1 \cap C_2 \neq \emptyset$ or $C_1 \cap \bar{C}_2 \neq \emptyset$. Then $\bigcup K$ is connected.⋄

A.2.2 Regular Points of Distributions/Codistributions

A point p is a regular point of a distribution Δ defined on the open set D if there exists a neighborhood of p, $U_p \subset D$, such that the rank of the vector fields forming Δ is constant everywhere in U_p (Isidori, 1995).

Lemma A.3 ((Elkin, 1999)) *The set of all regular points of a smooth distribution Δ defined on an open set D, is an open and dense subset of D.⋄*

Additional conditions on the distribution and the set D lead to a stronger result.

Proposition A.4

The set of all regular points of maximal rank of an analytic distribution Δ defined on an open and connected set D, is an open and dense subset of D.◇

Sketch of proof: We assume that Δ is a distribution spanned by r vector fields $f_1(x), \ldots, f_r(x)$. Let the function $h : D \to \mathbb{N}$ defined by $h(x) = rank\{f_1(x), \ldots, f_r(x)\}$ provide the maximum order of any non-vanishing determinant on D, and denote by k the maximal value of h (i.e., the maximal rank of the distribution Δ) over D. Notice that h is an algebraic function of analytic functions, that is, h is an analytic function (Boothby, 1986).

If $k = 0$ then the distribution has maximal rank over the whole of D thus proving the claim. Now suppose that p is a regular point of maximal rank $k > 0$. If $k < r$ then on D there are at most k linearly independent vector fields. In this case, one can simply redefine Δ so that it is spanned by the k vector fields that are linearly independent at p. Now we show by contradiction that the set of regular points with maximal rank forms an open and dense subset of D. Namely let us assume that $h^{-1}(\mathbb{R} \setminus \{0\})$ is not dense in D. Therefore there exists an open subset $U \subset D$ where the rank of Δ is less than k. Because h is analytic, it vanishes everywhere in the connected subset of D containing U. Since by assumption D is connected, then h vanishes everywhere in D, contradicting the fact that p is such that $h(x)|_{x=p} \neq 0$.□

Similar conclusions hold for codistributions.

A.2.3 Implicit Function Theorem

Theorem A.5 ((Isidori, 1995))

Let $A \subset \mathbb{R}^m$ and $B \subset \mathbb{R}^n$ be open sets. Let $f : A \times B \to \mathbb{R}^n$ be a smooth mapping. Let

$$(x, y) = (x_1, \ldots, x_m, y_1, \ldots, y_n) \tag{A.4}$$

denote a point of $A \times B$. Suppose that for some $(x^o, y^o) \in A \times B$, $f(x^o, y^o) = 0$ and the matrix

$$\frac{\partial f}{\partial y} = \begin{pmatrix} \frac{\partial f_1}{\partial y_1} & \cdots & \frac{\partial f_1}{\partial y_n} \\ \cdots & \cdots & \cdots \\ \frac{\partial f_n}{\partial y_1} & \cdots & \frac{\partial f_n}{\partial y_n} \end{pmatrix} \tag{A.5}$$

is nonsingular at (x^o, y^o). Then there exist open neighborhoods A_o of x^o in A and B_o of y^o in B and a unique smooth mapping $g : A_o \to B_o$ such that $f(x, g(x)) = 0$ for all $x \in A_o$.◇

A.2.4 Preimage Theorem

This theorem is also called the Submersions Theorem.

Theorem A.6 ((Abraham _et al._, 1988))

Let $f : M \to N$ be a smooth map between manifolds and let $n \in N$ be a regular value. Then the preimage $f^{-1}(n) = \{m \mid m \in M, f(m) = n\}$ is a submanifold of M with tangent space given by $T_m f^{-1}(n) = kernel(T_m f)$.◇

If N is finite dimensional and n is a regular value then $codim(f^{-1}(n)) = dim(N)$.

A.2.5 Sard's Theorem in $\mathbb{R}^n$

Theorem A.7 ((Abraham _et al._, 1988))

Let $U \subset \mathbb{R}^m$ be open and $f : U \to \mathbb{R}^n$ be of class C^k where $k > max(0, m-n)$. Then the set of critical values of f has measure zero in $\mathbb{R}^n$.◇

One can also find in (Abraham _et al._, 1988) a generalization of the above result for the case where the mapping involves manifolds.

A.3 Nonsmooth Analysis

A.3.1 Tangent Cone

From (Clarke, 1990), the (nonsmooth and Lipschitz) distance function from a point $p' \in D'$ to the set $\Omega(\hat{\Gamma})$ is defined as

$$d_{\Omega(\hat{\Gamma})}(p') = \min\{|p' - p| : p \in \Omega(\hat{\Gamma})\}. \tag{A.6}$$

The *generalized directional derivative* of $d_{\Omega(\hat{\Gamma})}$, when evaluated at p and in the direction $v \in \mathbb{R}^n$, is given by

$$d^0_{\Omega(\hat{\Gamma})}(p, v) := \limsup_{p' \to p, \ \lambda \downarrow 0} \frac{d_{\Omega(\hat{\Gamma})}(p' + \lambda v) - d_{\Omega(\hat{\Gamma})}(p')}{\lambda}. \tag{A.7}$$

The *tangent cone* to $\Omega(\hat{\Gamma})$ at a point $p \in \Omega(\hat{\Gamma})$ is given by

$$C_{\Omega(\hat{\Gamma})}(p) := \{v \in \mathbb{R}^n \mid d^0_{\Omega(\hat{\Gamma})}(p, v) = 0\}. \tag{A.8}$$

The following result establishes an equivalence between the elements of the tangent cone and some sequences.

Theorem A.8 ((Clarke, 1990))
An element v of $\mathbb{R}^n$ is tangent to $\Omega(\hat{\Gamma})$ at p if and only if, for every sequence p_i in $\Omega(\hat{\Gamma})$ converging to p and sequence β_i in $(\infty, 0)$ decreasing to 0, there is a sequence v_i in $\mathbb{R}^n$ converging to v such that $p_i + \beta_i v_i \in \Omega(\hat{\Gamma})$ for all $i.\diamond$

A.4 Control Theory

A.4.1 Class of Admissible Controls

Definition A.9 ((Nijmeijer and van der Schaft, 1990)) Let u be an input mapping $u : \mathbb{R}_{\geq 0} \to U$ where U is an input value set. The class of *admissible controls*, $\mathcal{U}$, consists of a family of input maps that is closed under concatenation, i.e., with

$u_1(\cdot), u_2(\cdot) \in \mathcal{U}$, and for any $\bar{t} \in \mathbb{R}$ and

$$\bar{u}(t) = \begin{cases} u_1(t), & t < \bar{t} \\ u_2(t), & t \geq \bar{t} \end{cases} \tag{A.9}$$

then $\bar{u}(\cdot) \in \mathcal{U}.\diamond$

A.4.2 Complete Vector Field

Definition A.10 ((Isidori, 1995)) A vector field $f(x)$ defined on a manifold M is *complete* if the flow ϕ of $f(x)$ is defined on the whole cartesian product $\mathbb{R} \times M.\diamond$

A.4.3 Complete Integrability

Definition A.11 ((Isidori, 1995)) A nonsingular d-dimensional distribution Δ, defined on an open set D of $\mathbb{R}^n$, is said to be *completely integrable* if, for each point x_0 of D there exist a neighborhood U_0 of x_0, and $n - d$ real-valued smooth functions $\lambda_1, \ldots, \lambda_{n-d}$, all defined on U_0, such that the annihilator of Δ, say $\Delta^\perp$, is such that $\Delta^\perp = span\{d\lambda_1, \ldots, d\lambda_{n-d}\}$ on $U_0.\diamond$

A.5 Exterior Differential Systems

The material presented here summarizes some concepts of exterior calculus. For a thorough treatment of the topic the reader is referred to (Edelen, 1985) and (Abraham *et al.*, 1988).

Recall that the tangent space to a manifold M at a point p is written as T_pM and that elements of T_pM are called vector fields. The tangent space to M turns out to be a vector space over $\mathbb{R}$ and with the Lie product it can be made into an algebra called the Lie algebra. In the next paragraphs, a similar procedure is performed for the dual of a tangent space, the cotangent space.

The cotangent space to M at a point p is denoted by T_p^*M and the elements of

T_p^*M are covectors. A differential form, or one-form, is a function ω that assigns to each point p of M a covector in T_p^*M. The collection of one-forms over T_p^*M is denoted by $\Lambda^1(M)$. The cotangent space can be made into a vector space over $\mathbb{R}$.

In order to make an algebra out of elements in T_p^*M, the cotangent space is equipped with a wedge product and an exterior algebra. The wedge product is a non-commutative product between two forms satisfying

$$
\begin{aligned}
(a\alpha_1 + b\alpha_2) \wedge \beta &= a\alpha_1 \wedge \beta + b\alpha_2 \wedge \beta, \text{ for } \alpha_1, \alpha_2, \beta \in \Lambda^1(M) \text{ and } a, b \in \mathbb{R} \\
\alpha \wedge (a\beta_1 + b\beta_2) &= a\alpha \wedge \beta_1 + b\alpha \wedge \beta_2, \text{ for } \alpha, \beta_1, \beta_2 \in \Lambda^1(M) \text{ and } a, b \in \mathbb{R} \quad \text{(A.10)} \\
\alpha \wedge \beta &= -\beta \wedge \alpha, \text{ for } \alpha, \beta \in \Lambda^1(M)
\end{aligned}
$$

The wedge product of k one-forms is called a k-form. The space of k-forms over M, denoted by $\Lambda^k(M)$, also defines a vector space over $\mathbb{R}$. The exterior algebra over M is the graded algebra

$$
\Lambda(M) := \Lambda^0(M) \oplus \cdots \oplus \Lambda^n(M), \tag{A.11}
$$

with $\Lambda^0(M) = C^0(M)$.

The exterior derivative of the smooth k-form $\omega = \sum_{i_1 \leq \cdots \leq i_k} a_{i_1 \cdots i_k} dx_{i_1} \wedge \cdots \wedge dx_{i_k}$ is the $(k+1)$-form

$$
d\omega = \sum_{i_1 \leq \cdots \leq i_k} da_{i_1 \cdots i_k} \wedge dx_{i_1} \wedge \cdots \wedge dx_{i_k}. \tag{A.12}
$$

The exterior derivative is such that (i) $d(\omega_1 + \omega_2) = d\omega_1 + d\omega_2$, (ii) $d(\omega \wedge \alpha) = d\omega \wedge \alpha + (-1)^k \omega \wedge d\alpha$, $\omega \in \Lambda^k(M)$, and (iii) $d(d\omega) = 0$.

A k-form that lies in the kernel of d is said to be *closed* whereas a k-form, $k \geq 1$, is *exact* when it lives in the range of d for some $(k-1)$-form. A collection of $k \leq n$ one-forms $\omega_1, \ldots, \omega_k$ is linearly independent if and only if

$$
\omega_1 \wedge \cdots \wedge \omega_k \neq 0. \tag{A.13}
$$

Appendix B

Program for Two-dimensional Systems

This appendix introduces some details about the program that generates FSM abstractions of two-dimensional systems.

B.1   Displacement along Leaves

In this section we present a few methods for moving along a leaf.

Method (I) Since the systems of interest live in $\mathbb{R}^2$, a leaf corresponds to a one-dimensional subspace on which a trajectory evolves, i.e., both the trajectory and the leaf are of the same dimension. Moreover the class of nearly integrable CSS has an integrable set of ODEs. Consequently it is possible to use numerical integration in order to move along a leaf in any direction (a reversal of time provides a displacement in the opposite direction). However this technique fails whenever a leaf contains equilibrium points. For this reason a more generic approach is proposed next.

Method (II) The present technique exploits the fact that each leaf L is characterized by a first integral $\gamma \in \Gamma$, which is an implicit function. Therefore

for any point of L the Implicit Function Theorem implies a local characterization. Also a metric is required.

The procedure is summarized by the following set of successive steps.

- Let $p \in L$ and identify an $i \in \{1, 2\}$ such that

$$\partial \gamma / \partial x_i|_{x=p} \neq 0 \text{ and } \|\partial \gamma / \partial x_i|_{x=p}\| \geq \|\partial \gamma / \partial x_j|_{x=p}\| \text{ for } j \neq i.$$

- Identify the characterization of L that holds at p, i.e., $x_i = h(x_j)$, and verify that $p_i = h(p_j)$ where $p = (p_1, p_2)$.

- Use the above characterization to define two points p^+ and p^- resulting from small perturbations $\pm\delta_j$ of p_j. In order to guarantee that both p^+ and p^- remain within a neighborhood of p check if $sign(\partial \gamma / \partial x_i|_{x=p}) = sign(\partial \gamma / \partial x_i|_{x=p^+})$ and $sign(\partial \gamma / \partial x_i|_{x=p}) = sign(\partial \gamma / \partial x_i|_{x=p^-})$. If not then divide δ_j until the condition is satisfied.

- The next step amounts to choosing which one among p^+ or p^- goes in the selected direction of search. At the first iteration one determines a direction by picking either p^+ or p^-. For the next iterations the method uses the predecessor of point p, say p_p. Namely if p^- is farther to p_p than p^+ is, then pick p^- as the next point on L matching the search direction, otherwise pick p^+.

- Repeat the procedure until the displacement along L leads to an intersection point, or until ∂E is encountered.

Method (III) By condition (4.3)(ii) the equilibrium points form a set of measure zero in D'. Consequently one can use Method (I) and switch to Method (II) whenever an equilibrium point is encountered.

B.2 Maple Output - Double Integrator

```
The system of interest is a double integrator
--------------------------------------------
```

$$vect\_field := \begin{bmatrix} x_2 \\ u_1 \end{bmatrix}$$

$$\phi 1 := x_1 - \frac{1}{2}\frac{x_2^2}{u_1} = cst$$

$$first\_integrals := \begin{bmatrix} x_1 - \frac{1}{2}\frac{x_2^2}{u_1} = cst \end{bmatrix}$$

$$inputs := \begin{bmatrix} 1 \\ -1 \\ 2 \end{bmatrix}$$

$$fic := \begin{bmatrix} -2 & 1 & 3 \\ -4 & 0 & 5 \\ -4 & 2 & 4 \end{bmatrix}$$

$$nts := \{x_2 = 0\}$$

$$region := \{-5 \le x_1,\ x_1 \le 11,\ x_2 \le 6,\ -6 \le x_2\}$$

```
Dimension=
```
$$2$$

```
The # fic per foliation =
```
$$3$$

```
The # inputs =
```
$$1$$

```
The # of input values is =
```
$$3$$

```
The list of intersection points is = [ index # of intersection point =

 [{index # of intersecting leaves} [coordinates of the int. pt]]
```

table([1 = $\begin{bmatrix} \{1\} & [-4., 0.] \end{bmatrix}$, 2 = $\begin{bmatrix} \{2\} & [-2.666666667, -2.309401077] \end{bmatrix}$,

3 = $\begin{bmatrix} \{2\} & [-2.666666667, 2.309401077] \end{bmatrix}$, 4 = $\begin{bmatrix} \{3\} & [-1., -3.464101615] \end{bmatrix}$,

5 = $\begin{bmatrix} \{3\} & [-1., 3.464101615] \end{bmatrix}$, 6 = $\begin{bmatrix} \{4, 8, 13\} & [3., 2.] \end{bmatrix}$,

7 = $\begin{bmatrix} \{4, 8, 13\} & [3., -2.] \end{bmatrix}$, 8 = $\begin{bmatrix} \{5\} & [4.333333333, -1.154700538] \end{bmatrix}$,

9 = $\begin{bmatrix} \{5\} & [4.333333333, 1.154700538] \end{bmatrix}$, 10 = $\begin{bmatrix} \{6\} & [6., 4.] \end{bmatrix}$,

11 = $\begin{bmatrix} \{6\} & [6., -4.] \end{bmatrix}$, 12 = $\begin{bmatrix} \{7\} & [10., -4.898979486] \end{bmatrix}$,

13 = $\begin{bmatrix} \{7\} & [10., 4.898979486] \end{bmatrix}$, 14 = $\begin{bmatrix} \{9\} & [7., -3.464101615] \end{bmatrix}$,

15 = $\begin{bmatrix} \{9\} & [7., 3.464101615] \end{bmatrix}$, 16 = $\begin{bmatrix} \{10\} & [5., 2.] \end{bmatrix}$,

17 = $\begin{bmatrix} \{10\} & [5., -2.] \end{bmatrix}$, 18 = $\begin{bmatrix} \{11\} & [-1., -1.414213562] \end{bmatrix}$,

19 = $\begin{bmatrix} \{11\} & [-1., 1.414213562] \end{bmatrix}$, 20 = $\begin{bmatrix} \{12\} & [1.500000000, -2.645751311] \end{bmatrix}$,

21 = $\begin{bmatrix} \{12\} & [1.500000000, 2.645751311] \end{bmatrix}$, 22 = $\begin{bmatrix} \{14\} & [4., -1.414213562] \end{bmatrix}$,

23 = $\begin{bmatrix} \{14\} & [4., 1.414213562] \end{bmatrix}$])

The list of 1D boundary elements is = [index # of 1D boundary element =

[leaf charact., time dir., ind. IP #1, ind. IP #2]]

table([1 = [[1, 1, 1], 1, 10, 13], 2 = [[1, 1, 1], −1, 10, 21],
3 = [[1, 1, 1], −1, 21, 19], 4 = [[1, 1, 1], −1, 19, 18], 5 = [[1, 1, 1], −1, 18, 20],
6 = [[1, 1, 1], −1, 20, 11], 7 = [[1, 1, 1], −1, 11, 12], 8 = [[1, 1, 2], 1, 6, 15],
9 = [[1, 1, 2], −1, 6, 7], 10 = [[1, 1, 2], −1, 7, 14], 11 = [[1, 1, 3], −1, 16, 23],
12 = [[1, 1, 3], −1, 23, 22], 13 = [[1, 1, 3], −1, 22, 17], 14 = [[2, 2, 2], −1, 2, 18],
15 = [[2, 2, 2], −1, 18, 19], 16 = [[2, 2, 2], −1, 19, 3], 17 = [[2, 2, 3], −1, 4, 20],
18 = [[2, 2, 3], −1, 20, 7], 19 = [[2, 2, 3], −1, 7, 22], 20 = [[2, 2, 3], −1, 22, 8],
21 = [[2, 2, 3], −1, 8, 9], 22 = [[2, 2, 3], −1, 9, 23], 23 = [[2, 2, 3], −1, 23, 6],
24 = [[2, 2, 3], −1, 6, 21], 25 = [[2, 2, 3], −1, 21, 5], 26 = [[3, 3, 1], 1, 1, 3],
27 = [[3, 3, 1], 1, 3, 5], 28 = [[3, 3, 1], −1, 1, 2], 29 = [[3, 3, 1], −1, 2, 4],
30 = [[3, 3, 2], 1, 6, 10], 31 = [[3, 3, 2], −1, 6, 7], 32 = [[3, 3, 2], −1, 7, 11],
33 = [[3, 3, 3], 1, 8, 9], 34 = [[3, 3, 3], 1, 9, 16], 35 = [[3, 3, 3], 1, 16, 15],
36 = [[3, 3, 3], 1, 15, 13], 37 = [[3, 3, 3], −1, 8, 17], 38 = [[3, 3, 3], −1, 17, 14],
39 = [[3, 3, 3], −1, 14, 12]])

The number of 2D elements is =

The set of 2D elements is =

[1 = table([1 = 10, 2 = 19, 3 = 13, 4 = 38]),
2 = table([1 = 30, 2 = 8, 3 = 36, 4 = 1]),
3 = table([1 = 27, 2 = 16, 3 = 3, 4 = 25]),
4 = table([1 = 12, 2 = 23, 3 = 31, 4 = 19]), 5 = table([1 = 13, 2 = 20, 3 = 37]),
6 = table([1 = 30, 2 = 24, 3 = 2]), 7 = table([1 = 29, 2 = 14, 3 = 5, 4 = 17]),
8 = table([1 = 11, 2 = 35, 3 = 8, 4 = 23]),
9 = table([1 = 28, 2 = 26, 3 = 16, 4 = 4, 5 = 14]),
10 = table([1 = 18, 2 = 6, 3 = 32]), 11 = table([1 = 10, 2 = 32, 3 = 7, 4 = 39]),
12 = table([1 = 31, 2 = 9]),
13 = table([1 = 15, 2 = 5, 3 = 18, 4 = 9, 5 = 24, 6 = 3]),
14 = table([1 = 15, 2 = 4]), 15 = table([1 = 33, 2 = 20, 3 = 12, 4 = 22]),
16 = table([1 = 33, 2 = 21]), 17 = table([1 = 22, 2 = 34, 3 = 11])]

The following set 1D element indices intersects with NTS
$$\{4, 9, 12, 15, 21, 31, 33\}$$

Transition table [2D source, input value, 1D element, 2D target]

table([1 = [1, 2, 10, 11], 2 = [1, 1, 19, 4], 3 = [1, 3, 19, 4], 4 = [1, 3, 13, 5],
5 = [2, 2, 8, 8], 6 = [3, 2, 3, 13], 7 = [4, 2, 12, 15], 8 = [4, 3, 12, 15],
9 = [4, 1, 23, 8], 10 = [4, 3, 23, 8], 11 = [4, 1, 31, 12], 12 = [4, 2, 31, 12],
13 = [5, 2, 13, 1], 14 = [5, 1, 20, 15], 15 = [5, 3, 20, 15], 16 = [6, 1, 30, 2],
17 = [6, 2, 30, 2], 18 = [7, 1, 14, 9], 19 = [7, 3, 14, 9], 20 = [7, 3, 5, 13],
21 = [8, 2, 11, 17], 22 = [8, 3, 8, 2], 23 = [9, 1, 16, 3], 24 = [9, 3, 16, 3],
25 = [9, 2, 4, 14], 26 = [9, 3, 4, 14], 27 = [10, 1, 18, 13], 28 = [10, 3, 18, 13],
29 = [11, 3, 10, 1], 30 = [11, 1, 32, 10], 31 = [11, 2, 32, 10], 32 = [12, 1, 31, 4],
33 = [12, 2, 31, 4], 34 = [12, 3, 9, 13], 35 = [12, 2, 9, 13], 36 = [13, 1, 15, 14],
37 = [13, 3, 15, 14], 38 = [13, 2, 5, 7], 39 = [13, 2, 9, 12], 40 = [13, 3, 9, 12],
41 = [13, 1, 24, 6], 42 = [13, 3, 24, 6], 43 = [13, 3, 3, 3], 44 = [14, 1, 15, 13],
45 = [14, 3, 15, 13], 46 = [14, 3, 4, 9], 47 = [14, 2, 4, 9], 48 = [15, 1, 33, 16],
49 = [15, 2, 33, 16], 50 = [15, 3, 12, 4], 51 = [15, 2, 12, 4], 52 = [15, 1, 22, 17],
53 = [15, 3, 22, 17], 54 = [16, 1, 33, 15], 55 = [16, 2, 33, 15], 56 = [17, 3, 11, 8],
57 = [1, 3, [19, 13], 15], 58 = [7, 3, [14, 5], 14], 59 = [14, 3, [4, 15], 3],
60 = [15, 3, [12, 22], 8]
])

The disable table [2D source, input value index, 1D element index] is =

table([1 = [2, 1, 36], 2 = [2, 2, 36], 3 = [2, 3, 1], 4 = [3, 1, 25], 5 = [3, 3, 25],
6 = [6, 3, 2], 7 = [7, 1, 29], 8 = [7, 2, 29], 9 = [8, 1, 35], 10 = [8, 2, 35],
11 = [9, 1, 28], 12 = [9, 2, 28], 13 = [10, 2, 6], 14 = [11, 2, 7], 15 = [16, 1, 21],
16 = [16, 3, 21], 17 = [17, 1, 34], 18 = [17, 2, 34], 19 = [2, 2, [8, 36]],
20 = [7, 1, [29, 14]], 21 = [8, 2, [11, 35]], 22 = [11, 2, [32, 7]], 23 = [13, 3, [24, 3]],
24 = [15, 1, [22, 33]]
])

The set of transitions with leaf segments intersecting with NTS =

[source cell, input value, leaf segment, target cell, leaf pts]

table([1 = [4, 2, 12000, 15, [[4., 1.414213562], [3., 0.]]], 2 = [4, 3, 12001, 15,
[[3., 0.], [4., −1.414213562]]], 3 = [4, 1, 31001, 12, [[2., 0.], [3., −2.]]],
4 = [4, 2, 31001, 12, [[2., 0.], [3., −2.]]], 5 = [9, 2, 4000, 14, [[−1., 1.414213562],
[−2., 0.]]], 6 = [9, 3, 4001, 14, [[−2., 0.], [−1., −1.414213562]]],
7 = [12, 1, 31000, 4, [[3., 2.], [2., 0.]]], 8 = [12, 2, 31000, 4, [[3., 2.], [2., 0.]]],
9 = [12, 3, 9000, 13, [[3., 2.], [1., 0.]]], 10 = [12, 2, 9001, 13, [[1., 0.], [3., −2.]]],
11 = [13, 1, 15000, 14, [[−1., −1.414213562], [0., 0.]]],
12 = [13, 3, 15000, 14, [[−1., −1.414213562], [0., 0.]]],
13 = [13, 2, 9000, 12, [[3., 2.], [1., 0.]]], 14 = [13, 3, 9001, 12, [[1., 0.], [3., −2.]]],
15 = [14, 1, 15001, 13, [[0., 0.], [−1., 1.414213562]]],
16 = [14, 3, 15001, 13, [[0., 0.], [−1., 1.414213562]]],
17 = [14, 3, 4000, 9, [[−1., 1.414213562], [−2., 0.]]],
18 = [14, 2, 4001, 9, [[−2., 0.], [−1., −1.414213562]]],
19 = [15, 1, 33001, 16, [[4., 0.], %1]], 20 = [15, 2, 33001, 16, [[4., 0.], %1]],
21 = [15, 3, 12000, 4, [[4., 1.414213562], [3., 0.]]],
22 = [15, 2, 12001, 4, [[3., 0.], [4., −1.414213562]]],
23 = [16, 1, 33000, 15, [[4.333333333, −1.154700538], [4., 0.]]],
24 = [16, 2, 33000, 15, [[4.333333333, −1.154700538], [4., 0.]]],
25 = [16, 1, 21001, [[5., 0.], %1]], 26 = [16, 3, 21001, [[5., 0.], %1]]
])
%1 := [4.333333333, 1.154700538]

The in-going transition table [2D source, input value, 1D source, largest
FIC interval, FIC interval 1D source, 1D target, 2D target] is =

table([1 = [1, 1, 38, [1., 3.], [1., 3.], 19, 4], 2 = [1, 2, 13, [5., 7.], [5., 7.], 10, 11],
3 = [1, 2, 38, [7., 13.], [7., 13.], 10, 11], 4 = [1, 3, 10, [2., 4.], [2., 3.500000000],
19, 4], 5 = [1, 3, 10, [2., 4.], [3.500000000, 4.], 13, 5], 6 = [2, 2, 30, [5., 14.],
[5., 13.], 8, 8], 7 = [3, 2, 27, [0., 5.], [−.5000000000 10^{-9}, 5.], 3, 13],
8 = [4, 1, 31000, [1., 2.], [1., 2.], 23, 8], 9 = [4, 1, 19, [1., 3.], [2., 3.], 23, 8],
10 = [4, 1, 19, [1., 3.], [1., 2.], 31, 12], 11 = [4, 2, 31000, [2., 5.], [3., 5.], 12, 15],
12 = [4, 2, 31000, [2., 5.], [2., 3.], 31, 12], 13 = [4, 2, 12001, [3., 5.], [3., 5.],
31, 12], 14 = [4, 3, 19, [2., 3.500000000], [3., 3.500000000], 12, 15],
15 = [4, 3, 19, [2., 3.500000000], [2., 3.], 23, 8],
16 = [4, 3, 12000, [3., 3.500000000], [3., 3.500000000], 23, 8],
17 = [5, 1, 37, [3., 3.666666667], [3., 3.666666667], 20, 15],
18 = [5, 2, 37, [4.999999999, 7.], [5., 7.], 13, 1],
19 = [5, 3, 13, [3.500000000, 4.], [3.500000000, 4.], 20, 15],
20 = [6, 1, 24, [−2., 1.], [−2., 1.], 30, 2],
21 = [6, 2, 2, [5., 14.], [5., 14.], 30, 2], 22 = [7, 1, 17, [−7., −2.],
[−5.333333334, −2.], 14, 9], 23 = [7, 3, 17, [−4., −.2500000000],
[−4.000000001, −1.500000000], 14, 9], 24 = [7, 3, 17, [−4., −.2500000000],
%1, 5, 13], 25 = [8, 2, 8, [5., 13.], [5., 7.], 11, 17],
26 = [8, 3, 23, [2., 3.500000000], [2., 3.500000000], 8, 2],
27 = [8, 3, 11, [3.500000000, 4.], [3.500000000, 4.], 8, 2],
28 = [9, 1, 26, [−5.333333334, −4.], [−5.333333334, −4.], 16, 3],
29 = [9, 1, 14, [−5.333333334, −2.], [−4., −2.], 16, 3],
30 = [9, 2, 26, [−4., 0.], [−2., −.5000000000 10^{-9}], 4, 14],
31 = [9, 3, 14, [−4.000000001, −1.500000000], [−4.000000001, −2.], 16, 3],
32 = [9, 3, 4000, [−2., −1.500000000], [−2., −1.500000000], 16, 3],
33 = [9, 3, 14, [−4.000000001, −1.500000000], [−2., −1.500000000], 4, 14]])
%1 := [−1.500000000, −.2500000000]

table([34 = [10, 1, 32, [−2., 1.], [−2., 1.], 18, 13],

35 = [10, 3, 6, [−.2500000000, 2.], [−.2500000000, 2.], 18, 13],

36 = [11, 1, 39, [−2., 1.], [−2., 1.], 32, 10],

37 = [11, 2, 10, [5., 13.], [5., 13.], 32, 10],

38 = [11, 2, 39, [13., 22.],

[13., 14.], 32, 10], 39 = [11, 3, 7, [2., 4.], [2., 4.], 10, 1],

40 = [12, 1, 31001, [1., 2.], [1., 2.], 31, 4],

41 = [12, 2, 9000, [1., 5.], [2., 5.], 31, 4], 42 = [12, 2, 9000, [1., 5.],

[1., 2.], 9, 13], 43 = [12, 2, 31001, [2., 5.], [2., 5.], 9, 13],

44 = [12, 3, 9001, [1., 2.], [1., 2.], 9, 13], 45 = [13, 1, 18, [−2., 1.],

[−2., 0.], 15, 14], 46 = [13, 1, 15001, [−2., 0.], [−2., 0.], 24, 6],

47 = [13, 1, 18, [−2., 1.], [0., 1.], 24, 6],

48 = [13, 2, 3, [−.5000000000 10^{-9}, 5.], [−.5000000000 10^{-9}, 1.], 5, 7],

49 = [13, 2, 9001, [1., 5.], [1., 5.], 5, 7],

50 = [13, 2, 3, [−.5000000000 10^{-9}, 5.], [1., 5.], 9, 12],

51 = [13, 3, 5, %1, %1, 15, 14],

52 = [13, 3, 18, [−.2500000000, 2.], [−.2500000000, 0.], 15, 14],

53 = [13, 3, 18, [−.2500000000, 2.], [1., 2.], 9, 12],

54 = [13, 3, 15001, [−1.500000000, 0.], [−.2500000000, 0.], 24, 6],

55 = [13, 3, 9000, [1., 2.], [1., 2.], 24, 6],

56 = [13, 3, 15001, [−1.500000000, 0.], %1, 3, 3],

57 = [14, 1, 15000, [−2., 0.], [−2., 0.], 15, 13],

58 = [14, 2, 4000, [−2., −.5000000000 10^{-9}], [−2., −.5000000000 10^{-9}],

4, 9], 59 = [14, 3, 15000, [−1.500000000, 0.], [−1.500000000, 0.], 15, 13],

60 = [14, 3, 4001, [−2., −1.500000000], [−2., −1.500000000], 4, 9],

61 = [15, 1, 33000, [3.666666667, 4.], [3.666666667, 4.], 33, 16],

62 = [15, 1, 20, [3., 3.666666667], [3., 3.666666667], 22, 17],

63 = [15, 2, 12000, [3., 5.], [4., 4.999999999], 33, 16],

64 = [15, 2, 12000, [3., 5.], [3., 4.], 12, 4],

65 = [15, 2, 33000, [4., 4.999999999], [4., 5.], 12, 4],

66 = [15, 3, 12001, [3., 3.500000000], [3., 3.500000000], 12, 4],

67 = [15, 3, 20, [3.500000000, 4.], [3.500000000, 4.], 22, 17],

68 = [16, 1, 21000, [3.666666667, 5.], [3.666666667, 4.], 33, 15],

69 = [16, 2, 33001, [4., 4.999999999], [4., 4.999999999], 33, 15],

70 = [17, 3, 22, [3.500000000, 4.], [3.500000000, 4.], 11, 8]

])

%1 := [−1.500000000, −.2500000000]

The in-going disable table [2D source, input value, 1D source, largest

FIC interval, FIC interval 1D source, 1D target] is =

table([1 = [2, 1, 30, [−2., 1.], [−2., 1.], 36], 2 = [2, 2, 30, [5., 14.], [13., 14.], 36],
3 = [2, 2, 1, [14., 22.], [14., 22.], 36], 4 = [2, 3, 8, [2., 4.], [2., 4.], 1],
5 = [3, 1, 27, [−7., −5.333333334], [−7., −5.333333334], 25],
6 = [3, 1, 16, [−5.333333334, −2.], [−5.333333334, −2.], 25],
7 = [3, 3, 16, [−4.000000001, −1.500000000], [−4., −1.500000000], 25],
8 = [3, 3, 3, [−1.500000000, −.2500000000], [−1.500000000, −.2500000000], 25],
9 = [6, 3, 24, [−.2500000000, 2.], [−.2500000000, 2.], 2],
10 = [7, 1, 17, [−7., −2.], [−7., −5.333333334], 29],
11 = [7, 2, 5, [−.5000000000 \, 10^{-9}, 5.], [0., 5.], 29],
12 = [8, 1, 23, [1., 3.], [1., 3.], 35], 13 = [8, 2, 8, [5., 13.], [7., 13.], 35],
14 = [9, 1, 14, [−5.333333334, −2.], [−5.333333334, −4.], 28],
15 = [9, 2, 26, [−4., 0.], [−4., −2.], 28],
16 = [9, 2, 4001, [−2., −.5000000000 \, 10^{-9}], [−2., 0.], 28],
17 = [10, 2, 32, [5., 14.], [5., 14.], 6], 18 = [11, 2, 39, [13., 22.], [14., 22.], 7],
19 = [16, 1, 33001, [3.666666667, 4.], [3.666666667, 4.], 21],
20 = [16, 1, 21000, [3.666666667, 5.], [4., 5.], 21],
21 = [16, 3, 21000, [4., 5.], [4., 5.], 21],
22 = [17, 1, 22, [3., 3.666666667], [3., 3.666666667], 34],
23 = [17, 2, 11, [5., 7.], [4.999999999, 7.], 34]
])

B.3 Maple Output - Exothermic Reactor

The transition structure is:

table([1 = [1, 2, 5, 14], 2 = [1, 1, 34, 17], 3 = [1, 1, 2, 22], 4 = [1, 1, 40, 17],
5 = [1, 2, 3, 10], 6 = [1, 2, 27, 4], 7 = [2, 1, 24, 5], 8 = [2, 2, 24, 5],
9 = [2, 1, 11, 3], 10 = [2, 1, 29, 15], 11 = [3, 1, 6, 4], 12 = [3, 1, 28, 14],
13 = [3, 2, 11, 2], 14 = [3, 2, 23, 21], 15 = [3, 2, 7, 6], 16 = [3, 1, 32, 10],
17 = [4, 2, 6, 3], 18 = [4, 1, 27, 1], 19 = [5, 1, 24, 2], 20 = [5, 1, 12, 21],
21 = [5, 1, 26, 6], 22 = [5, 2, 13, 8], 23 = [5, 2, 21, 20], 24 = [5, 2, 19, 8],
25 = [6, 1, 7, 3], 26 = [6, 1, 26, 5], 27 = [6, 2, 26, 5], 28 = [6, 1, 31, 9],
29 = [7, 1, 25, 8], 30 = [7, 2, 25, 8], 31 = [7, 1, 18, 2], 32 = [7, 2, 18, 2],
33 = [7, 1, 14, 6], 34 = [7, 2, 14, 6], 35 = [8, 1, 19, 5], 36 = [8, 2, 19, 5],
37 = [8, 1, 22, 18], 38 = [8, 2, 22, 18], 39 = [8, 1, 13, 5], 40 = [8, 2, 13, 5],
41 = [9, 1, 8, 10], 42 = [9, 2, 8, 10], 43 = [9, 1, 31, 6], 44 = [9, 2, 31, 6],
45 = [10, 2, 8, 9], 46 = [10, 2, 32, 3], 47 = [10, 1, 3, 1], 48 = [10, 2, 3, 1],
49 = [12, 1, 36, 15], 50 = [12, 2, 36, 15], 51 = [12, 1, 9, 13], 52 = [12, 2, 9, 13],
53 = [12, 1, 38, 9], 54 = [12, 2, 38, 9], 55 = [13, 1, 39, 10], 56 = [13, 2, 39, 10],
57 = [13, 1, 4, 17], 58 = [13, 2, 4, 17], 59 = [13, 1, 35, 14], 60 = [13, 2, 35, 14],
61 = [14, 2, 28, 3], 62 = [14, 1, 5, 1], 63 = [14, 2, 5, 1], 64 = [14, 2, 10, 15],
65 = [15, 1, 10, 14], 66 = [15, 2, 10, 14], 67 = [15, 1, 29, 2], 68 = [15, 2, 29, 2],
69 = [16, 1, 17, 15], 70 = [16, 2, 17, 15], 71 = [16, 1, 30, 7], 72 = [16, 2, 30, 7],
73 = [16, 1, 15, 9], 74 = [16, 2, 15, 9], 75 = [17, 1, 1, 19], 76 = [17, 2, 1, 19],
77 = [17, 1, 40, 1], 78 = [17, 2, 40, 1], 79 = [17, 1, 34, 1], 80 = [17, 2, 34, 1],
81 = [18, 1, 20, 20], 82 = [18, 1, 22, 8], 83 = [19, 2, 1, 17], 84 = [19, 2, 33, 22],
85 = [20, 2, 20, 18], 86 = [20, 1, 21, 5], 87 = [21, 2, 12, 5], 88 = [21, 1, 23, 3],
89 = [22, 2, 2, 1],
90 = [22, 1, 33, 19]
])

Vita

Name: Stéphane Blouin

Date of birth: August 30, 1969, Lévis, Québec

Education: M.Sc. Electrical Engineering
                     École Polytechnique, University of Montréal, 1998

                     B.Sc. Mechanical Engineering
                     Laval University, 1992

Experience: Teaching Assistant, Queen's University, 1999-2002.
                     Consultant in Automation, Walsh Automation, 1998.
                     Teaching Assistant, École Polytechnique, 1996-1998.
                     Production Engineer, SNC Industrial Tecnologies, 1995.
                     R&D Engineer, Falco Stainless Steel Equipment, 1994-1995.
                     Intern, Research Center in Shipbuilding (IRCN), France, 1992.

Awards: Thesis Writing Bursary, Queen's University, 2003.
                     Ontario Graduate Scholarship, Ontario, 2002-2003.
                     FCAR Ph.D. Schorlarship, Québec, 2001.
                     Queen's Graduate Award, 2000-2003.
                     T.F. Greenhalgh Scholarship, University of Alberta, 1999.
                     W. John Fellowship, University of Alberta, 1999.
                     NSERC PGSB Graduate Scholarship, 1999-2000.
                     CIME International Scholarship, France, 1991-1992.
                     Team Design Prize, Society of Automotive Engineering, 1991.

Publications: **Refereed Journal Publications**

                     S. Blouin, M. Guay and K. Rudie (2002), Discrete Abstractions for
                     Nearly Integrable Continuous Systems: The Two-dimensional Case.
                     International Journal of Hybrid Systems, 2(4), pp. 297-336.

                     S. Blouin, A. Hemami and M. Lipsett (2001), Review of Resistive Force
                     Models for Earthmoving Processes. *Journal of Aerospace Engineering*,
                     14(3), pp. 102-111.

Publications: **Refereed Conference Papers**

S. Blouin, M. Guay and K. Rudie, Discrete Abstractions for Two-dimensional Nearly Integrable Continuous Systems. In *Proceedings of the IFAC Conference on Analysis and Design of Hybrid Systems*, June 2003, pp. 383-388.

S. Blouin, M. Guay and K. Rudie, Discrete Control of Nearly Integrable Two-dimensional Systems. To appear in *ADCHEM 2004 International Symposium on Advanced Control of Chemical Processes.*

S. Blouin, M. Guay and K. Rudie, An Application of Discrete-Event Theory to Truck Dispatching. In *Proceedings of the American Control Conference*, June 2001, pp. 2315-2320.

J.C. Piedboeuf, R. Hurteau, S. Blouin and F. Germain, Friction and Stick-slip in Robot: Simulation and Experimentation. In *Proceedings of NATO Advanced Study Institute of Computational Methods and Mechanisms*, Bulgaria, June 1997, pp. 319-330.

Non-refereed Conference Papers

S. Blouin, M. Guay and K. Rudie, Hierarchical Hybrid Approach for Integrated Process Design.*AIChE Annual Meeting*, Los Angeles, USA, November 2000.

S. Blouin, R. Hurteau and R. Gourdeau, Identification paramétrique d'un environnement par une tâche de contact d'un manipulateur robotique. In *Proceedings of Third International Conference on Industrial Automation*, Montreal, Canada, June 1999, pp. 9.21-9.24.

R. Gourdeau, S. Blouin and R. Hurteau, Computed Torque Control of Robots Without Joint Velocity Measurements. In *Proceedings of 1999 IEEE CCECE*, Edmonton, Canada, May 1999, pp. 1413-1418.